City Research Online

City St George's, University of London

Citation: Akhavan-Rezayat, A. (1979). Measurement of the stopping powers of liquids and vapours for alpha-particles. (Unpublished Doctoral thesis, The City University)

This is the accepted version of the paper.

This version of the publication may differ from the final published version. To cite this item please consult the publisher's version.

Permanent repository link: https://openaccess.city.ac.uk/id/eprint/37401/

Copyright and Reuse: Copyright and Moral Rights remain with the author(s) and/or copyright holders. Copies of full items can be used for personal research or study, educational, or not-for-profit purposes without prior permission or charge, unless otherwise indicated, provided that the authors, title and full bibliographic details are credited, a hyperlink and/or URL is given for the original metadata page and the content is not changed in any way. For full details of reuse please refer to City Research Online policy.

City Research Online: http://openaccess.city.ac.uk/ publications@citystgeorges.ac.uk

THE CITY UNIVERSITY

NUCLEAR MEASUREMENT LABORATORY

DEPARTMENT OF PHYSICS

Measurement of the stopping powers of liquids and vapours for alpha-particles

By

A. AKHAVAN-REZAYAT

A thesis submitted for the degree of

Doctor of Philosophy

April 1979

CONTENTS

Symbols

Z_1	=	Alpha-particle electric charge
M	=	Alpha-particle mass
v	=	Alpha-particle velocity
E	=	Alpha-particle energy
e	=	Electronic charge
m	=	Mass of electron
ε_o	=	Permittivity of free space
Q	=	The energy which can be transferred to an electron in a single collision
τ	=	Orbital period of electron
ω	=	$\frac{1}{\tau}$
b	=	impact parameter
N	=	Number of stopping atoms per unit volume
Z_2	=	Nuclear charge
h	=	Planck constant
I	=	Mean ionisation and excitation potential
fi	=	Oscillator strength of each possible excitation
Ei	=	excitation energy
B	=	Stopping number
C	=	Speed of light
β	=	$\frac{v}{c}$
δ	=	Density correction
σ	=	Standard deviation
Z_{leff}	=	Effective charge of an alpha-particle
σ_c	=	Electron capture cross section

σ_I = Electron loss cross section

a_H = Bohr radius

m_o = Electron rest mass

v_H = Velocity of an electron in the first Bohr orbit of hydrogen

N_A = Avogadro constant

η_k = $\frac{mv^2}{2(Z_2-0.3)2Ry}$ (Corresponding definition for η_L)

θ_k = Observed ionization potential for K shell

Ry = Ionization potential of the hydrogen atom

N_m = Number of moleculer per unit volume

q = $K_B/4$ Ry

K_B = I_{mean}/Z_2

t = Thickness

s = Area of the substrate

f = Density

R_o = Mean range

R = Extrapolated range

R_p = range at any required pressure

D = Distance

P = Pressure

ACKNOWLEDGEMENTS

I wish to thank my supervisor Dr. R. B. J. Palmer for her patient, skillful and sympathetic guidance throughout all stages of this research.

Sincere thanks are offered to [redacted] technician in charge of the Nuclear Measurements Laboratory who willingly undertook the many problems inherent in complying with my precise requirements.

Thanks are also due to all technicians and workshop personnel of the Physics Department especially [redacted] who helped in many ways.

In addition I would like to express my gratitude to [redacted] who undertook the typing of this thesis.

Finally I would like to thank [redacted] as this work would not have been completed without their constant encouragement and understanding.

ABSTRACT.

Measurements have been carried out of the molecular stopping power for alpha-particles over the energy range 1 to 8 Mev of oxygen, water, methyl, ethyl and propyl alcohols, dichloromethane, trichloromethane and carbontetrachloride in the liquid and vapour states. These results are compared with calculated stopping power values and discussed with reference to the charge state of the alpha-particles at various energies. The methods used include a new technique for measurements with liquids. The molecular stopping powers of all materials in the vapour phase are found to be significantly higher than those in the corresponding liquid phase except for CH_2Cl_2 (above 2 Mev), $CHCl_3$ and CCl_4.

Stopping cross sections for oxygen, - CH_2 -, - C - and - Cl - have been determined from the experimental measurements using Bragg's Rule.

1. Introduction

1.1 Basic interaction of charged particles with matter

When a charged nuclear particle passes through matter, it ionises or excites the atoms of the medium and loses energy. This interaction with the atomic electrons is through the Coulomb force; the energy transferred to the electrons represents a loss of kinetic energy of the moving particle which therefore will slow down, and eventually stop. This constitutes the major mechanism of energy loss; however at very low energies interaction with nuclei takes place and gives rise to scattering.

The strength of these interactions and the magnitude of the energy loss depend on the charge and velocity of the particles and on the character of the medium. The different types of charged particles can be classified into two main groups: electrons, and heavy charged particles. The latter include, for example, protons, alpha-particles, mesons, and atomic and molecular ions. The fundamental difference in behaviour between the electron and all the other charged particles is that the electron rest mass m, is very small. When an electron collides with another electron, it can lose a large part of its energy in a single interaction and also can be deflected through a large angle, but a heavy particle will lose only a small fraction of its energy, and will only be deflected through a very small angle in a single collision.

1.2 Classical Calculation of the Energy loss

The classical calculation of the energy loss of a charged particle travelling through an absorbing medium was first carried out by N. Bohr (1948). Consider an incident particle of electric charge Z_1e, mass M,

velocity v, and kinetic energy E, moving along X axis as in Fig. 1.1 which interacts with a free electron -e and mass m situated on the axis Y.

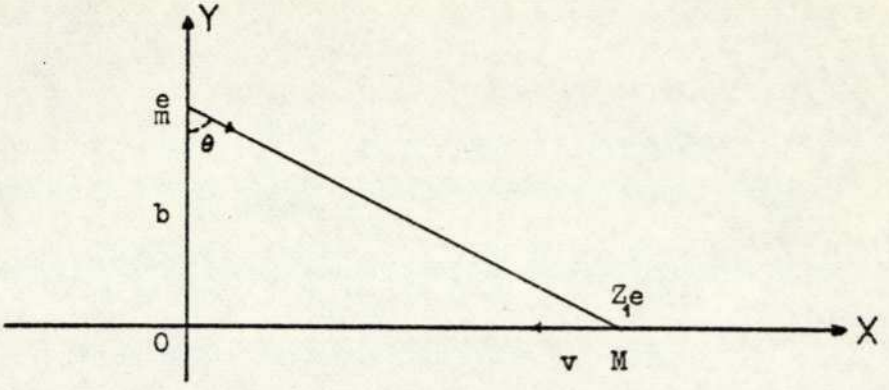

Fig. 1.1 Diagram for collision of heavy positive charged particle with electron.

In order that momentum and energy should be conserved the maximum energy that can be transferred to an electron is $2mv^2$, and this occurs when the minimum impact parameter $b_{min} = \frac{Z_1e^2}{4\pi\varepsilon_o mv^2}$ where ε_o is permittivity of free space.

For a bound electron the minimum energy Q_{min} that can be transferred in a single collision is determined by the collision time which must be less than the orbital period, τ, of the electron,

$$Q_{min} = \frac{2Z_1^2e^4\omega^2}{(4\pi\varepsilon_o)^2 mv^4}$$

when $\omega = \frac{1}{\tau}$. This loss will occur at a maximum impact parameter, b_{max}, where b_{max} is of the order $\frac{V}{\omega}$

From these considerations it can be shown that the rate of energy loss in the medium,

$$\frac{\Delta E}{\Delta X} = \frac{4\pi Z_1^2 e^4 NZ_2}{mv^2} \ln \frac{bmax}{bmin} = \frac{Z_1^2 e^4 NZ_2}{4\pi\varepsilon_o^2 mv^2} \ln \frac{4\pi\varepsilon_o mv^3}{Z_1 e^2 \omega}$$

where N is the number of stopping atoms per cm^3, and Z_2 is the nuclear charge. Calculation using this formula presents problems owing to the presence of the parameter ω. In simple cases this can be calculated for each electron and a mean obtained.

The Bohr treatment can be shown, due to the uncertainty principle, to be valid only if $\frac{Z_1 e^2}{4\pi\varepsilon_0 \hbar v} \gg 1$. Bethe (1930) using a quantum mechanical treatment obtained an expression of similar overall form, but with a different logarithmic term which is valid if the Born approximation holds, i.e. for $\frac{Z_1 e^2}{4\pi\varepsilon_0 \hbar v} \ll 1$.

Bloch (1933) developed a general formula which reduces to Bohr's and Bethe's expressions in the two extreme limits, his calculation being based upon a continuous distribution of electron charge from the nucleus to the radius of the atom. The stopping power formula is most conveniently expressed in terms of the mean ionisation and excitation potential of the atoms of the absorbing medium I which is defined as

$$Z_2 \ln I = \sum_i f_i \ln E_i \qquad (1.1)$$

where f_i is the oscillator strength of each possible excitation or ionization from the ground state to the excited state i, E_i is the excitation energy and Z_2 is the nuclear charge. Since the spectroscopic values of the oscillator strengths are generally not well known in the range of the most important excitation energies, there are serious difficulties in determining I from the above definition for a given material.

The stopping power formula may be written

$$-\frac{dE}{dx} = \frac{Z_1^2 e^4}{4\pi\varepsilon_0^2 mv^2} NB \qquad (1.2)$$

where B is the stopping number and is given by the expression

$$B = Z_2 \ln(2\ mv^2/I) \quad (1.3)$$

In practice, I can be obtained experimentally by using stopping power measurements. To determine this accurately, however, the Bethe equation has to be corrected for several effects not allowed for in the simple theory.

It should be noted that, since only the logarithm of I enters the expression directly, a large uncertainty in I introduces only a relatively small uncertainty in stopping power.

A number of workers have calculated values for I relating to various materials using experimental values of $\frac{dE}{dX}$ and equating this to the expression (1-2). If the Bethe formula is correct, $\frac{dE}{dX}$ is proportional to $Z_2 \ln \frac{2mv^2}{I}$, Bloch suggested that $\frac{I}{Z_2}$ may be regarded as a constant K. On this basis, approximate values for I were calculated from stopping power measurements on a limited number of materials.

Jensen (1937) suggested that experimental I values increase as Z_2 increases. He explained that, this is due to electron exchange effects. Dalton and Turner (1968) obtained I values for a number of substances of interest in radiation dosimetry. They have obtained I values by calculation, using equation (1.1), for the simplest atoms, and by the use of equation (1.2) with experimental values of $\frac{dE}{dX}$ for heavier atoms. They found that, I as a function of Z_2 could be obtained by using the following empirical formulae,

$$I_{(ev)} = 11.2 + 11.7\, Z_2, \quad Z_2 \leqslant 13$$

$$I_{(ev)} = 52.8 + 8.71\, Z_2, \quad Z_2 > 13$$

For most elements the value of I, using these equations was given, to within $\pm$ 4% of the value recalculated from experiment.

Further stopping power measurements on a wider range of materials have subsequently shown that K is not a true constant, but has a periodic variation as a function of Z_2, especially for low Z_2, ($Z_2 < 30$).

The values of the ratio $\frac{I}{Z_2}$ decrease at high Z_2 values as the atomic number of the element increases. Bichsel (1970) suggested that K is expected to be a constant if I is evaluated using the Thomas Fermi model. However he presented a curve based on experimental values which show that $\frac{I}{Z_2}$ is not constant but varies as shown in Fig. (1.2). As can be seen, the $\frac{I}{Z_2}$ value has its maximum values for rare gases and minimum values in the middle of rows in the periodic table.

Inokuti (1978) explained this as a reflection of the shell structure of atoms, which is not explicitly taken into account in the Thomas Fermi model.

Turner et al (1970) found I values by making a few modifications of their earlier work. (Dalton and Turner 1968). They presented a table listing I values for the chemical elements. Computational methods have now been devised in the main for simple light media, based on experimental data on oscillator strengths (Zeiss et al 1977), but for condensed phases and complex media there are serious difficulties. They found I values for the isolated H atom 14.99 ev, and for H_2 about 19.3 ev. The 30% increase is due to higher electron density near the two protons.

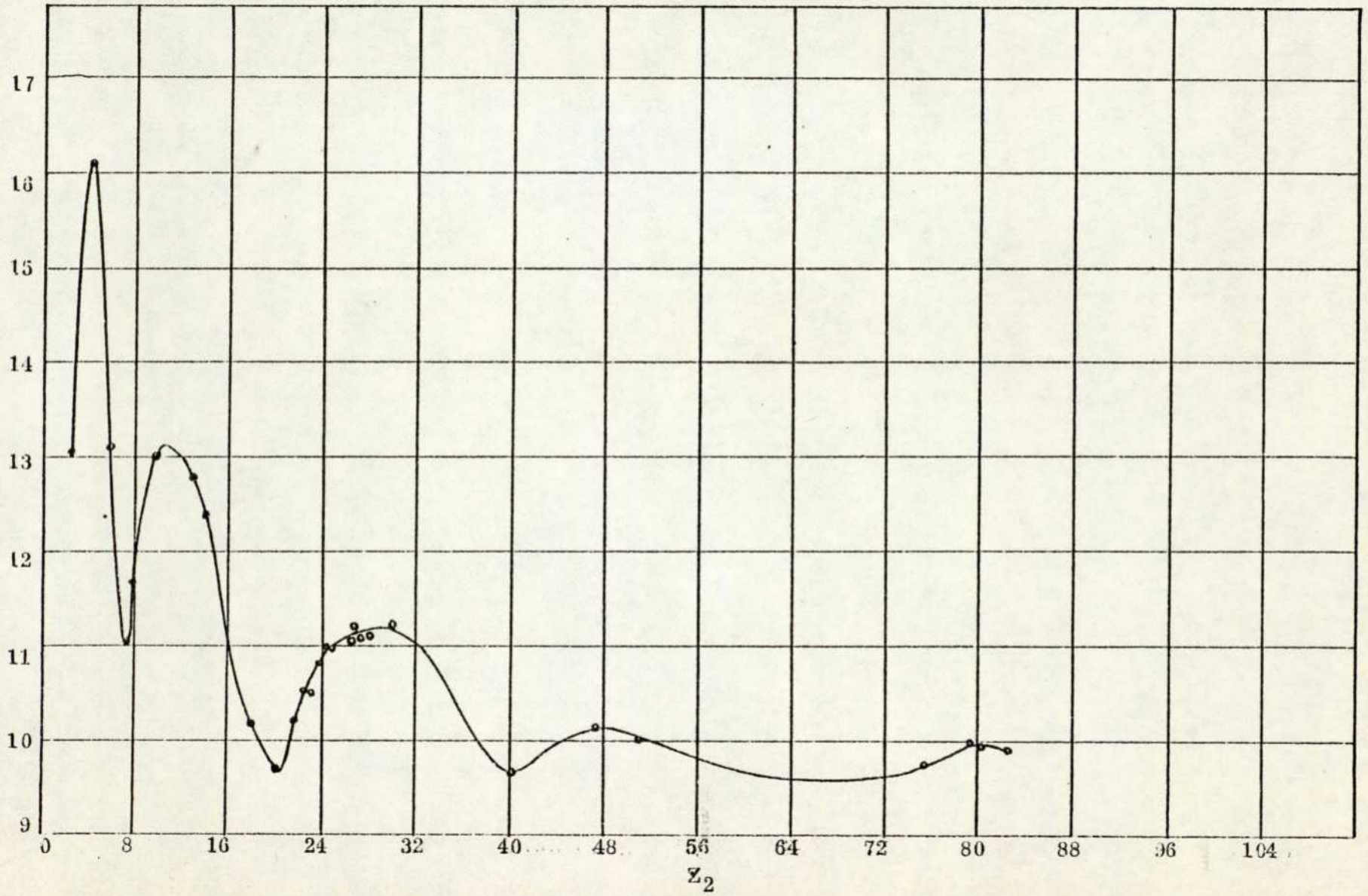

Fig (1-2) The mean excitation energy I_{ave} for different elements (Bischsel 1970).

which causes a higher value for I. Considering the effect of chemical binding on I, they suggested that in all molecules except those which contain hydrogen atoms, the effect is very small, because only valence electrons are modified by binding and valence electrons are only a small fraction of all electrons. By similar reasoning the influence of phase upon the I value is inevitable, but its magnitude may be negligible. One of the important reasons why we have different stopping power values for matter in different states could be due to the change in I with phase (Matteson et al 1977).

Bichsel (1974) suggested that the I value in the condensed phase owing to the modified energy state of the outer electrons is greater than that in vapour phase. On this reasoning the experimental stopping power of particles in the condensed state is expected to be lower than the stopping power of the same material in the vapour phase.

1.3 Modifications to the Bethe formula.

For an accurate assessment of stopping power, however, a number of corrections must be made to the Bethe formula, since some of the assumptions made in the derivation are not always valid.

At high energy i.e. when the particle is moving at relativistic velocities the stopping power formula must be corrected to include a modified value of B. Under these conditions the form of equation (1.3) must be re-written $B = Z_2(\ln \frac{2mv^2}{I(1-\beta^2)} - \beta^2 - \frac{1}{2}\delta)$ (1.4)

where $\beta = \frac{v}{c}$, c is the speed of light and δ is the density correction.

We shall ignore the density effect δ in the region of energy which has been used in this work because it only has to be considered at very high energies in condensed materials, otherwise the density effect is negligible. With 1 Gev protons in Cu, for example, the density effect reduces the stopping power by 0.5%, Fano (1964), (Cf. Table 10A, P.123)

Therefore the form of equation (1.4) can be rewritten as

$$B = Z_2\left(\ln \frac{2mv^2}{I(1-\beta^2)} - \beta^2\right) \quad (1.5)$$

For alpha-particles of energy less than 8 Mev, β^2 can also be neglected since $\frac{v^2}{c^2}$ at 8 Mev is about 0.004.

1.3a Electron Capture and Loss by ions

The charge on the incident particle can only be assumed to be 2e at high energies, and at low velocity the effective charge $Z_{1\,eff}\,e$ is not very well known. When an incident particle traverses a sufficient amount of homogeneous material, it reaches a new equilibrium charge state which is related to its velocity. This is due to the continuous process of capture and loss of electrons by the ion from the atoms of the stopping medium. There is considerable doubt as to the value of the alpha-particle charge at various velocities.

Electron pick-up occurs when the ion velocity is sufficiently reduced, and statistically the mean ion charge becomes less than 2e, so that the relevant value of Z_1 becomes less than 2, and the stopping power is reduced accordingly. However the process of capture and loss of electrons provides a further energy loss mechanism, and the effective charge on the alpha-particle $Z_{1\,eff}$ at energies less than 3 or 4 Mev is difficult to estimate accurately.

If all other parameters in the Bethe formula were accurately known one could, from accurate experimental measurements of stopping power, obtain values of Z_{1eff} at various energies, but there are further corrections to the formula at low energies, all of which introduce considerable uncertainty into calculations. The phenomenon of charge exchange has been extensively studied particularly for fission fragments which carry a large number of electrons because of their high nuclear charge.

The first authors which examined theoretically the range and effective charge of heavy ions in gas were Bohr (1940, 1941), and Knipp and Teller (1941). Bohr shows that, in a medium of light atomic number some electrons have speeds as large as the velocity of the incident particle. He presented an equation for the capture cross section from the Thomas-Fermi model

$$\sigma_c \sim 4\pi a_H^2 Z_2^{\frac{1}{3}} (V_H/V)^6$$

where, a_H is the Bohr radius and is $a_H = \frac{4\pi\varepsilon_0 \hbar}{m_0 e^2} = 0.53 \times 10^{-8}$ cm, $V_H = Z_1 e^2/4\pi\varepsilon_0\hbar$ is the velocity of an electron in the first Bohr orbit of hydrogen and V is the velocity of the particle. This equation is valid only for $V \gg V_H$. For lighter absorbers, $Z_2 = 1$ to 4, Bohr's equation for electron loss cross section is

$$\sigma_\ell = 4\pi \left(\frac{a_H}{Z_1}\right)^2 (Z_2^2 + Z_2)\left(\frac{V_H}{V}\right)^2$$

For $Z_2 \simeq 4$ to 6, Bohr's equation is

$$\sigma_\ell = \pi \frac{a_H^2}{Z_1} Z_2^{\frac{2}{3}} \frac{V_H}{V}$$

and for $Z_2 > 6$, the dependence of electron loss cross section σ_ℓ on the velocity of the incident particle V, is expected to become weaker, until for very heavy element, σ_ℓ becomes substantially independent of V.

Bohr assumes as a first approximation that the fragment will take off all electrons for which the orbital velocity in the atom is smaller than the velocity of the fragment. The equation below with a rough estimate based on the Thomas-Fermi statistical model obtains $Z_{1\,eff}$

$$Z_{1eff} = Z_2^{\frac{1}{2}} \frac{4\pi\varepsilon_0 hv}{e^2}$$

where V is the velocity of the particle.

Bethe et al (1953) have found experimentally and theoretically that if the particles velocity V, is very much greater than the Bohr orbital velocity for a K electron in the moving particle, the probability of electron loss by a particle is much greater than electron capture $\sigma_\ell \gg \sigma_c$, where σ_c and σ_ℓ are the capture and loss cross section per atom of absorber. At lower particle velocity V the pick-up process is highly probable.

Bell (1953) theoretically investigated the capture and loss of electrons by fission fragments in low pressure gas. He suggested that the effective charge changes with the velocity of the fission fragment and also with the nature of the gas which particles pass through. He suggested that, those electrons whose orbital velocities are close to the ion velocity have more probability to be captured by the fragment. He also mentioned that, total capture cross section in argon are nearly twice as large as that in oxygen, this is due to the number of electrons in the atoms which are available for capture and have $V_H \cong V$. It means that in the heavier gases, because of the low velocity of the valence electrons, compared with the velocity of the fission fragment, the capture cross section in these gases is larger.

Gluckstern (1955) investigated the capture and loss cross section for ions of intermediate atomic numbers, $8 \leqslant Z_2 \leqslant 18$, passing through low pressure gas, by using a modified form of Bell's model, He pointed out that the capture cross section depend on the particles velocity and charge, and is independent of the particular ion. He also suggested that in a single collision, capture and loss of two electrons is significant, but the effect on the charge distribution should not be too great. He argues that Bell's capture cross sections are too large because they contain contributions from all electrons in a target atom. One should not sum the individual capture cross section especially in collisions with small impact parameters, for which the capture cross sections are greatest, but should instead consider, at any impact parameter, the probability of capturing any electron. Betz (1972) has also mentioned that there is the possibility that in a single collision more than one electron may be transferred, but this probability is very small. He pointed out that multiple-electron loss occurs with more probability than multiple-electron capture. Allison (1958) has reviewed the experimental data on charge changing collisions of hydrogen and helium atoms and ions.

Much experimental work has been carried out since on the measurement of capture and loss cross-sections in various materials, and these are classified in the literature, (e.g. Mapleton 1972 and Massy and Gilbody 1974).

Studies of capture and loss of electrons do not, in themselves, provide a solution to the problem of knowing what is the effective charge associated with an alpha particle as it traverses matter. This problem

was appreciated by early experimental workers who attempted to measure the proportion of He^{+} to He^{++} emerging from various absorbers. An equilibrium charge state is reached for any velocity, but this is changing as the particles slow down.

Heckman et al (1963) by measuring the equilibrium distributions of electronic-charge states of C^{12}, N^{14}, O^{15} and Ne^{20} ions in Zapon at 1.59 to 10.5 Mev/nucleon and nonequilibrium charge distributions for ions in Zapon 10.2 Mev/nucleon, pointed out that a beam of ions after passing through a matter reaches an equilibrium charge distribution, which depends on the characteristic of the material, the ion's nuclear charge and the velocity of the ion.

The variations in cross-section for pick-up and loss of electrons in different gases showed that the equilibrium charge may depend on the nature of substance to be examined, but Ziegler (1978) evaluated the effective charge of H and He ions in all elements and showed that the effective charge of these two ions could be almost independent of the target.

There are indication (see later) that the molecular stopping power of the condensed phase is lower than that of the vapour phase. If this is due to charge exchange effects it would suggest that the charge state is lower in the condensed phase than the vapour phase. Betz (1972, 1976) discusses heavy ions and for these the evidence is that the charge state is higher in the solid state. However, for these ions the situation is different from that of the alpha-particle since these ions are not completely stripped of electrons. Much

of the heavy ion data and calculations are therefore not necessarily relevent in the present discussion. This is borne out by the experiments of Meckbach and Allison (1963) who measured the stopping power of Cd solid and vapour for He ions and H ions from 148 to 920 kev energies. They found that for He ions between 575 and 920 kev energy, the effective charge in the gas is higher than in solid.

1.3 b Shell-corrections

The Bethe equation is valid provided that the velocity of the incident particle is large compared with the velocity of the atomic electrons, $V \gg V_H$, where V_H is the orbital velocity of the electrons bound in the shell. If it is not large compared with the velocity of some of the atomic electrons, correction must be made for this condition, for example, the condition of $V \gg V_H$ for the inner orbit of heavy elements is rarely fulfilled and even at high energies of incident particles the shell correction may have an appreciable value.

The stopping number B must be calculated separately for each shell since each responds differently to the incident particle, and will in fact cease to influence it at different energies, depending upon the velocity of the atomic electrons concerned. The total stopping is calculated from the sum of the contributions of the various shells.

Walske (1952, 1955) has calculated the stopping power of K and L electrons for a limited range of Z_2 and V, and expressed them in a form convenient for computation, so that the simple Bethe formula can be corrected normally by the subtraction of the terms C_k and C_L hence

$$-\frac{dE}{dx} = \frac{Z_1^2 e^4 N Z_2}{4\pi\varepsilon_0^2 mv^2}\left(\ln\frac{2mv^2}{I} - \sum\frac{C}{Z_2}\right) \qquad (1.6)$$

For atoms of low atomic number with which we are at present concerned only C_k is relevant. Walske has given curves of C_k against $^1/_{\eta_k}$ over the range $0 < {}^1/_{\eta_k} < 2$ for various θ_k. θ_k is the observed ionization potential or the energy difference between the ground state and lowest unoccupied state in units Z_{keff}^2 Ry

$$\eta_k = \frac{mv^2}{2Z_{eff}^2\,\text{Ry}} = \frac{Em}{MZ_{eff}^2\,\text{Ry}}$$

where Ry is the ionization potential of the hydrogen atom and $Z_{eff} \approx Z_2 - 0.3$ is the effective nuclear charge in the k shell, m is the electron rest mass and M is the mass of the ionizing particle of energy E. η_k is thus dimensionless. By calculating η for any value of the incident particle's energies, C_k can be obtained from the curve, and a correction made to the stopping power value.

These calculations do not merely allow for the non-participation of certain (e.g. k shell) electrons in the stopping at a critical energy of the incident particle, but also allow for the fact that one cannot assume for low energy incident particles that the electrons with which they are interacting are stationary. This false assumption leads to the incorrect condition implied by the simple Bethe formula that where $2mv^2 < I$, $\frac{dE}{dx}$ becomes - ve, and obviously as $2mv^2$ approaches this limiting value the Bethe formula will be incorrect.

Khandelwal and Merzbacher (1966) have calculated the M-shell binding correction to Bethe's formula and also Khandelwal (1968) has

made K- and L- shell corrections by calculations similar to Walske's, to cover the entire periodic table. His corrections agreed very well with Walske's.

Bonderup (1967) used the Lindhard and Winther electron gas model to calculate shell corrections for all elements. Walske's and Bonderup's shell corrections have the same asymptotic values at high velocities.

Andersen et al (1969) calculated the shell corrections for the elements Z_2=20 to Z_2=30 from stopping power measurements with 5-12 Mev protons and deuterons. The result which they obtained in some cases are smaller than Walske's calculated corrections, for lower Z_2. This, they suggested, could be because Walske's corrections are too large, but it could also arise because their calculated corrections indicate the deviations from the simple Bethe formula which means that they include all types of deviations and not merely those due to non-participation of the inner shell electrons. In fact this would include the Z_1^3 correction, not appreciated at the time, and this would in fact reduce the overall correction and make the shell correction appear to be smaller.

1.3 c The Barkas effect

Barkas et al (1963) found that the stopping power of a material for slow positive ions was larger than that for negative ions at the same velocities, and suggested that this fact was not in agreement with the current theory based on the first Born approximation.

According to equation (1.6), if we measure the stopping power of

a material for alpha particles and for protons, we can have the following equation at identical velocities for both particles,

$$\left(\frac{dE}{dx}\right)_a = 4\left(\frac{dE}{dx}\right)_p \quad (1.7) \quad \text{Since } Z_a = 2Z_p$$

Anderson et al (1969) measured the stopping power of aluminium and tantalum for different particles and found that the double-charged ions lose energy at a rate 1-2.5% higher than would be predicted by equation (1.7). They also compared the energy loss of helium ions in thin metal foils with the energy loss of hydrogen ions of identical velocity in the same foils, and found that the ratio between the two sets of data is larger than the factor $\underline{4}$ predicted by the Bethe theory.

Heckman et al (1969) investigated the stopping power differences between +ve and -ve pions at low velocities, and they found similar results to Barkas et al. They suggested that the difference in the stopping power for positive and negative particles is due to the difference in direction of the coulomb force acting on the particles within the negative electron cloud of the atom. As a result the rate of energy-loss of positively charged incident particles increases, conversely, slow negative particles will repel the electrons of the media, and the strength of the interactions between the particles and the electrons will be smaller and therefore the energy-loss rate will be reduced, and the range will be increased. They suggested that the use of the second-order Born approximation treatment would introduce an extra term in the stopping power that is proportional to third power of the incident particle charge.

In the Bethe theory equation (1.6), the stopping power of a medium for a particle of charge number, Z_1e is proportional to $(Z_1e)^2$. Also

Ashley et al (1972), Jackson and McCarthy (1972), Ashley et al (1973) and Ashley (1973) extended the stopping power theory to include a term proportional to the third power of the charged carried by the particle, and evaluated the effect of this contribution in a number of materials.

If So (X_c) is the stopping power uncorrected for the Z_1^3 effect the corrected stopping power $S(X_c)$ is

$$S(X_c) = So(X_c) \quad 1 + \frac{Z_1 k (b, X_c)}{Z_c^{\frac{2}{3}} \cdot X_c} \quad f (Z_c, X_c)$$

where $f (Z_c, X_c) = \frac{Z_c^{\frac{1}{2}}}{Z_c^{\frac{3}{2}}} \quad (1 + \frac{\ln \bar{Z}_c / \bar{Z}'_c}{\ln \frac{X_c}{q}})$

$$Z_c^{\frac{1}{2}} = \frac{\Sigma_{ni} Z_{2i}}{\Sigma_{ni} Z_{2i}}$$

$$\ln \bar{Z}_c = \frac{\Sigma_{ni} Z_{2i} \ln Z_{2i}}{\Sigma_{ni} Z_{2i}}$$

$$\ln \bar{Z}'_c = \frac{\Sigma_{ni} Z_{2i}^{3/2} \ln Z_{2i}}{\Sigma_{ni} Z_{2i}^{3/2}}$$

$Xc = 40.2 E_1/M_1 \bar{Z}_c$ where M_1 is the mass of alpha-particle in a.m.u, and E_1 is the energy in Mev.

If $Z_1 \neq 2$ due to charge exchange we use Z_{1eff} instead of Z_1.

$q = K_B/4R_y$ where $K_B = \frac{I_{mean}}{Z_2}$ and R_y is the ionization potential of the hydrogen atom.

Lindhard (1976) reported on a new calculation of the Z_1^3 correction, and the result obtained was approximately twice the magnitude of Ashley et al's earlier calculation. He also introduced another correction significant only for very low energy particles. The additional term is proportional to the fourth power of the charge of the particle.

Anderson et al (1977) investigated these effects experimentally by measuring the stopping power of hydrogen, helium, and lithium ions in

in five different materials, and confirmed the Lindhard correction.

Finally, Ritchie and Brandt (1978) have investigated the stopping power data of solids with atomic number $13 \leqslant Z_2 \leqslant 79$ for ions in the ranges $1 \leqslant Z_1 \leqslant 9$ with velocities $7 \leqslant v_1/v_2 \leqslant 12$ in terms of the Z_1^3 effect and effective ion charges, and have suggested that the stopping power data are consistent with the theory of Ashley et al.

1.3.d. Bragg's rule.

Bragg's rule states that the stopping cross section of compounds can be obtained by adding the stopping cross section of the component elements. If the Bethe formula applies, Bragg's rule must also hold. If, however, corrections to the Bethe formula are necessary, Bragg's rule may, or may not be true depending upon the nature and reason for the corrections.

Physical-state effects and chemical-binding effects can be considered in the experimental tests of Bragg's rule.

If $\sigma(X_mY_n)$ is the stopping cross section $\frac{1}{N_m}\frac{dE}{dx}$ of the molecule X_mY_n, where N_m is the number of molecules per unit volume, and $\sigma(X)$ and $\sigma(Y)$ are the stopping cross section of the component elements X and Y, respectively. Bragg's rule is stated as follows:

$$\sigma(X_mY_n) = m\ \sigma(X) + n\ \sigma(Y),$$

When a compound is formed, the wave functions of the outer electrons will slightly change, the binding will become tighter, and therefore the average excitation potential will change and an increase of the ionisation

potential of the valence electrons would be expected. Hence an increase in the value of I, the mean ionisation and excitation potential seems not unreasonable, although this could be quite small.

It is also reasonable to suppose that the physical state of an absorber will, under certain circumstances affect its stopping power. In the condensed phase the outer electronic levels can be slightly affected due to inter-molecular forces. In addition the close proximity of other atoms on molecules can influence distant collisions. This can affect direct energy losses and could also affect the equilibrium charge on the incident particle as mentioned previously in the section on charge exchange.

Experimental measurements of the stopping cross sections for given atoms in different states of chemical combination and phase have been carried out. A number of measurements have been made with solids and vapours, and a few with liquids. There is still, however, some disagreement regarding the effect of phase upon the stopping power of particles. There is also some disagreement due to the effect of chemical binding upon stopping power. Bakker and Segre (1951) have suggested that the effect of chemical binding upon I is too small to affect the stopping power.

Experimental measurements by Palmer (1966) using alpha-particles over the energy range 1-8 Mev on gaseous hydrocarbon targets, indicated that the effect of chemical binding on the range of 8 Mev alpha-particle is negligible. Lodhi and Powers (1974) find additivity anomalies with double-bonded hydrocarbons and Bourland and Powers (1971) tested the additivity of atomic stopping cross sections for alpha-particles in a number of gaseous compounds and suggested that Bragg's rule can be applied to

the gaseous compounds with single and double bands, but with triple-bonded hydrocarbons at energies below 2 Mev they obtained deviations as great as 12.8%.

Baglin and Ziegler (1973) have measured the energy loss of $^{+}$He ions up to 2 Mev in a number of elements and in their solid compounds like RhSi, H_fSi, SiO_2, Al_2O_3, Si_3N_4, AlN, W_2N_3 and for melamine and adenine. They had good agreement with Bragg's rule, and they did not find any deviation from the additivity rule for triple-bonded solid targets.

Zeiss et al (1977) calculated atomic and molecular stopping powers for a number of gases by calculating excitation energies from oscillator strength distributions for gaseous atoms and molecules. They found that, for all atoms except those involving the hydrogen atom, the errors in using the additivity rules would be less than 1.5% at 0.5 Mev per amu for the incident particle, but for hydrogen atoms the error is estimated to be 6% at this energy. They expect deviations from the additivity rule in condensed phases.

Chau and Powers (1978) measured the molecular stopping cross section of aldehydes and ketones and hence calculated the atomic stopping cross section of oxygen in double-bonded and three-membered ring-structure C-H-O compounds. They also measured stopping cross-sections in a straight-chain single band, for 0.3 to 2.0 Mev He^{+} ions. In contrast to Baglin and Ziegler (1973), they found that the stopping cross section for oxygen in a double-bonded structure is 6-17% greater than that in a three membered ring structure, and the stopping cross section in a three

membered ring structure is 3.1-10.4% greater than that in the single bond, for energies less than 0.7 Mev.

Palmer and Simons (1959) observed the stopping cross section for alpha-particles to be less in the liquid than in the vapour state for H_2O and certain organic compounds.

Williamson and Watt (1972) measured the stopping power of alpha-particles in hydrocarbon compounds in the gaseous and solid state. They found that the stopping cross section in the condensed state was lower than that for the corresponding gaseous state. They suggested that these differences are completely due to charge exchange effects. Palmer (1961) has measured the stopping power of ethyl alcohol and carbontetrachloride in liquid and vapour states for 2-8 Mev alpa-particles. She found that the molecular stopping power for both liquids was lower than that of the corresponding vapour especially at lower energies, and in (1973) has measured the stopping power of carbon tetrachloride and several hydrocarbon liquids for 1-8 Mev alpha-particles. Comparing the molecular stopping power of alpha-particles in these liquids for different energies with that for corresponding vapours, she found that the stopping power for liquid hydrocarbons were lower than those of the corresponding vapours at lower energies. She suggested that these differences are caused by different charge exchange effects in the liquids and vapours, and polarization of the absorbing liquid medium by low velocity alpha-particles. Bichsel (1974) suggested that the stopping power of condensed media is lower than that of the corresponding gases because the condensed phase leads to a modified energy state of the outer electrons and an increased value of I. Matteson,

Power and Chau (1977), measuring the stopping cross section of H_2O ice and vapour for 0.3-2.0 Mev alpha-particles found that the stopping cross section of H_2O vapour was 4-12% higher than that of H_2O ice. Their results indicated that a physical-state effect does indeed exist in the stopping cross-section of H_2O for alpha-particles and they suggested this is due to charge-exchange effects. Thwaites and Watt (1978) suggested that this deviation is largely due to changes in electronic excitation levels when the phase is changed.

Feng, Chu and Nicolet (1974), measuring the stopping power of 1-2 Mev alpha-particles in five solid oxides, found no observable chemical effect in the stopping power of alpha-particles by these solid oxides. However they have observed that the stopping cross section of oxygen in a solid metal oxide for alpha-particles less than 2 Mev is 6-22% lower than that of gaseous diatomic oxygen. They suggested that the differences in the stopping cross section of oxygen between the two forms was due to a physical state effect.

Further measurements of the stopping powers of liquids and solids for alpha-particles which show deviations from calculated values and from the stopping power in the vapour phase at the identical velocities are as follows. Palmer (1966, 1973,Liquid and Vapour), Williamson and Watt (1972,Solid and Vapour), Venkataraman et al (1975, Solid and Vapour) Burgess (1975, Solid, Liquid and Vapour), Palmer and Akhavan-Rezayat (1978, Liquid and Vapour).

Whillock and Edwards (1978) by measuring the experimental stopping cross section of ethylene and polyethylene in solid and gaseous states

using 1.5–4.2 Mev alpha-particles, found no differences in stopping cross section between the two set of values. Chu et al (1978) have measured the energy loss of 0.5–2.0 Mev ^{4}He ions in argon, oxygen and CO_2 in the solid phase, they compared their result of stopping cross-sections with corresponding gaseous-target values in the literature. They concluded that, at energies above 1 Mev, the stopping cross section data agree with the corresponding gaseous-target values, and at lower energies the solid-target data were 5–10% lower than for the gaseous phase.

2. Experimental Procedure

2.1 Nature of investigations

As may be seen in the previous section, extensive measurements of stopping power of organic vapours and solids, and a number of liquids for charged particles have been performed.

Accurate stopping power values are available for protons and alpha-particles in certain solids and gases especially at fairly high energies, but there are few accurate values available for liquids and vapours. Calculations, particularly at low energies are not reliable and the effect of chemical binding and phase upon the molecular stopping power, especially at low energies, is uncertain. The measurements reported here have been made in order to provide more data concerned with the liquid phase, and, by comparing with the vapour phase, to indicate any phase dependance of the stopping power.

The materials which were selected for this investigation are shown in table 2.1.

These materials have been chosen because their boiling points made it possible to investigate the penetration of alpha-particles in both liquid and vapour states at or near room temperature. Also they included adjacent members of homologous series, enabling comparisons of the effect of chemical groups to be made. They were also available in a high state of purity.

	Chemical formula	Melting point (^{o}C)	Boiling point (^{o}C)	Density g/cm^{3}	Molecular weight	Purity
Oxygen	O_2				15.9994	99.6%
Water	H_2O			0.9977	18.0153	
Methyl alcohol	CH_3OH	-97.8	64.96	0.9714	32.0424	99.86%
Ethyl alcohol	C_2H_5OH	-117.3	78.50	0.7893	46.0695	99.56%
Propyl alcohol	$(CH_3)_2CHOH$	-127	97.10	0.7796	60.0966	99.80%
Dichloromethane	CH_2Cl_2	-97	40.10	1.3350	84.933	99.95%
Trichloromethane (Chloroform)	$CHCl_3$	-63.5	61.20	1.4916	119.378	99.95%
Carbontetrachloride	CCl_4	-22.95	76.75	1.5942	153.823	99.95%

Table 2.1 The properties of organic materials (Purities as stated by manufacturers).

2.2 General techniques

Two separate types of alpha-emitting source were used for the stopping power measurement: ^{212}Bi which has a double alpha-emission with energies of 8.78 Mev and 6.05 Mev and also emits beta particles which cause a noise signal in the detector especially at energies below 1 Mev. The ^{212}Bi source was electrostatically deposited which gave a very thin source so that straggling effects due to self absorption in it were negligible.

^{241}Am has been used to cover the lower part of the energy range from 0.25 Mev to 5.48 Mev, and has the advantage that there is no beta emission in this source and hence less noise.

The residual energies of alpha particles have been measured after the particles passed through a known path in vapour or liquid. Pulses produced by alpha particles in the detector were fed via a Tennelec 100B charge-sensitive preamplifier and Harwell 2000 Series main amplifier into a 400 channel Laben pulse height analyser, as shown in Fig. 2.1.

The residual energies of alpha-particles in various liquids and vapours were measured by means of a lithium drifted silicon detector with sensitive area of 3.14 cm^2.

The advantages of solid state detectors as compared with the scintillation detectors are as follows: (a) the energy resolution is better, (b) the charge pulse produced is linearly dependent upon the energy deposited in the sensitive volume of the detector.

There is a thin dead layer on the surface of a semiconductor

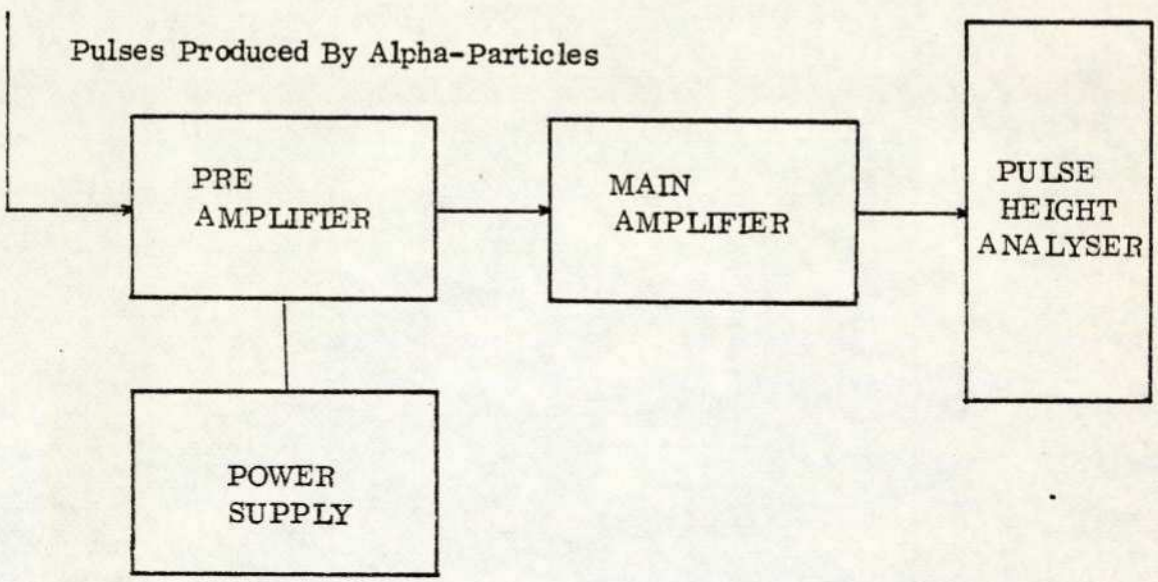

Fig 2.1. Block diagram of electronic system.

detector but correction was made for this as follows:

The range of alpha-particles in air was found for both ^{212}Bi and ^{241}Am sources by the method described in section 2.3, and the result was compared with the established range-energy curve (Segre, 1953). The difference between the apparent range of particles from each source and that of the corresponding established range represented the amount of energy loss in the detector's dead layer. The energy loss in the window thickness was found to be 0.06 ± 0.02 Mev at 8.78 Mev. This represents up to 0.12 Mev at very low energy.

The ratio of the stopping power of silicon to that of any organic liquid or vapour at any particlar energy was assumed to be approximately constant, over the whole energy range 0.5 to 8.50 Mev. Hence the stopping effect of the window in the detector could be assumed to be equivalent to that of a liquid or vapour layer, the thickness of which would be the same for all energies. The layer thickness could be approximately evaluated and was found to be of the order of 1 μm for the liquids and correspondingly more in vapours at any given pressure. Any error in this evaluation would contribute to the error in the total range but would have negligible effect on the stopping power value. $\frac{dE}{dx}$.

The back bias on the detector was adjusted so that the noise level was a minimum consistent with the particles being completely stopped in the depletion layer thus giving a maximum signal to noise ratio. The bias voltage used was 90 V. The linear ity of the detection system has been checked by means of a pulse generator. There was a slight deviation

from linearity of the pulse height analyser at upper levels for which correction was made where applicable.

2.3 Experimental arrangement for the vapour measurements.

For the vapour measurements, the experimental arrangement of the apparatus is shown in Fig. 2.2.

The cylindrical gas chamber, 0.54 m long, was supported with its axis horizontal. The detector was mounted at one end and the source was attached to the end of a horizontal rod which could be adjusted in position so that the alpha particles emitted from it passed through a known path length of the gas to be studied, and their residual energy could be measured in the detector.

The minimum distance between the detector and source was 20 cm in the case of the ^{241}Am source and 40 cm in the case of the ^{212}Bi source, thus ensuring that the maximum variation in path length of the particles due to the finite size of the source and detector was 0.2 - 0.3% for ^{241}Am and 0.05 - 0.06% for ^{212}Bi.

The vacuum system could be evacuated to less than 0.01 mm.Hg and could be used at any pressure up to atomspheric.

At the lowest pressure, the rate of outgassing into the chamber was negligible.

A mercury manometer was used to measure the gas pressure. Before beginning the measurements, the chamber was flushed with each of the vapours many times.

Readings were estimated to an accuracy of $\pm$ 0.02 to $\pm$ 0.04 mm (depending upon pressure and temperature conditions) by means of a cathetometer.

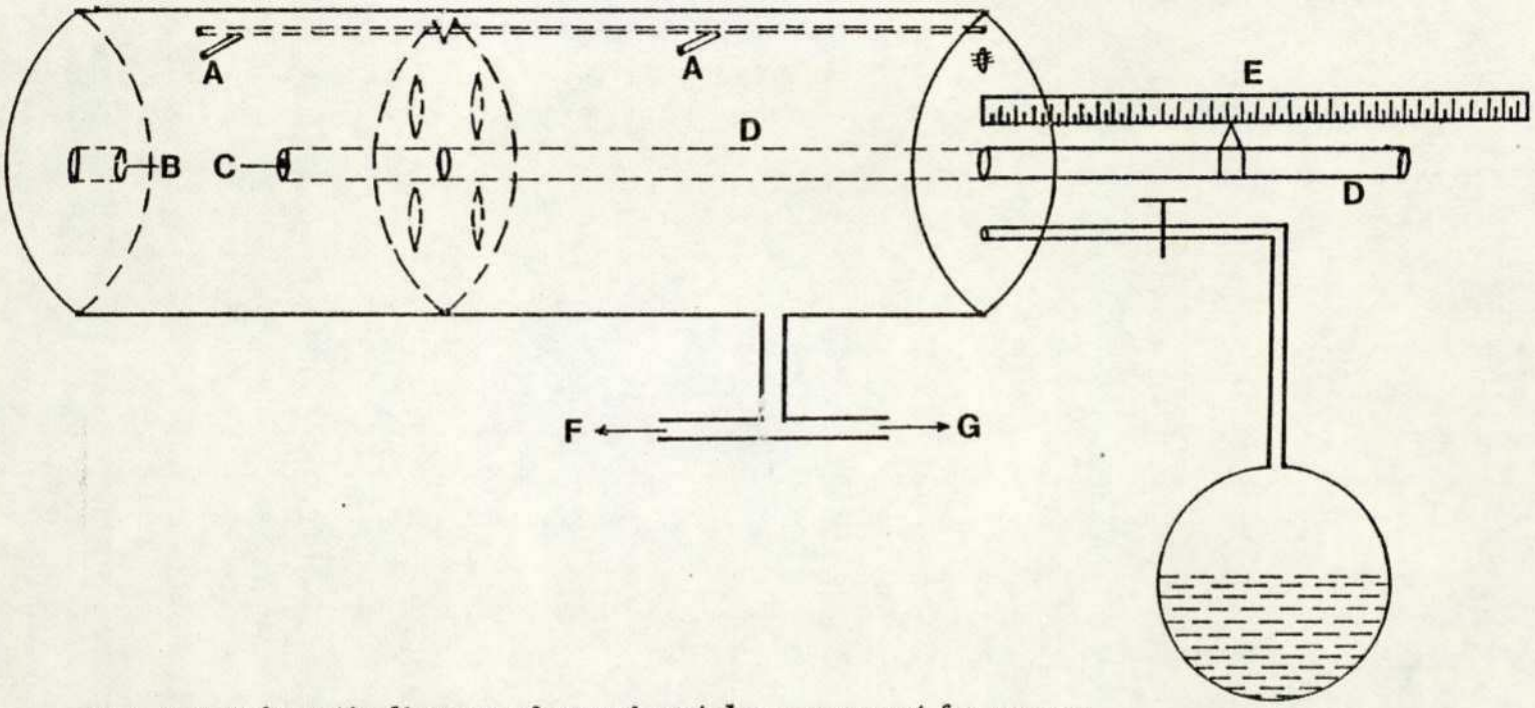

Fig. 2.2 Schematic diagram of experimental arrangement for vapour

A = Thermistor thermometers

B = Detector

C = Source

D = Adjustment rod

E = Steel rule

F = Vacuum pump

G = Mercury manometer

The temperature of the chamber was measured by means of two thermistors in order to determine the vapour density.

The distance from the source to the detector was determined to within $\pm$ 0.2 mm by means of a steel rule.

The cylinder was initially evacuated and the pulse height corresponding to the maximum energy of alpha-particles was noted, vapour at various pressures was then introduced and the pulse heights corresponding to the reduced energies of the alpha-particles were measured.

The chamber could be heated slightly but the detector could not be operated at a temperature above 30°C.

Because of its low saturation vapour pressure, water presented a problem. This was overcome by the use of thin aluminium foils of uniform thickness varying from 3 to 42 μm, which enabled the alpha-particle energy to be reduced by convenient increments, so that the whole energy range from 8.78 Mev to about the relevant noise level could be investigated. Assuming that the energy loss is a function of the product of vapour pressure and path length traversed, each stopping pressure corresponding to a fixed path could be replaced by an equivalent path at a common pressure and temperature of 3 cm of mercury and 15° centigrade respectively, and hence a range-energy relation for these conditions was deduced.

The residual energy of the alpha-particles after passing through a known length of liquid or vapour was measured by the energy corresponding to the maximum of the peak displayed by the pulse height analyser. Under optimum conditions i.e. with no vapour in the apparatus and with the detector bias adjusted to give the best signal to noise ratio the spectral peak was

symmetrical and the spectral width was approximately 100 kev (f.w.h.m). When the alpha-particles were reduced to low energies the spectral spread increased to approximately 200 kev below 2 Mev and there was some assymetry in the form of a low energy tail. A comparison was made between the energy corresponding to the peak maximum and to the average energy of pulses in several typical spectra. It was found that the average values were about 20 kev lower than the peak value for energies between 1 and 2 Mev, which was less than the uncertainty in individual peak measurements at these low energies. Therefore, peak values were used in all cases.

2.4 Experimental arrangement for the liquid measurements.

A new technique (method I) has been devised for measuring the residual alpha-particle energy after the particles have traversed a known path in liquid, the experimental arrangement for this being shown in Fig. 2.3. The source was coated on a source holder consisting of a flat surface with a number of annular steps as shown in Fig. 2.4. This was to be placed on a flat collimator covered with a thin film in such a way that a liquid drop could be trapped between the upper surface of the collimator and the source. Particles from the source could thus traverse different path lengths through the liquid and only those travelling in a direction normal to the collimator surface could pass through to the detector on which the collimator was positioned. Due to the steps in the source holder discrete path lengths would be traversed by the particles in the liquid.

Several methods of preparing the source holder were attempted. The precision required was too demanding for mechanical cutting of the steps, since the depth of step required varied from 1 μ m up to 10 μ m. An electroplating method was attempted. The best results were obtained with the following conditions:

Plating Solution

$Cu\ So_4,\ 5\ H_2O$	60g./l
Na CN	41g./l
$Na_2\ CO_3$	25g./l

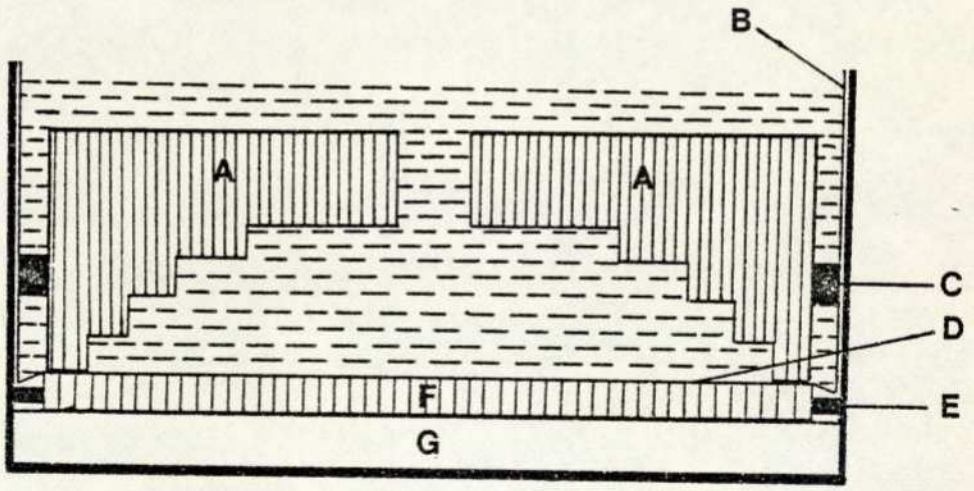

Fig. 2.3 Schematic diagram of experimental arrangement for liquid method I (not to scale)

A = Source holder

B = Cylindrical brass tube (film holder)

C = A brass ring to keep the source holder in a central position.

D = Film

E = A ring to keep the collimator in a central position.

F = Collimator

G = Semiconductor detector

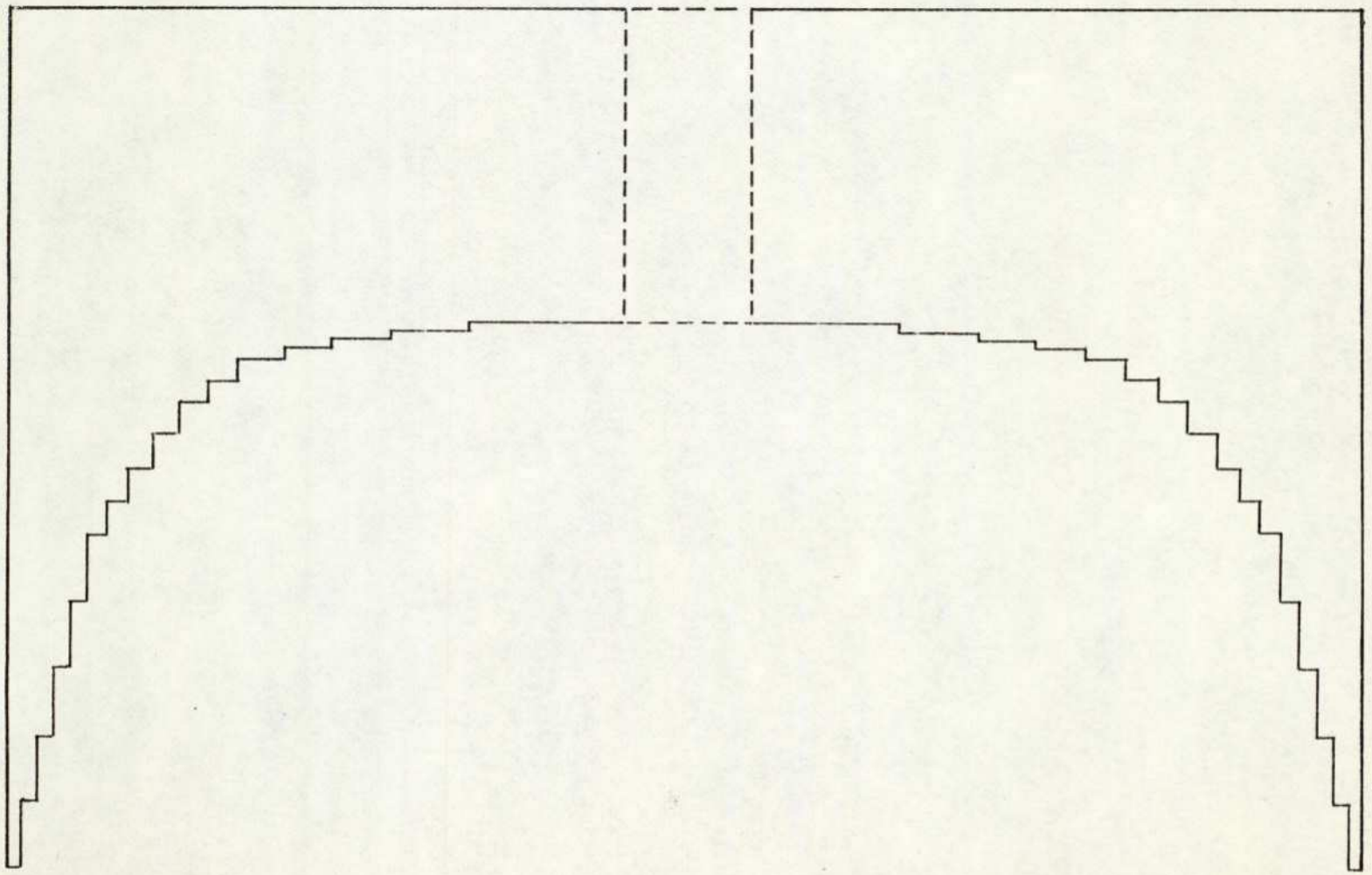

Fig. 2.4 Schematic diagram of source holder consisting of a flat surface with fifteen annular steps.

Na OH	3 g./l
Rachellesalt	37 g./l
Temperature	60°C
Current density	15 mA/cm^2

The specimen source holder was mounted on a rotatable cathode in the electroplating solution. A very thin nylon screen was inserted between the copper anode and the cathode to prevent impurities reaching the cathode.

In order to make a flat, homogeneous surface with sharp edges, conditions were varied as follows: current between 5 and 30 mA, temperature between 60 and 90°C, rotation rate between 90 and 120 r.p.m. The best results were obtained by a current of 15 mA through the solution at 60°C with a rotation rate of 90 r.p.m. This plated 2 μm on the surface in 30 minutes. With this method steps of thickness up to 2 microns were found to be satisfactory, the surface of the plating being very flat and homogeneous, but at greater thicknesses the surface became irregular.

An evaporation technique was tried and found to produce superior results, although the step thickness obtained was still limited by practical considerations i.e. mainly expense and time available.

2.4.1. Preparation and plating of substrates.

The vacuum system used was based on an oil diffusion system with a rotary backing pump. A thermoelectric cold trap was mounted between the diffusion pump and evaporation chamber to prevent backstreaming vapour and its subsequent deposition on to the substrates.

The ultimate pressure which could be reached by this system was

of the order of 2×10^{-5} torr after about one hour. Over-heating of the substrate was avoided by supporting it on a brass heat sink and the apparatus was cooled in general by a water-cooling system mounted on the evaporation chamber.

Pure aluminium was chosen for evaporating on to a silver steel disc. The factors governing the selection of this material were:

1 - The tolerance on residual pressure in the system for the metal being evaporated.

2 - The temperature to which the system was subjected.

3 - The cost of this material, and ease of obtaining it.

4 - The ease of obtaining a uniform evaporated coating which was chemically stable, and produced a good surface.

During a trial run a molybdenum boat was used to evaporate some aluminium onto a substrate. It was found that the aluminium reacted with the molybdenum, causing pitting and holing and thus loss of evaporant.

Boats of thicker molybdenum were tried but without success. As it was required to evaporate larger amounts of aluminium a small carbon crucible indirectly heated by electron bombardment was tried but again the problem of perforation was encountered. Finally, a large tungsten filament was used and this, although still attacked by the molten aluminium, lasted long enough to enable a fair amount of plating to be achieved.

The amount of evaporant which could be accommodated by the filament was generally insufficient to deposit all but the thinnest layer i.e. $< 1\ \mu m$ so the need arose to provide some means of feeding a quantity of aluminium on to the filament during plating.

Several methods were tried but the most successful was achieved by using an externally controlled sealed rotary arm, to raise and lower a rod from which several pieces of 18 s wg pure aluminium wire were suspended. (The apparatus assemblies are shown in photograph 2.1 and 2.2). When the wire came into contact with the heated filament evaporation resulted and in this manner quite large deposits could be obtained, without having continually to open and shut the evaporation chamber. This resulted in much purer films as well as a great saving in time.

The maximum thickness which could be obtained per run was governed by two factors; first, the amount of alumium wire which could be loaded on to the carrier and second, the ability of the filament to resist attack by the molten aluminium. Generally the first was the limiting factor and this restricted the maximum amount of evaporant laid down to about 5 microns in one operation. During plating, a quartz crystal monitor was used to estimate the thickness of the deposition. This was calibrated by mounting suitably prepared microscope slides inside the evaporation chamber and evaporating onto them. The distance between the filament and substrates was 24 cm. One half of each slide was masked so that no deposition could occur on it. This was used as the reference surface and enabled the thickness of the plated metal to be determined.

The thickness of the deposit on the slides was determined by using several methods in turn i.e. mechanical, by using a talystep, and optical, using both interference and optical focusing techniques. One of the simplest methods of measuring the thickness of evaporated film is to weigh the substrate before and after deposition. The thickness of the film is then

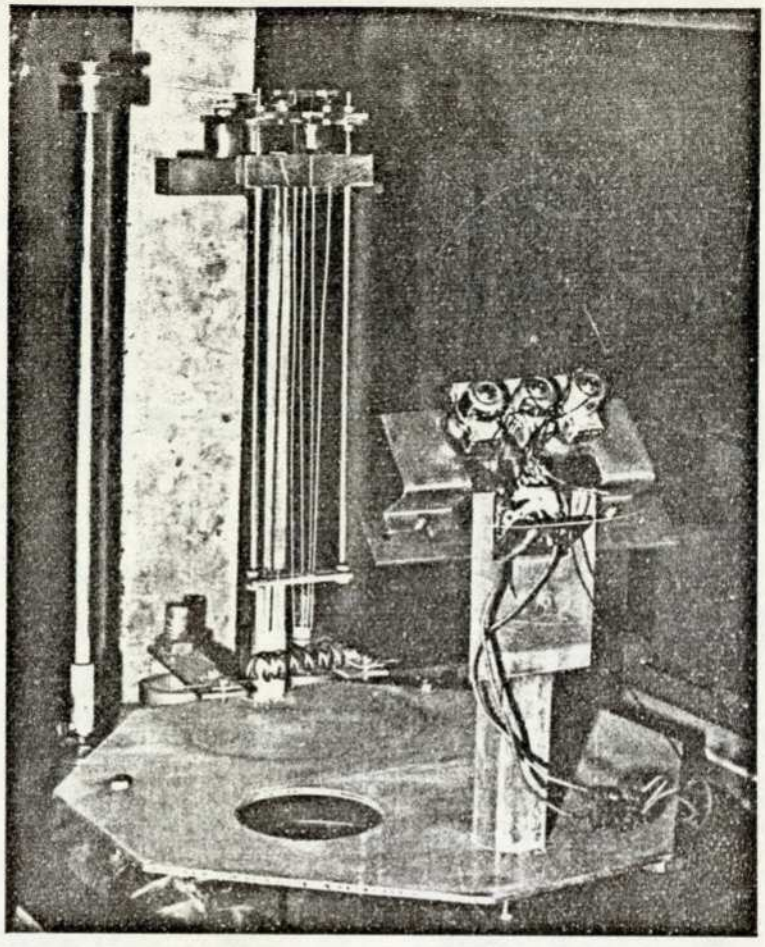

Photograph 2.1

Apparatus assemblies for preparation and

Plating of Substrates.

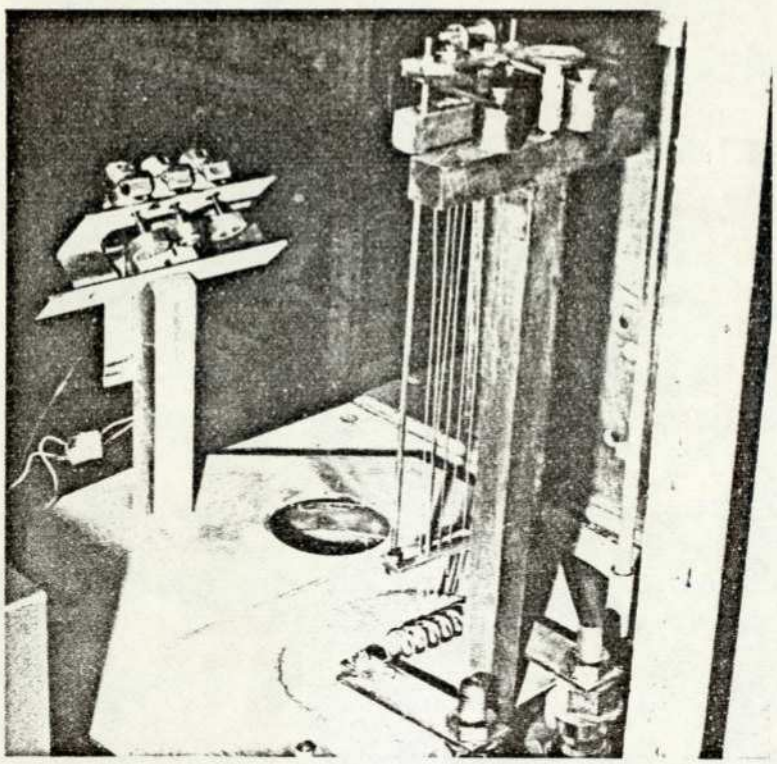

Photograph 2.2

Apparatus assemblies for preparation and

Plating of Substrates.

determined from the equation, $t = m/s.\rho$

where t is the thickness, m is the increase in mass of the substrate, s is the area of the substrate and ρ is the density of aluminium. These methods gave very good agreement. The mechanical method by using a Talystep was preferred, the overall accuracy of this method, including the calibration accuracy of the instrument and repeatability of the step measurements being usually less than $\pm 2\%$ and in all cases less than $\pm 4\%$ for thickness measurements between 1 μm and 10 μm. For calibration of the monitor as shown in graph 2.1, the frequency of oscillation of the crystal loaded by the aluminium deposit is plotted against the thickness of the deposit as measured by means of the Talystep which is used as a standard.

Each substrate was made from a silver steel disc of approx. 2 cm diameter and 5 mm thickness, in the centre of which a 2 mm diameter hole was bored. One face of each substrate was surface ground using a very fine wheel and then lapped down to a $\frac{1}{4}$ μm finish. After preparation the substrates were thoroughly cleaned in trichloroethylene by ultrasonic agitation and then they were placed in a vacuum chamber and cleaned by ionic bombardment for about 20 minutes before being placed in the plating apparatus.

Building up a stepped surface on the substrates was accomplished by preparing a number of aluminium masks of various diameters, each having a central 2 mm hole which enabled it to be attached to the steel substrate as required.

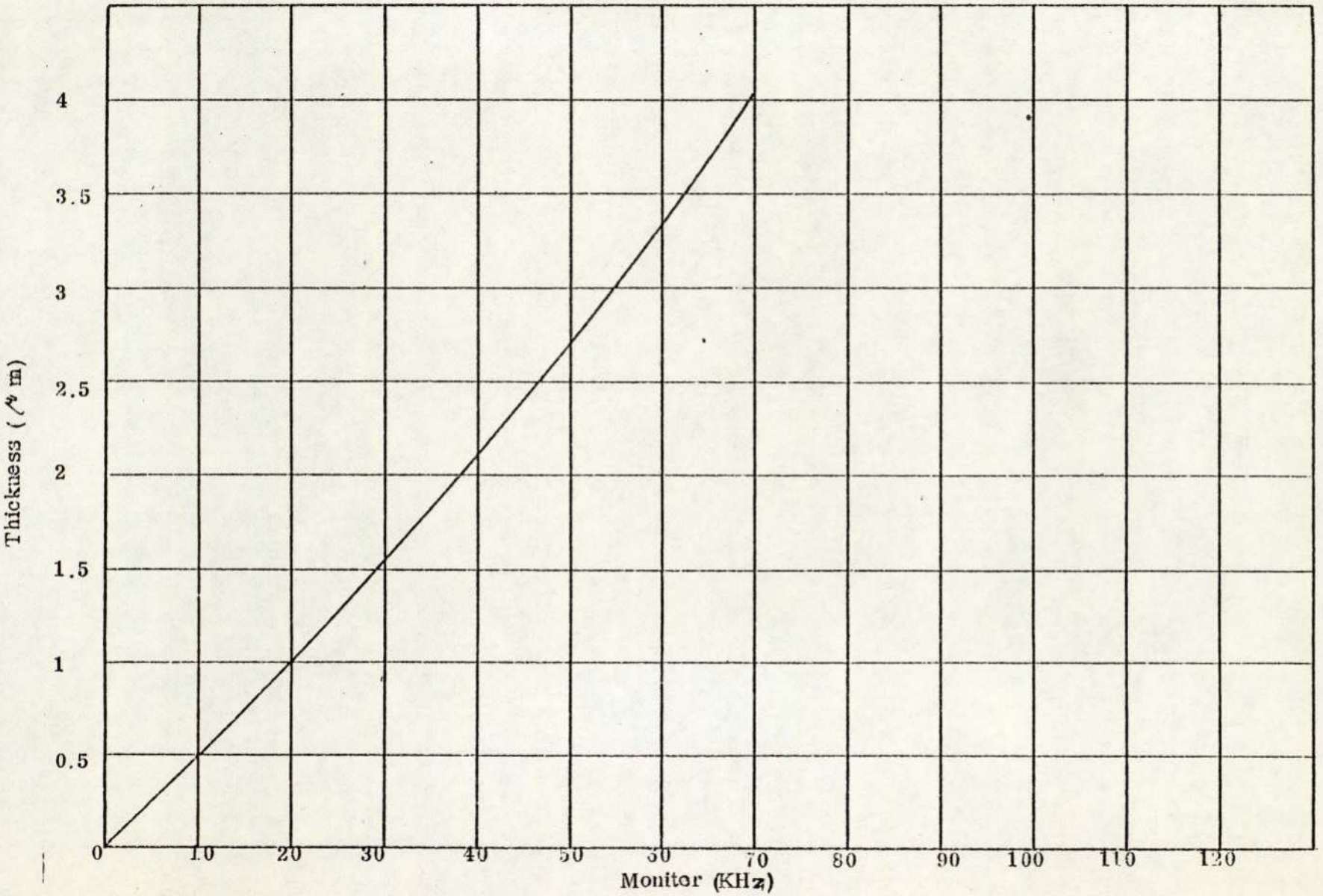

Graph 2.1. Calibration of monitor.

One problem which arose was the difficulty in obtaining a perfectly flat deposit on the substrate simply by mounting it in a fixed jig, due to the geometrical disposition of the hot source and the substrate. A variation in thickness of the deposit over the substrate was avoided by rotating it during deposition. For this purpose three small electric motors were mounted in the vacuum system and arranged so that the substrates could be individually fixed on to the shafts facing the filament, when coating was started the substrates were rotated at a steady rate of approximately 120 r.p.m. until the desired thickness was obtained. By this means quite flat coatings were achieved.

Initially fifteen steps were prepared on the substrates as indicated below.

Step	Outer Diameter of annulus (mm)	Area of annulus (mm^2)	Height of Step (μm)
1st	20.00	14.29	10
2nd	19.54	14.55	10
3rd	19.06	15.36	10
4th	18.54	15.49	10
5th	18.00	15.31	10
6th	17.45	17.48	5
7th	16.80	18.09	5
8th	16.10	19.73	5
9th	15.30	20.54	5
10th	14.42	21.87	3
11th	13.43	26.67	3
12th	12.10	26.74	2
13th	10.60	26.73	1
14th	8.85	28.33	1
15th	6.50	30.04	1

When a deposit of ^{212}Bi was formed on this surface it was "sealed" by flashing it with a very thin evaporated layer of aluminium (less than 0.1 μm). Any loss in energy in this layer was so small that it could

not be detected as a shift in the peak energy, when the source was placed on the detector surface.

With a liquid drop trapped between the source and detector it was hoped that a series of at least fifteen peaks would be observed, possibly with complications due to the lower energy components from the ^{212}Bi (6.05 Mev initial energy). Some problems were introduced due to the presence of air bubbles, but with care these could be overcome. However, the resolution obtainable for the individual peaks was limited to an extent which made neighbouring peaks overlap and the results were very difficult to interpret.

It was therefore decided to limit the number of steps used on a single substrate and the optimum number for the size of detector used was about 4 or 5.

The most satisfactory source-holder prepared was of the dimensions given below:

Step	Outer Diameter of annulus (mm)	Area of annulus (mm^2)
1st	20.00	54.00
2nd	18.20	54.04
3rd	16.20	62.98
4th	13.50	64.60
5th	10.00	75.40

Three different substrates were actually used. The heights of steps on each substrate were as follows:

1st) 1,1, 2, 3 μm. 2nd) 3,4,5,5, μ m. 3rd) 8,8,10,10 μm.

The collimator of thickness 2.4 mm and 21 mm in diameter and with holes of diameter 0.35 mm was positioned on the lithium drifted silicon detector.

The surface of the collimator was originally prepared to give a flat $\frac{1}{4}$ μm surface finish and a cylindrical brass tube which was covered at one end with 1 to 2 μm thickness polymer film (Polyethylene Terephthalate) was positioned on the collimator, and the liquid was placed on the upper surface of the film, so that the film prevented liquid from penetrating into the collimator. The stepped source holder previously activated was then centrally positioned on the collimator. After passing through the liquid the alpha-particles passed through the film of previously determined stopping power and then through 2.4 mm of air (due to the collimator). There was a further energy loss in the 'window' of the detector before the residual energy was deposited and measured in the detector.

The energy losses on leaving the liquid are estimated as follows:

1. Energy loss in 2.4 mm of air is about 0.145 Mev at 8.78 Mev alpha-particle energy.
2. Energy loss in the 1-2 μm film was at most 0.125 Mev at 8.78 Mev alpha-particle energy.
3. The energy loss in the dead layer of the detector was about 0.06 Mev at 8.78 Mev alpha-particle energy.

However, the relevant energy loss in the film, air and silicon surface is that which would take place, not at 8.78 Mev but at the energy of entry of the particles into the silicon. The correction for this is made as follows:

Energy loss at maximum alpha-particle energy 8.78 Mev is:

$$\Delta E = 0.145 + 0.123 + 0.06 = 0.330 \text{ Mev}$$

Energy loss at any other level of energy E_i is:

$$\Delta E_1 = \Delta E \frac{\left(\frac{dE}{dX}\right)_{air} \text{ at } E_i}{\left(\frac{dE}{dX}\right)_{air} \text{ at 8.78 Mev}}$$

Graph 2.2. Energy losses in air, film and detector window as a function of residual alpha-particle energy.

The differential stopping power of air for alpha-particles between 0.25 and 8.78 Mev has been found by using the range - energy curve previously quoted. The energy loss ΔE_i is shown in graph 2.2. From this graph the appropriate correction at any energy E could easily be deduced, and this was added to each residual energy measurement.

In order to test this system for accuracy and reproducibility of results separate experiments have been performed using a 2 cm diameter flat silver steel disc, prepared and polished as previously described with a 2mm diameter hole in the center.

This disc was used as a ^{212}Bi source prepared by electrostatic deposition as before. For these measurements, two pieces of melinex foil of thickness uniform to within ±2% were inserted under the disc, as shown in Fig (2.5). The distance between source and collimator surface could be changed by using foils of different known thickness. The foils were positioned on the film and the flat source was placed on the foils, the residual energies of alpha-particles being measured after they had passed through a thickness of the liquid equal to that of the foils. The results of these measurements were found to be reproducible to within the expected accuracy of the assessment of the liquid layer.

An unexpected difficulty arose in this method due to the problem associated with cutting a small piece of melinex so that the uniformity in thickness was maintained at the cut edge. Careful cutting by means of a sharp razor or by several different form of guillotine did not produce the required degree of uniformity, giving increased edge thickness of up to 25% in some cases, and being generally unreliable.

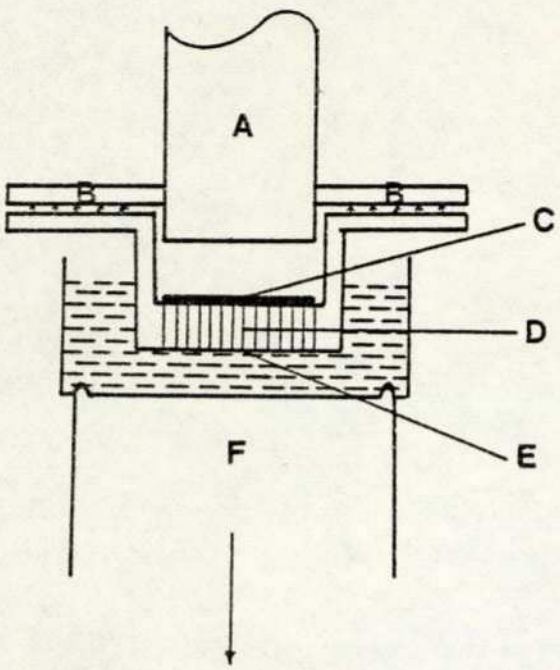

Fig. 2.6 Schematic diagram of experimental arrangement for liquid (method II).

A = Micrometer shaft

B = Steel magnet

C = Alpha-particle source

D = Collimator

E = Melinex film

F = A lithium-drifted silicon detector

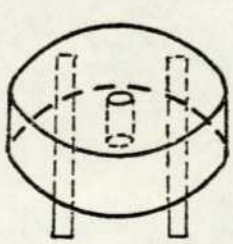

Fig. 2.5 Schematic diagram of experimental arrangements for testing reproducibility of measurements in method I.

Satisfactory results were in fact produced using a pair of very sharp scissors. These in fact gave an edge which was about 10% thinner than the main part of the foil, but this was acceptable for the use intended.

The thickness of the foils was measured by means of a dial comparator thickness gauge. The consistency of the measurements was about 2% for foils of 15 μm thickness, improving to less than 1% for thicker foils up to 75 μm.

Before the foils were placed on the film the film and foils were carefully cleaned by pure methanol and were blown dry by dust-free compressed air. With care errors due to dust on the surface of the foils and film could be made negligible.

2.4.2 A second technique (method II) has been used to measure alpha-particle range energy relations in the liquid phase in order to have comparative measurements in the same liquids by different methods. This was similar to that described in papers by Palmer (1966, 1973) and Palmer and Akhavan-Rezayat (1978). This also enabled measurements to be extended to lower energies. The experimental arrangement is shown in Fig. 2.6. In this method two separate sources ^{212}Bi with 8.78 and 6.05 Mev energies and ^{241}Am with 5.48 Mev were used.

The ^{212}Bi source was deposited by electrostatic attraction on a flat steel disc. This was positioned on a collimator consisting of 0.35mm diameter holes drilled in brass, 2.6 mm thick.

The collimator was polished flat on its lower surface and was covered by a melinex film (polyethylene Terephthalate) or polypropylene film of 1 to 1.5 μm thickness.

The collimator was supported on a flat steel magnet holder and the holder was supported on the non-rotating shaft of a micrometer, so that

by adjusting the micrometer setting the distance between the source and detector could be changed whilst still retaining their parallel condition.

The micrometer was calibrated in 2μm divisionswith a vernier setting calibrated to $\frac{1}{5}$ μm.

The detector was fixed on the centre of a large base plate and this was supported on three ball bearings at points near its circumference. These could be raised or lowered by means of adjusting screws, giving a sensitive means of levelling the detector relative to the lower surface of the collimator.

The residual alpha-particle energies were measured after the particles had passed through a known path in liquid which could be noted on the micrometer.

However there were also small energy losses before and after the alpha-particles traversed the liquid, and allowance had to be made for these losses.

The energy loss in 2.6 mm of air in the collimator was 147 Kev for the 8.78 Mev alpha-particles, 218 Kev for the 6.05 Mev alpha-particles and 237 Kev for the 5.48 Mev Alpha-particles.

The melinex film was between 1 and 1.5μm in thickness and the energy loss in the film was measured before and after each experiment. It was found to be approximately 120 Kev in most cases. The energy loss in the detector's dead layer as it has been described before was 60 Kev at 8.78 Mev.

For an 8.78 Mev alpha-particle therefore the total energy losses consisted of a constant energy loss of approximately 270 Kev before entering the liquid and a smaller variable energy loss after the liquid which could be equated to the loss in a liquid layer of constant thickness as previously discussed.

The calibration of the pulse height analyser in terms of Mev per channel is therefore obtained by dividing 8.78 Mev by the maximum peak channel number.

2.5 Alpha-particle range measurement.

Because of statistical variations in individual energy transfers to atoms or electrons in the stopping medium, a group of particles of initially uniform velocity, after passage through a certain thickness of matter, will show a distribution of energies. Similarly, there would be a statistical fluctuation in the range of these particles. These fluctuation effects are known as "straggling". The average thickness of material which particles traverse is called the projected range, and the thickness of material at which one half of the particles in transmitted is called the median projected range.

Range measurements

With vapours, as in the stopping power measurements, the distance between the source and detector was kept constant, and the amount of absorber between the source and the detector was changed by changing the pressure inside the chamber.

The counting rate above a fixed noise level taken for various pressures is shown in graph 2.3. The bell shaped curve is obtained by taking the slopes of the range curve. This curve is known as the number-range curve, and its shape is Gaussian. R_o, indicates the mean range, where the counts decrease by half, and R is the extrapolated range, which is obtained by drawing the tangent to the curve at its inflection point and noting where the tangent crosses the pressure axis.

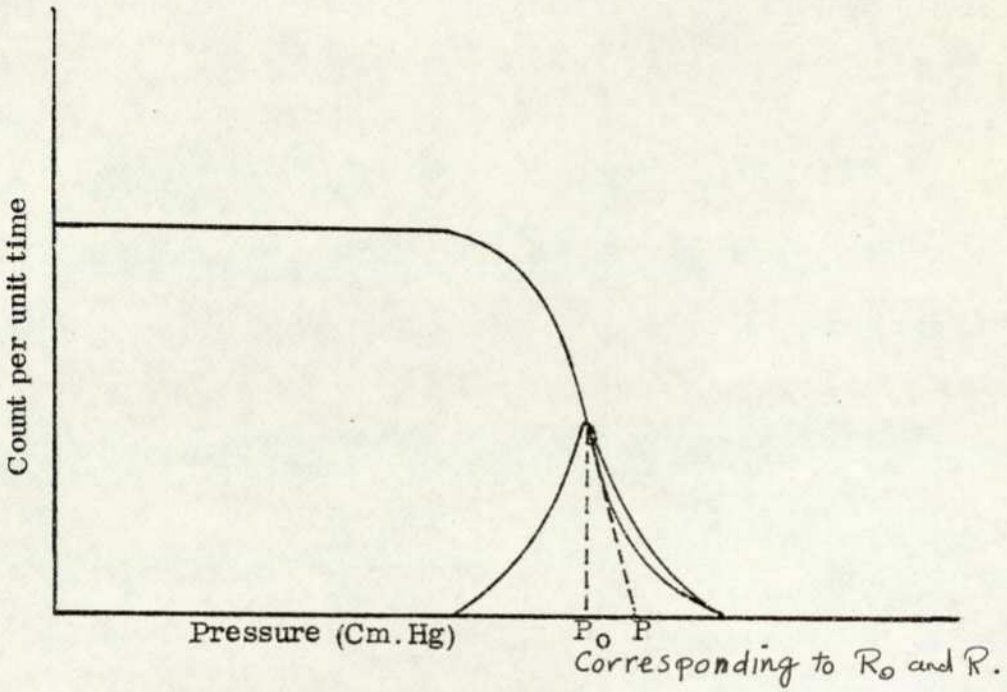

Graph 2.3. Alpha counts as a function of gas pressure. R_o, indicates the mean range and R is the extrapolated range.

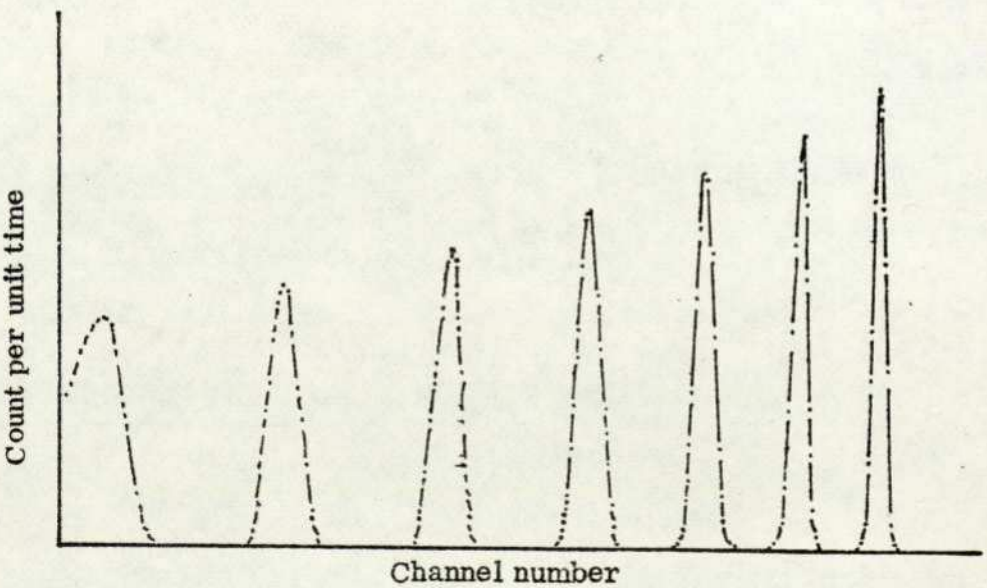

Graph 2.4. Several energy spectra of alpha-particles after traversing a known length of a vapour material at various gas pressure.

In an alternative approach, the residual alpha particle spectrum was observed on the multichannel analyzer as the pressure approached the stopping pressure. The alpha particle peaks became wider as the pressure in the chamber increased, and also, due to the increase in straggling, some assymetry in the peaks appeared in the form of a low energy tail before the peaks disappeared into the noise spectrum. Graph 2.4.

A typical spectral series was analysed, the energy corresponding to the maximum count in each peak being compared with the mean energy over the major part of the spectral peak. For energies above 2 Mev there was no significant difference between the peak and mean energies. Below 2 Mev, the average value was about 0.02 Mev lower than the peak. This difference is smaller than the expected errors in individual peak measurements; therefore peak values were used in all cases.

In order to obtain the effective range of the alpha particles, a curve was plotted of peak channel energy against pressure. This was then extrapolated down to the pressure axis as shown in graph 2.5., the extrapolation error being estimated at about 1.5%. The range $R_{p'}$ at any required pressure P' could then be found from the relation

$$R_{p'} = \frac{DP(273+15)}{P'(273+t)}$$

where D is the distance between the source and detector.

For some vapours it was necessary to use aluminium filters as previously described in order to stop the alpha particles, and due allowance was made for this.

The range of alpha particles in liquids was found in a similar way,

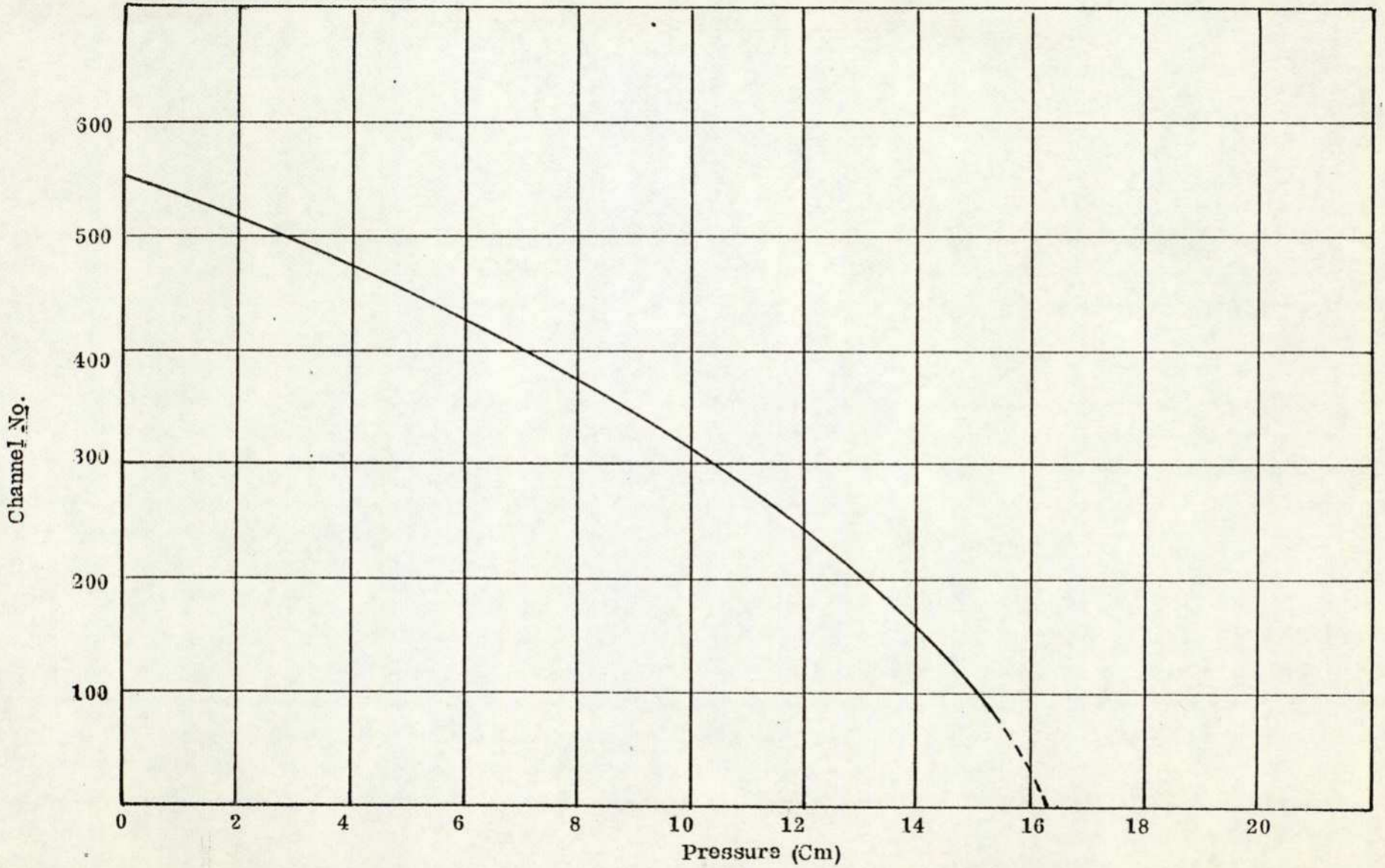

Graph 2.5. Channel No — Pressure curve for oxygen (Sample).

except that a range value was obtained by extrapolating the graph of channel peak against distance to intersect the distance axis. In this case a value had to be decided for the initial position of the source when the alpha particles reaching the detector were of maximum energy. Range measurements carried out with the same liquid but with different polymer film covering the collimator were always in agreement within $\pm$ 2%.

3. Treatment of results and assessment of errors.

3.1. For liquid and vapour measurements, as has been mentioned before, range values, R, were obtained corresponding to the complete stopping of the particles by extrapolation of the path length, x, to zero residual energy. Having the total range value, R, the range-energy relation was obtained by plotting (R-x) as a function of the corresponding residual energy values. To obtain reliable results, for each vapour measurement, at least ten separate sets of experimental values with both alpha-particle sources has been carried out. For each liquid measurement eight separate experiments were carried out using the method I, and using the method II eight separate experiments were carried out for each liquid using ^{212}Bi and five using ^{241}Am. To obtain the final range-energy relation and the stopping power, $\frac{dE}{dX}$, at various energies, range-energy data from separate experiments was analysed by computer and an estimate of reliability of the stopping power values was obtained by comparing the results at corresponding energies.

3.2. The possible sources of error.

Some of the most likely sources of error in the experimental measurement of stopping power are mentioned in the previous section, e.g. in the vapour measurements, errors in the gas pressure, gas temperature, and in the separation distance of the source and detector. In the liquid measurements errors in the assessment of the film and air absorption in the collimator, and in both cases linearity of the detection system, and end effects due to the detector window, noise, etc.

Considering the accuracy of the peak measurement in the residual energy spectra, the peak energy showed a standard deviation varying from $\pm$ 0.01 Mev at high energies to $\pm$ 0.05 Mev just above noise level.

An other very important point in the liquid measurements with both techniques which must be carefully considered is the distortion of the film across the collimator holes due to the presence of the liquid. This is shown in Fig (3.1), and it may be seen that the liquid path length can be increased in this way at the centre of the collimator holes especially if the film is rather slack across the collimator surface. This will give rise to a poor spectral shape, especially at low residual energies, and will also lead to an error in assessing the total range. Increasing the tension of the film decreased this effect.

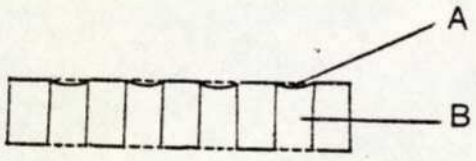

Fig 3.1. Schematic diagram of distortion of the film across the collimator holes.

A = Film
B = Collimator

3.3. Computing.

In order to obtain the final range-energy relation and the stopping power values, $\frac{dE}{dX}$, at specific energies, the experimental results were analysed by computer. Quadratic, cubic and quartic curves were fitted to the data, covering energy ranges of 3 Mev (e.g. from 0 to 3.0 Mev, 0.5 to 3.5 Mev, 1.0 to 4.0 Mev etc.), the overlapping regions of these computed curves were compared and found to be in good agreement. Graph 3.1 shows a typical result obtained.

The stopping power values were taken mainly from the quadratic curves except at the lowest and highest energies. The values of $\frac{dE}{dX}$ from the middle portions of the quadratic curves were found to be in good agreement at corresponding energies, and the stopping power values obtained in this way were noted at 0.25 Mev intervals between 1 and 8.5 Mev for all independent series of readings with each vapour and liquid wherever the experimental points justified this. A mean value of stopping power was then calculated for each energy and an estimate of reliability was obtained by comparing the results of different experimental runs at corresponding energies.

An alternative analysis was carried out in which the experimental points were fitted to a rising exponential of the forms

1) $E = (C_1 + C_3x)(1 - e^{-C_2x})$ Fit 1

2) $E = (C_1 + C_3x)(1 - C_4e^{-C_2x})$ Fit 2

3) $E = (C_1 + C_3x + C_5x^2)(1 - C_4e^{-C_2x})$ Fit 3

This was carried out using a package available from Mr. J. Snell of the Computer Science Division of the City University. This uses a

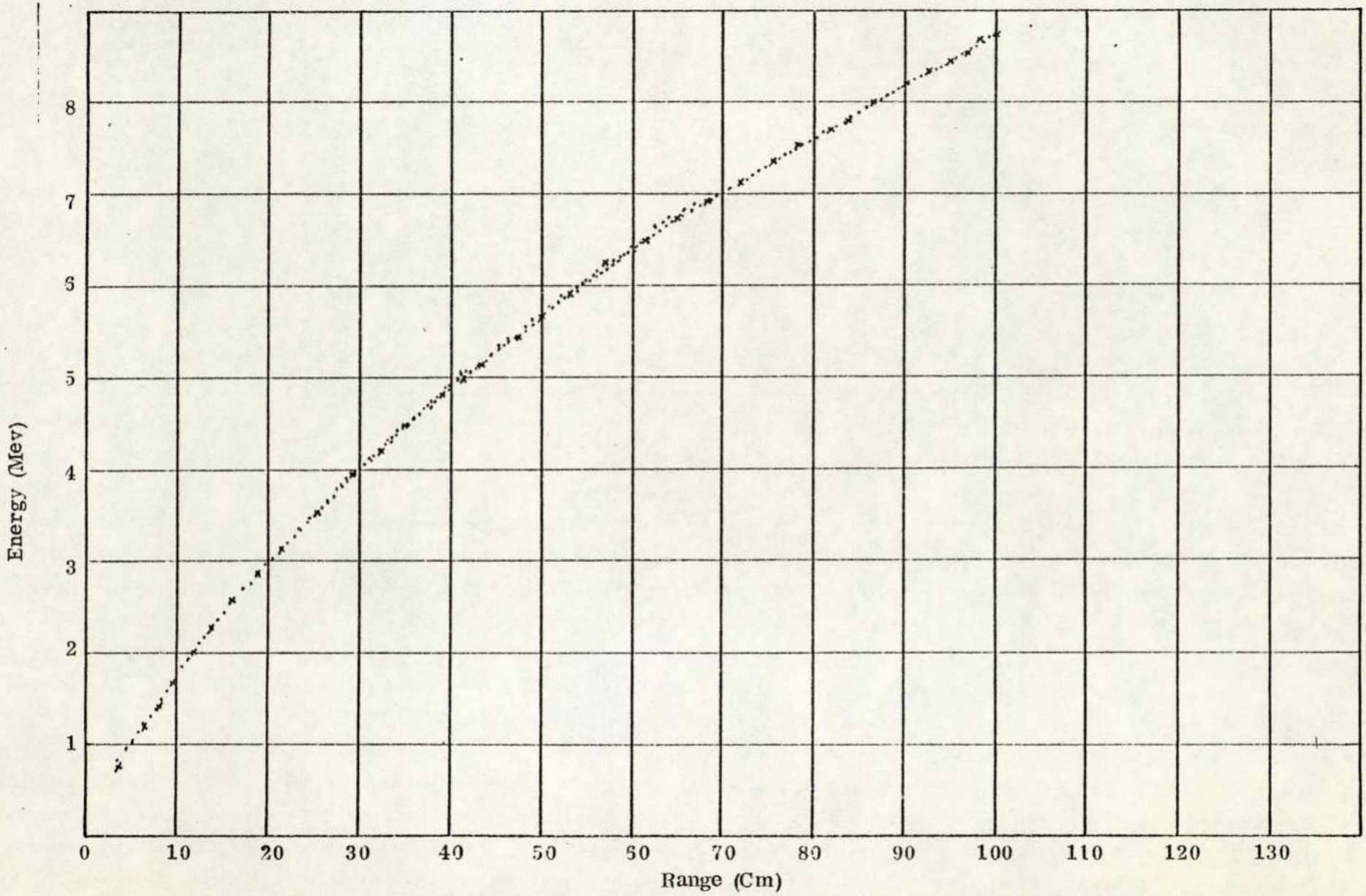

Graph 3.1. Comparison of experimental range-energy data (x) with points(•) obtained by least-squares computer fitting of quadratic curves to sections of experimental data.

least squares minimisation technique described by J. Walsh (1966).

The fitting was very sensitive to small differences in the experimental data. In some cases, Fit 1 was found to be a good fit, the sum of the squares of the deviations from the curve being very small. In other cases the values did not show a rapid convergence to a suitable curve and the programme terminated before the required fitting was achieved. Then the alternative Fit 2 or Fit 3 were tried with more successful results. The derivatives of the curves were obtained at energy intervals of 0.25 Mev as in the previous analysis. It was found that there was no significant difference between the results of these two separate methods of analysis, but the first method was more reliable and easier to apply.

The listings of the programs used to calculate $\frac{dE}{dX}$ with both methods can be viewed in appendix (I).

3.4. Total range value.

In method (II) a correction had to be made due to the fact that on average 0.27 Mev of energy was lost in the collimator and film before entering the liquid.

The point R_1 was determined by extrapolation of the experimental curve to the distance axis as discussed for the vapour measurements. Minimum readings of spectral peaks could be made down to about 0.35 Mev for ^{241}Am source and 1.25 Mev for ^{212}Bi source.

As discussed by Palmer (1973) the maximum energy value was obtained before the end of the collimator was in contact with the detector and this maximum was not as high as the peak obtained with no liquid present. It was assumed that a liquid layer was absorbed into the polymer film, possibly with some displacement of the film as discussed in section 3.2. The curve was extrapolated back to the channel corresponding to the maximum peak with no liquid in the apparatus in order to determine the effective zero distance as indicated in Graph 3.2.

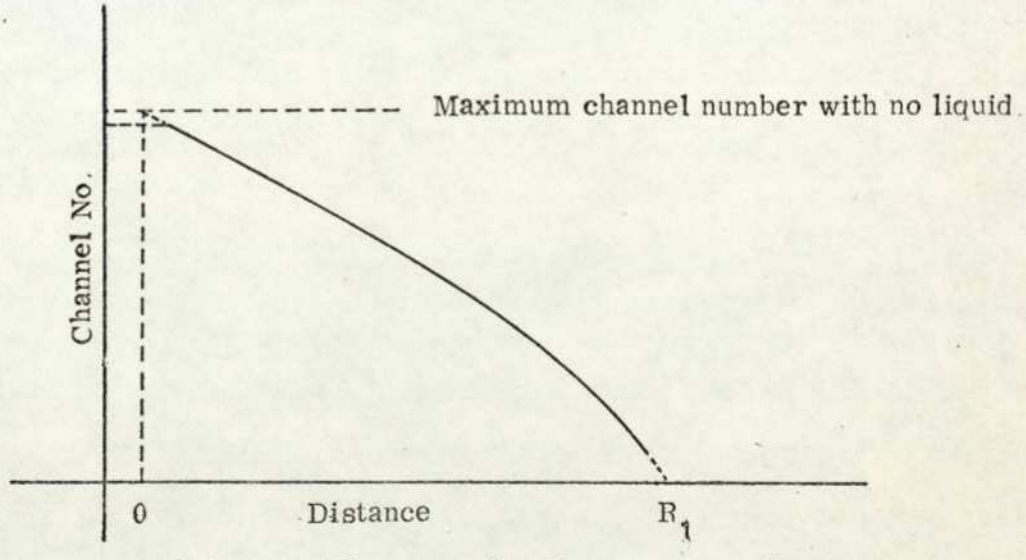

Graph 3.2. Total range value R_1, corresponding to the total average energy (8.78 - 0.27) Mev.

4. The results of experimental measurements with vapours and liquids

4.1 In this section all the stopping power data obtained from experimental work is presented e.g. range-energy relations, stopping power data . Also molecular stopping powers calculated from the uncorrected Bethe formula at various alpha-particle energies for all vapour and liquid (with both methods) materials separately are given. A critical appraisal of the stopping power measurements in vapour and liquid phases and also comparison of the present work with other workers results is deferred until the next section.

The values of I, mean ionisation and exitation potential used in these calculations were for hydrogen 19.2 ev, for oxygen 93 ev, for carbon 78 ev and for chlorine 175 ev.

In tables 4.1 - 4.2, range values are given for Oxygen, and Water, Methyl alcohol, Ethyl alcohol, Propyl alcohol, Dichloromethane, Trichloromethane and Carbontetrachloride all in vapour and liquid states at energies ranging 1 to 8 Mev. Vapour ranges for all compounds are corrected to 3 cm. Hg pressure and 15°C temperature. These values represent the mean results of all separate sets of vapour and liquid measurements in each vapour and liquid material.

Energy (Mev)	O_2	H_2O	CH_3OH	C_2H_5OH
1.00	10.0 ± 0.3	9.2 ± 0.3	6.5 ± 0.2	4.3 ± 0.1
1.25	13.0 ± 0.3	12.7 ± 0.3	8.3 ± 0.3	5.6 ± 0.1
1.50	16.3 ± 0.3	16.8 ± 0.2	10.5 ± 0.2	6.9 ± 0.2
1.75	19.5 ± 0.2	21.4 ± 0.3	12.8 ± 0.4	8.5 ± 0.3
2.00	23.2 ± 0.5	26.3 ± 0.7	15.4 ± 0.4	10.1 ± 0.2
2.25	26.8 ± 0.5	31.7 ± 0.8	18.2 ± 0.5	11.8 ± 0.3
2.50	31.0 ± 0.7	37.3 ± 0.7	21.0 ± 0.4	14.0 ± 0.4
2.75	35.0 ± 0.5	43.0 ± 0.4	24.2 ± 0.7	16.1 ± 0.5
3.00	39.8 ± 0.4	49.5 ± 0.8	27.5 ± 0.6	18.4 ± 0.5
3.25	44.3 ± 0.4	56.2 ± 0.6	31.2 ± 0.9	20.7 ± 0.4
3.50	49.2 ± 0.5	63.3 ± 0.6	34.9 ± 0.8	23.5 ± 0.5
3.75	54.5 ± 0.6	70.4 ± 0.8	38.4 ± 0.8	26.0 ± 0.4
4.00	49.3 ± 0.5	77.5 ± 0.9	42.7 ± 0.9	29.0 ± 0.6
4.25	65.0 ± 0.4	85.0 ± 0.8	47.0 ± 0.8	31.9 ± 0.5
4.50	70.5 ± 0.8	92.8 ± 1.0	51.3 ± 0.9	35.0 ± 0.7
4.75	76.5 ± 0.6	101.0 ± 1.2	55.8 ± 1.1	38.2 ± 0.8
5.00	82.5 ± 0.5	109.5 ± 1.0	61.0 ± 1.0	41.4 ± 0.7
5.25	89.0 ± 0.6	118.2 ± 1.5	66.0 ± 1.0	44.7 ± 0.9
5.50	95.8 ± 0.7	127.0 ± 1.3	71.0 ± 0.9	48.1 ± 1.2
5.75	102.0 ± 0.9	136.2 ± 1.6	76.2 ± 1.2	51.5 ± 1.3
6.00	109.0 ± 0.8	145.5 ± 1.8	81.6 ± 1.1	55.0 ± 1.2
6.25	116.0 ± 0.5	155.0 ± 2.0	87.5 ± 1.2	58.7 ± 1.5
6.50	123.8 ± 0.6	165.0 ± 1.8	93.0 ± 1.3	62.5 ± 1.7
6.75	131.0 ± 1.0	175.0 ± 2.2	99.0 ± 1.3	66.2 ± 1.6
7.00	139.5 ± 1.2	185.5 ± 2.0	105.0 ± 1.2	70.0 ± 1.8
7.25	147.0 ± 1.0	196.2 ± 2.2	111.3 ± 1.5	74.0 ± 2.0
7.50	155.5 ± 1.2	207.0 ± 2.1	117.8 ± 0.9	78.2 ± 2.2
7.75	164.5 ± 1.3	219.0 ± 2.3	124.2 ± 1.4	82.3 ± 1.8
8.00	173.5 ± 1.5	230.5 ± 2.5	131.2 ± 1.5	87.0 ± 1.6
8.25	183.0 ± 1.2	242.7 ± 2.5	138.7 ± 1.4	91.7 ± 1.5
8.50	193.5 ± 1.2	255.0 ± 2.5	146.6 ± 1.4	96.5 ± 1.2

Table 4.1 Range values (Cm) of 1 - 8.5 Mev alpha-particles in oxygen, water vapour, methyl and ethyl alcohol vapour at 3 cm. Hg pressure and 15°C temperature.

Energy (Mev)	$(CH_3)_2CHOH$	CH_2Cl_2	$CHCl_3$	CCl_4
1.00	3.6 ± 0.1	3.2 ± 0.1	2.8	2.5
1.25	4.7 ± 0.1	4.3 ± 0.1	3.8	3.2
1.50	5.8 ± 0.1	5.7 ± 0.1	4.8 ± 0.1	4.1 ± 0.1
1.75	7.1 ± 0.2	7.1 ± 0.1	5.8 ± 0.1	5.0 ± 0.1
2.00	8.5 ± 0.1	8.7 ± 0.3	6.9 ± 0.2	5.8 ± 0.1
2.25	9.9 ± 0.3	10.5 ± 0.2	8.2 ± 0.1	6.8 ± 0.2
2.50	11.4 ± 0.2	12.2 ± 0.3	9.5 ± 0.2	7.9 ± 0.1
2.75	13.0 ± 0.3	14.0 ± 0.3	10.8 ± 0.2	9.1 ± 0.2
3.00	14.8 ± 0.3	15.9 ± 0.4	12.3 ± 0.1	10.2 ± 0.2
3.25	16.6 ± 0.2	17.8 ± 0.2	13.7 ± 0.1	11.3 ± 0.2
3.50	18.6 ± 0.4	20.0 ± 0.2	15.4 ± 0.3	12.6 ± 0.3
3.75	20.8 ± 0.3	22.2 ± 0.3	17.1 ± 0.2	13.8 ± 0.2
4.00	23.0 ± 0.5	24.5 ± 0.5	18.9 ± 0.3	15.2 ± 0.2
4.25	25.4 ± 0.4	26.7 ± 0.5	20.8 ± 0.3	16.5 ± 0.3
4.50	28.0 ± 0.6	29.2 ± 0.4	22.7 ± 0.2	18.1 ± 0.4
4.75	30.5 ± 0.9	31.7 ± 0.6	24.7 ± 0.4	19.6 ± 0.4
5.00	33.1 ± 0.7	34.2 ± 0.5	26.8 ± 0.3	21.1 ± 0.3
5.25	35.7 ± 0.7	37.2 ± 0.7	29.0 ± 0.4	22.7 ± 0.5
5.50	38.5 ± 0.8	40.0 ± 0.4	31.2 ± 0.5	24.3 ± 0.4
5.75	41.2 ± 0.9	42.7 ± 0.5	33.3 ± 0.5	26.0 ± 0.4
6.00	44.0 ± 0.7	45.6 ± 0.6	35.6 ± 0.7	27.8 ± 0.5
6.25	47.2 ± 1.0	48.6 ± 0.5	37.9 ± 0.6	29.7 ± 0.7
6.50	50.2 ± 0.9	51.7 ± 0.7	40.4 ± 0.9	31.8 ± 0.5
6.75	53.2 ± 1.2	55.0 ± 0.7	42.8 ± 0.8	33.3 ± 0.8
7.00	56.3 ± 1.0	58.3 ± 0.9	45.3 ± 0.7	35.8 ± 0.6
7.25	59.8 ± 1.1	61.7 ± 0.8	47.9 ± 0.7	38.2 ± 0.7
7.50	63.1 ± 0.8	65.4 ± 1.2	50.7 ± 0.6	40.5 ± 0.5
7.75	66.5 ± 0.8	69.0 ± 1.0	53.4 ± 0.9	42.8 ± 0.6
8.00	70.2 ± 1.0	72.7 ± 0.8	56.1 ± 1.2	45.2 ± 0.9
8.25	73.8 ± 0.7	76.7 ± 0.6	58.9 ± 1.0	47.6 ± 0.7
8.50	77.6 ± 1.0	81.0 ± 0.7	61.9 ± 0.8	50.2 ± 0.8

Table 4.1a Range Values (Cm) of 1 - 8.5 Mev alpha-particles in propyl alcohol, dichloromethane, trichloromethane and carbontetrachloride vapour at 3 Cm Hg pressure and 15°C temperature.

Energy (Mev)	H_2O	CH_3OH	C_2H_5OH	$(CH_3)_2CHOH$
2.00	8.9 ± 0.3	9.8 ± 0.4	9.2 ± 0.3	10.2 ± 0.4
2.25	10.9 ± 0.3	11.8 ± 0.4	11.0 ± 0.3	12.0 ± 0.4
2.50	12.8 ± 0.2	13.7 ± 0.3	12.9 ± 0.2	13.9 ± 0.3
2.75	14.8 ± 0.3	15.8 ± 0.4	15.0 ± 0.4	16.2 ± 0.3
3.00	17.1 ± 0.4	18.0 ± 0.5	17.2 ± 0.3	18.5 ± 0.5
3.25	19.2 ± 0.4	20.3 ± 0.4	19.6 ± 0.4	20.7 ± 0.5
3.50	21.5 ± 0.5	22.8 ± 0.5	22.1 ± 0.3	23.3 ± 0.4
3.75	23.7 ± 0.4	25.5 ± 0.5	24.6 ± 0.4	25.8 ± 0.5
4.00	26.1 ± 0.6	28.4 ± 0.5	27.4 ± 0.5	28.6 ± 0.4
4.25	28.5 ± 0.5	31.5 ± 0.6	30.5 ± 0.4	31.6 ± 0.6
4.50	31.2 ± 0.7	34.7 ± 0.7	33.6 ± 0.5	34.6 ± 0.6
4.75	33.5 ± 0.7	37.7 ± 0.6	36.6 ± 0.6	37.5 ± 0.7
5.00	36.2 ± 0.7	41.1 ± 0.6	40.1 ± 0.6	40.9 ± 0.6
5.25	38.7 ± 0.8	44.5 ± 0.7	43.5 ± 0.5	44.2 ± 0.7
5.50	41.4 ± 0.7	48.2 ± 0.7	47.2 ± 0.7	47.7 ± 0.8
5.75	44.3 ± 0.9	51.6 ± 0.6	50.7 ± 0.7	51.2 ± 0.8
6.00	47.25 ± 0.8	55.2 ± 0.7	54.7 ± 0.6	55.0 ± 0.8
6.25	50.2 ± 0.8	59.3 ± 0.8	57.7 ± 0.8	58.7 ± 0.9
6.50	53.3 ± 0.9	63.4 ± 0.8	62.8 ± 0.9	62.5 ± 0.8
6.75	56.6 ± 0.8	67.4 ± 0.8	67.0 ± 0.9	66.2 ± 0.9
7.00	59.7 ± 1.0	71.6 ± 0.7	71.2 ± 0.9	70.6 ± 0.9
7.25	63.2 ± 1.0	76.0 ± 09	76.2 ± 0.8	75.0 ± 1.0
7.50	66.8 ± 0.9	80.6 ± 0.8	81.2 ± 0.8	79.1 ± 1.1
7.75	70.6 ± 0.9	85.0 ± 0.9	86.3 ± 0.9	83.4 ± 1.0
8.00	74.6 ± 1.0	90.0 ± 1.0	91.3 ± 1.0	87.7 ± 1.0
8.25	78.5 ± 0.9	94.8 ± 1.0	97.5 ± 1.0	92.6 ± 1.1
8.50	83.2 ± 1.0	100.3 ± 1.1	103.2 ± 1.1	97.8 ± 1.1

Table 4.2 Range values (/^{4}m) of 2 - 8.5 Mev alpha particles in water, methyl, ethyl and propyl alcohol liquid with method I.

Energy (Mev)	CH_3OH	C_2H_5OH	$(CH_3)_2CHOH$
1.00	4.7 ± 0.2	3.9 ± .2	4.2 ± 0.2
1.25	5.9 ± 0.2	5.1 ± 0.1	5.7 ± 0.2
1.50	7.3 ± 0.2	6.7 ± 0.2	7.3 ± 0.2
1.75	8.9 ± 0.3	8.2 ± 0.2	9.2 ± 0.2
2.00	10.6 ± 0.3	10.0 ± 0.3	10.9 ± 0.3
2.25	12.4 ± 0.3	11.7 ± 0.2	12.9 ± 0.3
2.50	14.3 ± 0.3	13.8 ± 0.3	15.0 ± 0.3
2.75	16.4 ± 0.4	16.0 ± 0.4	17.2 ± 0.4
3.00	18.6 ± 0.3	18.4 ± 0.4	19.7 ± 0.3
3.25	21.0 ± 0.4	20.7 ± 0.5	22.2 ± 0.4
3.50	23.3 ± 0.5	23.3 ± 0.5	24.8 ± 0.4
3.75	25.9 ± 0.5	25.9 ± 0.6	27.5 ± 0.3
4.00	28.7 ± 0.6	28.6 ± 0.8	30.5 ± 0.5
4.25	31.7 ± 0.5	31.1 ± 0.7	33.5 ± 0.5
4.50	34.7 ± 0.7	34.9 ± 0.8	36.5 ± 0.5
4.75	37.9 ± 0.7	38.2 ± 0.9	39.8 ± 0.7
5.00	41.2 ± 0.8	41.9 ± 1.0	43.3 ± 0.7
5.25	44.7 ± 0.9	45.5 ± 1.1	46.7 ± 0.6
5.50	48.3 ± 0.8	49.2 ± 0.9	50.0 ± 0.6
5.75	51.5 ± 0.7	53.0 ± 0.9	54.1 ± 0.7
6.00	55.8 ± 0.6	57.1 ± 0.7	57.7 ± 0.8
6.25	59.8 ± 0.6	61.2 ± 0.7	61.9 ± 0.7
6.50	63.9 ± 0.7	65.2 ± 0.6	65.8 ± 0.7
6.75	68.0 ± 0.7	69.4 ± 0.6	70.0 ± 0.8
7.00	72.3 ± 0.6	73.8 ± 0.7	74.4 ± 0.9
7.25	76.8 ± 0.8	78.5 ± 0.7	78.8 ± 0.8
7.50	81.3 ± 0.8	83.0 ± 0.8	83.0 ± 0.9
7.75	86.0 ± 0.9	88.1 ± 0.7	87.6 ± 0.9
8.00	90.8 ± 0.8	93.8 ± 0.8	92.2 ± 0.8

Table 4.2a Range values (μm) of 1 - 8 Mev alpha-particles in methyl, ethyl and propyl alcohol liquid with method II.

Energy (Mev)	CH_2Cl_2	$CHCl_3$	CCl_4
1.00	4.4 ± 0.1	3.5 ± 0.1	3.5 ± 0.1
1.25	5.8 ± 0.2	4.5 ± 0.1	4.6 ± 0.2
1.50	7.2 ± 0.2	5.6 ± 0.2	5.8 ± 0.1
1.75	8.8 ± 0.2	7.0 ± 0.2	7.3 ± 0.2
2.00	10.5 ± 0.3	8.5 ± 0.2	8.7 ± 0.2
2.25	12.2 ± 0.3	10.0 ± 0.3	10.5 ± 0.3
2.50	14.1 ± 0.2	11.7 ± 0.3	12.2 ± 0.3
2.75	16.0 ± 0.3	13.6 ± 0.3	13.8 ± 0.4
3.00	18.2 ± 0.4	15.7 ± 0.4	15.9 ± 0.4
3.25	20.2 ± 0.4	17.8 ± 0.3	17.8 ± 0.4
3.50	22.6 ± 0.3	20.2 ± 0.4	20.0 ± 0.3
3.75	25.0 ± 0.5	22.5 ± 0.4	22.0 ± 0.5
4.00	27.5 ± 0.4	25.1 ± 0.4	24.3 ± 0.4
4.25	30.2 ± 0.5	27.6 ± 0.5	26.7 ± 0.5
4.50	32.7 ± 0.5	30.5 ± 0.4	29.0 ± 0.5
4.75	35.5 ± 0.5	33.1 ± 0.4	31.5 ± 0.4
5.00	38.2 ± 0.6	36.2 ± 0.5	34.0 ± 0.5
5.25	41.3 ± 0.5	39.2 ± 0.5	36.8 ± 0.6
5.50	44.2 ± 0.6	42.2 ± 0.5	39.6 ± 0.6
5.75	47.2 ± 0.7	45.2 ± 0.6	42.4 ± 0.6
6.00	50.6 ± 0.6	48.4 ± 0.5	45.0 ± 07
6.25	53.8 ± 0.7	51.7 ± 0.7	48.3 ± 0.6
6.50	57.2 ± 0.7	55.0 ± 0.6	51.4 ± 0.7
6.75	60.7 ± 0.7	58.2 ± 0.7	54.3 ± 0.6
7.00	64.3 ± 0.8	61.5 ± 0.7	57.6 ± 0.6
7.25	68.0 ± 0.8	65.3 ± 0.6	60.7 ± 0.7
7.50	71.5 ± 0.7	68.9 ± 0.7	64.2 ± 0.7
7.75	75.5 ± 0.7	72.7 ± 0.7	67.5 ± 0.6
8.00	79.3 ± 0.8	76.7 ± 0.7	71.0 ± 0.7

Table 4.2b Range Values (mm) of 1 - 8 Mev alpha-particles in dichloromethane, trichloromethane and carbontetrachloride liquid with method II.

4.2 The results of experimental measurements with vapours.

4.2 a Oxygen O_2

The range-energy relation for alpha-particles in oxygen is shown in graph 4.1.

In table 4.3 the experimental stopping power and molecular stopping power at various alpha-particle energies for oxygen are shown in columns (1) and (2) respectively. Column (3) shows the calculated molecular stopping power obtained from the uncorrected Bethe formula. In column (4) the values in (3) have been corrected for the anomalous stopping contribution of the K shell electrons in oxygen as described by Walske (1952). This correction factor increases the stopping power by about 11% at 1 Mev, and by about 1% at 2 Mev. Above 2 Mev it lowers the value calculated from the simple Bethe formula by 1 - 3%.

In column (5) the values in column (4) have been corrected for the Z_1^3 effect as suggested by Ashley et al (1973). This is a positive correction factor at all energies, the correction being greatestat lowest energy and falling to about 1% at 4 Mev. In comparing the two columns (3) and (5), it may be seen that the two corrections (C_k and Z_1^3), virtually cancel each other at energies about 4 Mev, but at lower energies the values of calculated stopping power with these corrections are very much higher than that calculated from the uncorrected Bethe formula. The accuracy of these calculations, however, is significantly dependent upon the value of Z_1 assumed for the alpha-particles, and as stated previously, at low energies the effective value of Z_1 is not accurately known. The value assumed in these calculations is 2e.

Table 4.3 Oxygen O_2

Energy Mev	(1)	(2)	(3)	(4)	(5)
1.00	8.91 ± 0.15	8.85 ± 0.15	10.84	11.63	13.62
1.25	8.51 ± 0.10	8.45 ± 0.10	9.76	10.56	12.06
1.50	7.96 ± 0.07	7.91 ± 0.07	8.88	9.39	10.52
1.75	7.56 ± 0.10	7.51 ± 0.10	8.15	8.24	9.11
2.00	7.14 ± 0.10	7.09 ± 0.10	7.54	7.62	8.34
2.25	6.71 ± 0.15	6.66 ± 0.15	7.02	6.96	7.55
2.50	6.30 ± 0.13	6.26 ± 0.13	6.58	6.49	6.99
2.75	5.95 ± 0.12	5.91 ± 0.12	6.19	6.05	6.47
3.00	5.60 ± 0.10	5.56 ± 0.10	5.86	5.71	6.07
3.25	5.34 ± 0.03	5.30 ± 0.03	5.56	5.41	5.73
3.50	5.10 ± 0.02	5.07 ± 0.02	5.29	5.13	5.41
3.75	4.89 ± 0.01	4.86 ± 0.01	5.05	4.90	5.15
4.00	4.68 ± 0.03	4.65 ± 0.03	4.83	4.67	4.89
4.25	4.49 ± 0.04	4.46 ± 0.04	4.64	4.49	4.69
4.50	4.31 ± 0.03	4.28 ± 0.03	4.46	4.31	4.49
4.75	4.17 ± 0.04	4.14 ± 0.04	4.29	4.15	4.31
5.00	4.03 ± 0.04	4.00 ± 0.04	4.14	4.00	4.15
5.25	3.90 ± 0.03	3.87 ± 0.03	4.00	3.86	4.00
5.50	3.78 ± 0.02	3.75 ± 0.02	3.87	3.74	3.87
5.75	3.66 ± 0.04	3.64 ± 0.04	3.75	3.62	3.74
6.00	3.56 ± 0.03	3.54 ± 0.03	3.64	3.52	3.63
6.25	3.44 ± 0.03	3.42 ± 0.03	3.53	3.41	3.51
6.50	3.32 ± 0.01	3.30 ± 0.01	3.43	3.32	3.41
6.75	3.21 ± 0.03	3.19 ± 0.03	3.34	3.23	3.32
7.00	3.10 ± 0.04	3.08 ± 0.04	3.25	3.14	3.22
7.25	3.01 ± 0.02	2.99 ± 0.02	3.17	3.07	3.14
7.50	2.92 ± 0.02	2.90 ± 0.02	3.09	2.99	3.06
7.75	2.82 ± 0.03	2.80 ± 0.03	3.02	2.93	3.00
8.00	2.73 ± 0.03	2.71 ± 0.03	2.95	2.86	2.92

Columns (1) and (2) list experimental stopping powers (10^{-2} Mev/cm) and molecular stopping powers (10^{-24} Mev.m^2.mol^{-1}) of oxygen respectively.

Columns (3) - (5) list calculated stopping powers (10^{-24} Mev.m.^{2}mol^{-1}).

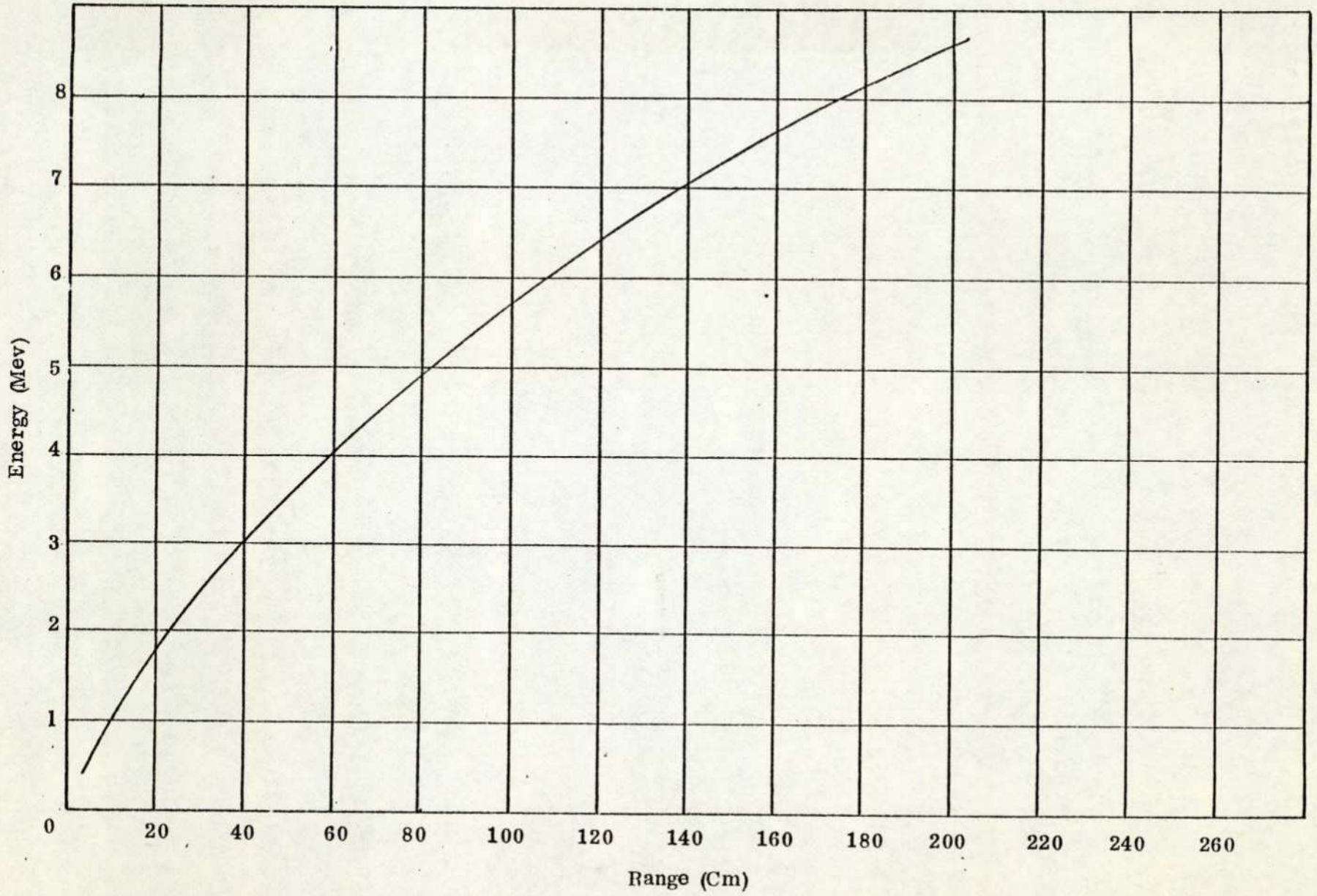

Graph 4.1. Range-energy relation for alpha-particles in oxygen at 3 cm. Hg pressure and 15 ^{o}C.

The experimental stopping power values are lower than those calculated from the Bethe formula. The differences at energies below 2 Mev is as high as 18 - 54% lower than those calculated from the Bethe formula with both C_k and Z_1^3 corrections. This differences is certainly due at least in part to the effect of charge exchange in the stopping medium. There is no definite theory from which an accurate value of the effective charge can be calculated at low energies. In table 4.3 a, column (1) gives the value of Z_1eff which would be required for oxygen in order to make the calculated values agree with the experimental values. Comparing these values with the value for Z_1eff derived by Evans (1955) from early experiments, column (2), and those calculated from a formula suggested by Barkas (1963), column (3), these values are not unreasonable.

It should also be recognised that the values of stopping power cannot be quoted to the extreme ends of the curve and the values quoted near to the ends have greater uncertainty than the others.

The molecular stopping power of oxygen is plotted as a function of alpha-particle energy in graph 4.2. This is compared with some of the published stopping power values from some other workers. (Bourland et al 1971, Venkataraman et al 1975 and Hanke and Laursen 1978). At higher energies above 2 Mev the results by Venkataraman et al are the same as the present results and Hanke et al's results are 1 - 1.5% lower than those present in this work. At energies below 2 Mev it may be seen from the graph the differences between results by various other workers.

Table 4.3 a Values of Z_{leff} for oxygen O_2

Energy Mev	(1)	(2)	(3)
1.00	1.61	1.71	1.77
1.25	1.67	1.80	1.82
1.50	1.73	1.85	1.85
1.75	1.82	1.88	1.87
2.00	1.84	1.91	1.89
2.25	1.88	1.93	1.90
2.50	1.89	1.94	1.91
2.75	1.91	1.95	1.92
3.00	1.92	1.96	1.93
3.25	1.92	1.96	1.94
3.50	1.94	1.97	1.94
3.75	1.94	1.97	1.95
4.00	1.95	1.97	1.95
4.25	1.95	1.98	1.95
4.50	1.95	1.98	1.96
4.75	1.96	1.98	1.96
5.00	1.96	1.98	1.96
5.25	1.97	1.98	1.96
5.50	1.97	1.98	1.96
5.75	1.97	1.98	1.97
6.00	1.98	1.99	1.97
6.25	1.97	1.99	1.97
6.50	1.97	1.99	1.97
6.75	1.96	1.99	1.97
7.00	1.96	1.99	1.97
7.25	1.95	1.99	1.97
7.50	1.95	1.99	1.98
7.75	1.93	1.99	1.98
8.00	1.93	1.99	1.98

Column (1) gives the value of Z_{leff} for oxygen which would bring the calculated stopping power in column (5) table 4.3 into agreement with the experimental values in column (2).

Columns (2) and (3) give the values of Z_{leff} according to Evans (1955) and Barkas (1963) respectively.

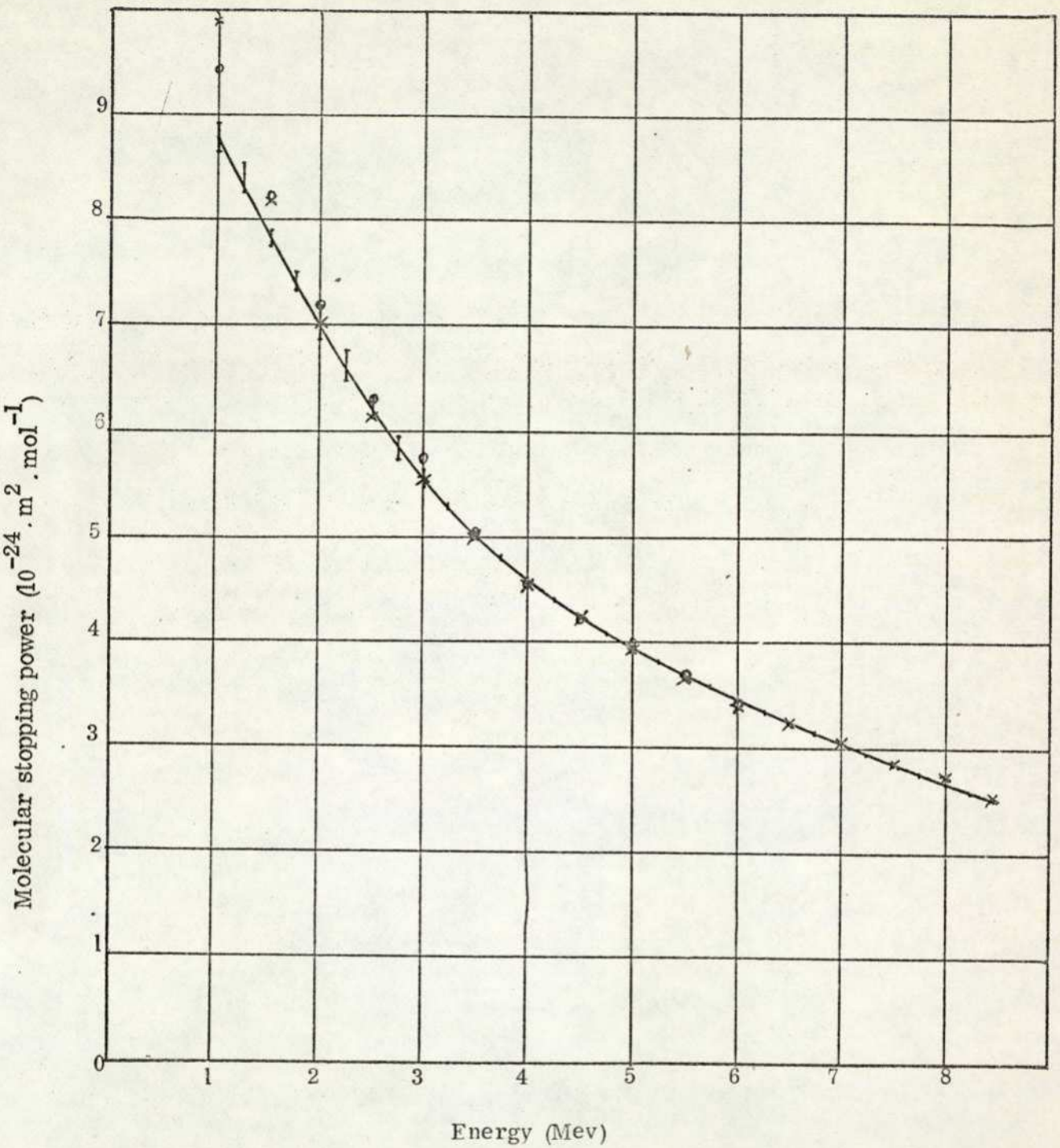

Graph 4.2 Variation of molecular stopping power of oxygen with alpha-particle energy.

O Venkataraman et al (1975)

x Hanke and Laursen (1978)

4.2 b Water (H_2O) vapour

For the water vapour measurements because the detector could not be operated at a temperature above 30°C this presented a problem owing to the low saturation vapour pressure of water at ambient temperatures. By using thin metal foils of uniform thickness varying from 3 to 42 μm, the energy of the alpha-particles leaving the source could be reduced and whole energy range from 8.78 Mev down to noise level could be investigated.

The range-energy relation for alpha-particles in water vapour is shown in graph 4.3 and represents the results of all separate sets of vapour measurements with overlapping energy ranges obtained by the use of different foils and sources.

The stopping powers, molecular stopping powers and molecular stopping powers calculated from the uncorrected Bethe formula at various alpha-particle energies for water vapour are shown in table 4.4.

Graph 4.4 shows the molecular stopping power of water vapour as a function of alpha-particle energy.

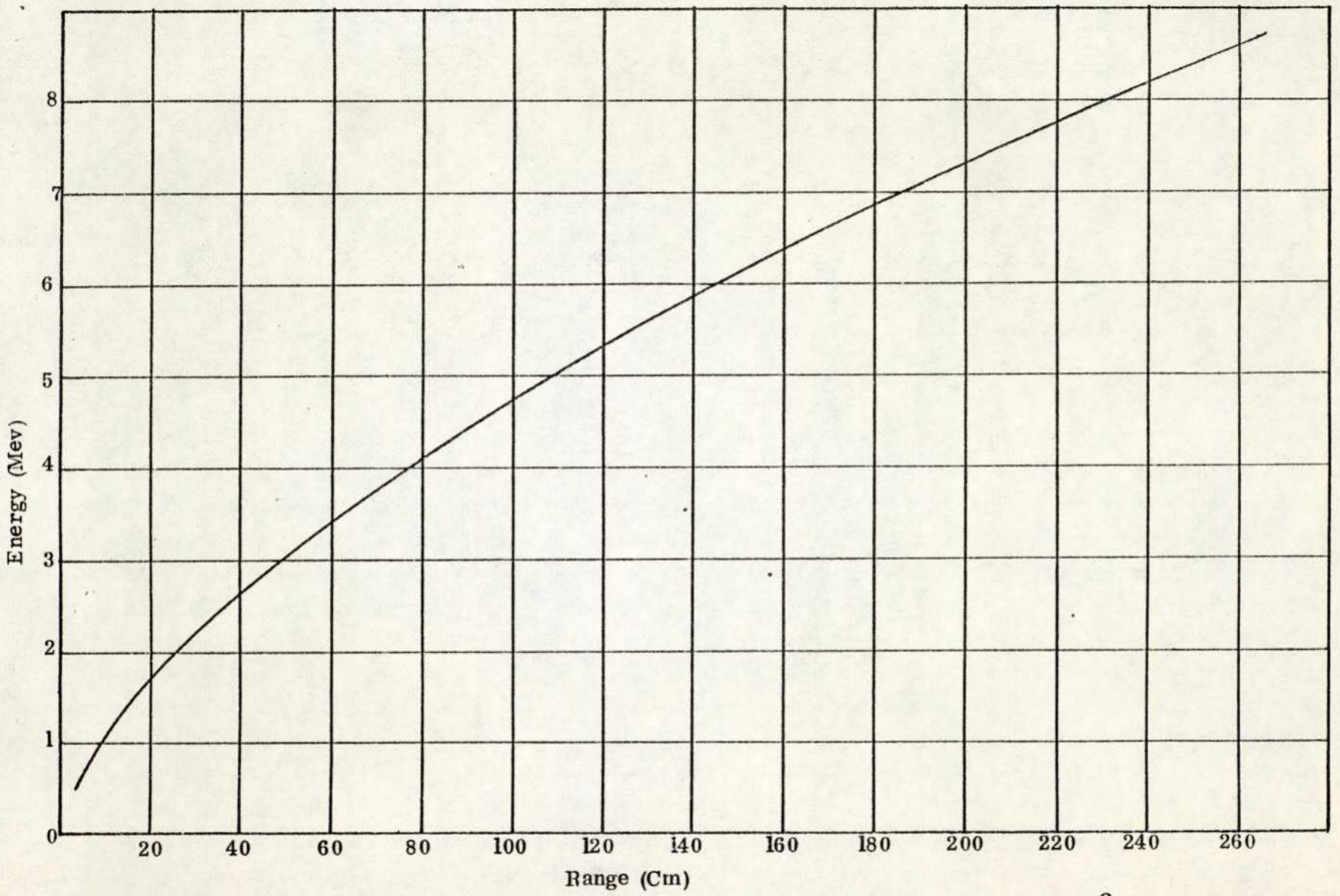

Graph 4.3 Range energy relation for alpha-particles in water vapour at 3cm. Hg pressure and 15°C.

Energy (Mev)	$\frac{dE}{dx} \times 10^2$ Mev/cm	10^{-24} Mev m^2 mol^{-1} $\frac{dE}{dx}/N$ experimental	$\frac{dE}{dx}/N$ caiculated
1.00	7.10 ± 0.24	7.05 ± 0.24	7.97
1.25	6.70 ± 0.23	6.65 ± 0.23	7.06
1.50	5.92 ± 0.16	5.88 ± 0.16	6.34
1.75	5.53 ± 0.11	5.49 ± 0.11	5.77
2.00	5.11 ± 0.03	5.08 ± 0.03	5.29
2.25	4.77 ± 0.05	4.74 ± 0.05	4.93
2.50	4.51 ± 0.03	4.48 ± 0.03	4.57
2.75	4.26 ± 0.08	4.23 ± 0.08	4.30
3.00	4.00 ± 0.10	3.97 ± 0.10	4.06
3.25	3.82 ± 0.10	3.79 ± 0.10	3.85
3.50	3.65 ± 0.09	3.63 ± 0.09	3.64
3.75	3.46 ± 0.05	3.44 ± 0.05	3.46
4.00	3.33 ± 0.05	3.31 ± 0.05	3.31
4.25	3.19 ± 0.03	3.17 ± 0.03	3.19
4.50	3.07 ± 0.03	3.05 ± 0.03	3.04
4.75	2.97 ± 0.07	2.95 ± 0.07	2.93
5.00	2.85 ± 0.06	2.83 ± 0.06	2.82
5.25	2.77 ± 0.05	2.75 ± 0.05	2.72
5.50	2.70 ± 0.04	2.68 ± 0.04	2.63
5.75	2.63 ± 0.04	2.61 ± 0.02	2.54
6.00	2.57 ± 0.02	2.55 ± 0.02	2.46
6.25	2.52 ± 0.01	2.50 ± 0.01	2.39
6.50	2.47 ± 0.01	2.45 ± 0.01	2.39
6.75	2.41 ± 0.01	2.39 ± 0.01	2.26
7.00	2.36 ± 0.02	2.34 ± 0.02	2.20
7.25	2.30 ± 0.03	2.28 ± 0.03	2.14
7.50	2.24 ± 0.03	2.22 ± 0.02	2.09
7.75	2.16 ± 0.01	2.15 ± 0.01	2.03
8.00	2.08 ± 0.01	2.07 ± 0.01	1.99

Table 4.4 Water (H_2O) vapour

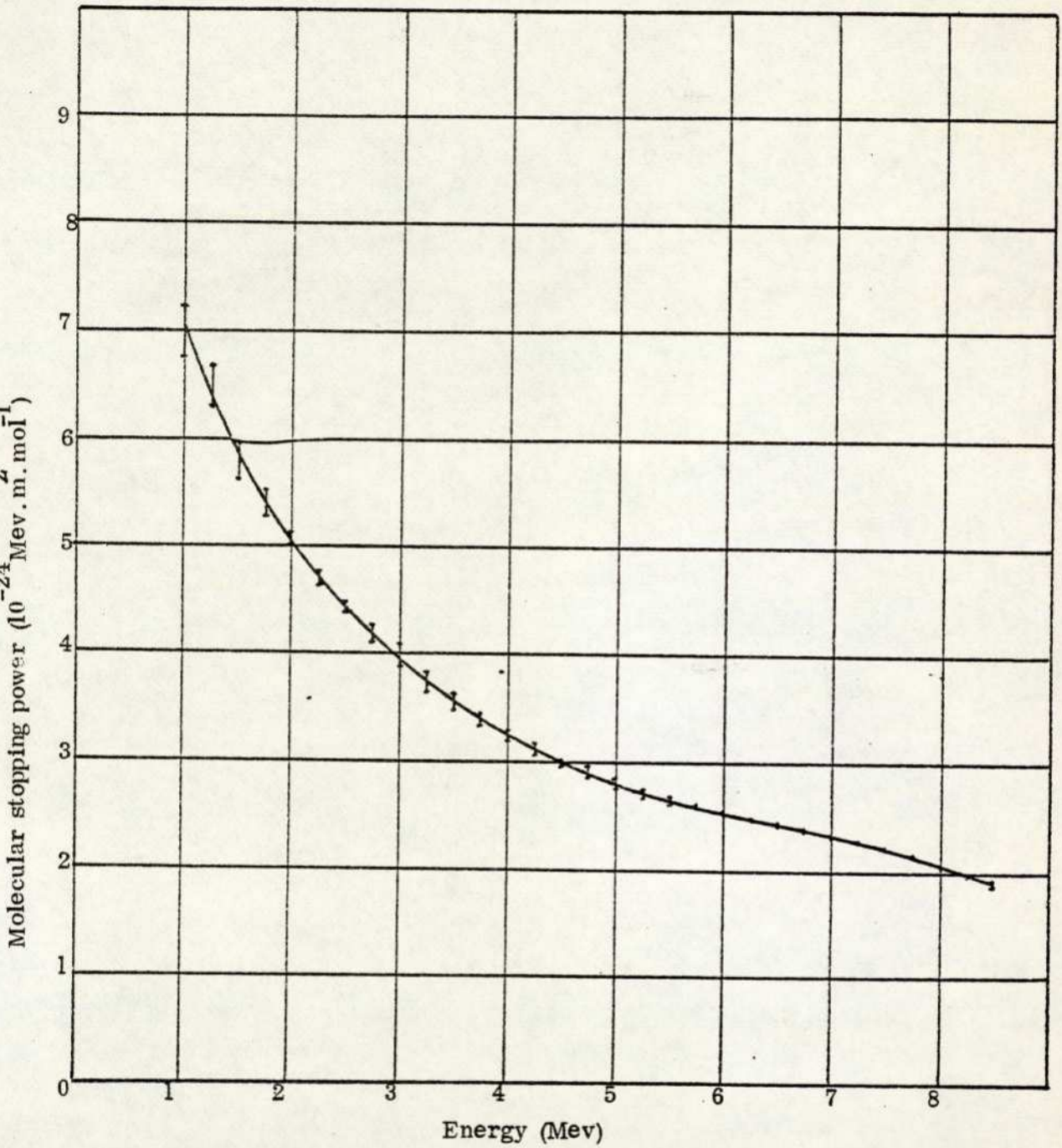

Graph 4.4 Variation of molecular stopping power of water vapour with alpha-particle energy.

4.2 c Methyl alcohol (CH_3OH) Vapour

The range-energy relation for alpha-particles in methyl alcohol vapour is shown in graph 4.5 and represents the results of all separate sets of vapour measurements by using different sources.

The stopping powers, molecular stopping powers and molecular stopping powers calculated from the uncorrected Bethe formula at various alpha-particle energies for methyl alcohol vapour are shown in table 4.5 .

Graph 4.6 shows the molecular stopping power of CH_3OH vapour as a function of alpha-particle energy.

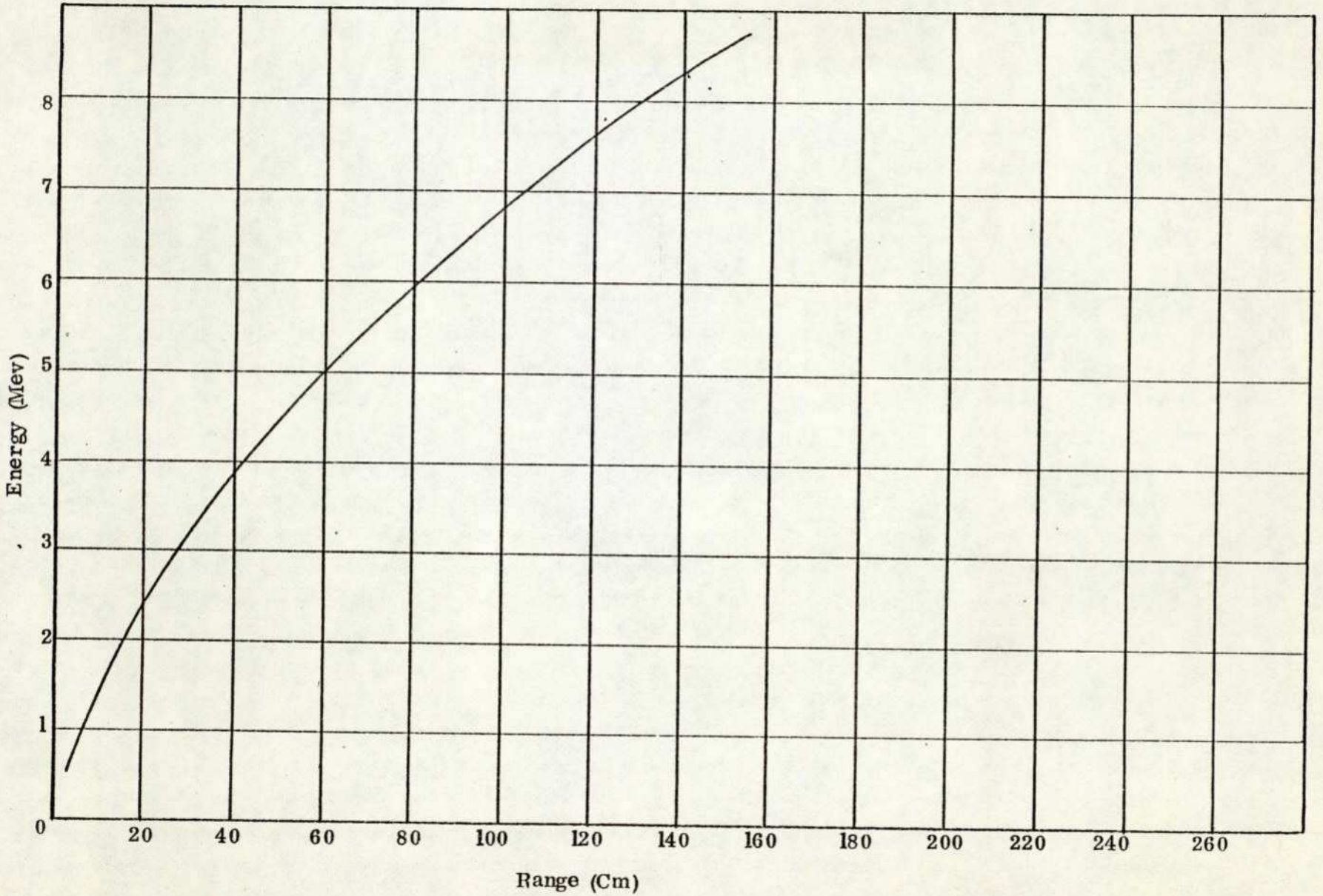

Graph 4.5 Range energy relation for alpha-particles in methyl alcohol vapour at 3 cm. Hg pressure and 15 ^{o}C.

Energy (Mev)	$\frac{dE}{dx}$ x 10^2 Mev/cm	$\frac{dE}{dx}$ experimental / N	$\frac{dE}{dx}$ calculated / N
		10^{-24} Mev m^2 mol^{-1}	
1.00	13.47 ± 0.21	13.38 ± 0.21	15.01
1.25	12.50 ± 0.18	12.42 ± 0.18	13.24
1.50	11.60 ± 0.25	11.52 ± 0.25	11.87
1.75	10.65 ± 0.35	10.58 ± 0.35	10.78
2.00	9.89 ± 0.35	9.82 ± 0.35	9.89
2.25	9.25 ± 0.35	9.19 ± 0.35	9.16
2.50	8.44 ± 0.10	8.38 ± 0.10	8.53
2.75	7.95 ± 0.19	7.90 ± 0.19	7.99
3.00	7.40 ± 0.08	7.35 ± 0.08	7.53
3.25	7.02 ± 0.09	6.97 ± 0.09	7.12
3.50	6.62 ± 0.04	6.58 ± 0.04	6.76
3.75	6.34 ± 0.05	6.30 ± 0.05	6.43
4.00	6.02 ± 0.06	5.98 ± 0.06	6.14
4.25	5.78 ± 0.05	5.74 ± 0.05	5.88
4.50	5.56 ± 0.02	5.52 ± 0.02	5.64
4.75	5.32 ± 0.05	5.28 ± 0.05	5.42
5.00	5.12 ± 0.06	5.09 ± 0.06	5.22
5.25	4.92 ± 0.07	4.89 ± 0.07	5.04
5.50	4.76 ± 0.06	4.73 ± 0.06	4.87
5.75	4.62 ± 0.05	4.59 ± 0.05	4.71
6.00	4.48 ± 0.05	4.45 ± 0.05	4.56
6.25	4.35 + 0.05	4.32 ± 0.05	4.42
6.50	4.22 ± 0.05	4.19 ± 0.05	4.29
6.75	4.09 ± 0.03	4.06 ± 0.03	4.17
7.00	3.95 ± 0.04	3.92 ± 0.04	4.06
7.25	3.81 ± 0.03	3.78 ± 0.03	3.95
7.50	3.68 ± 0.03	3.66 ± 0.03	3.85
7.75	3.56 ± 0.03	3.54 ± 0.03	3.76
8.00	3.46 ± 0.04	3.44 ± 0.04	3.67

Table 4.5 Methyl alcohol (CH_3OH) Vapour

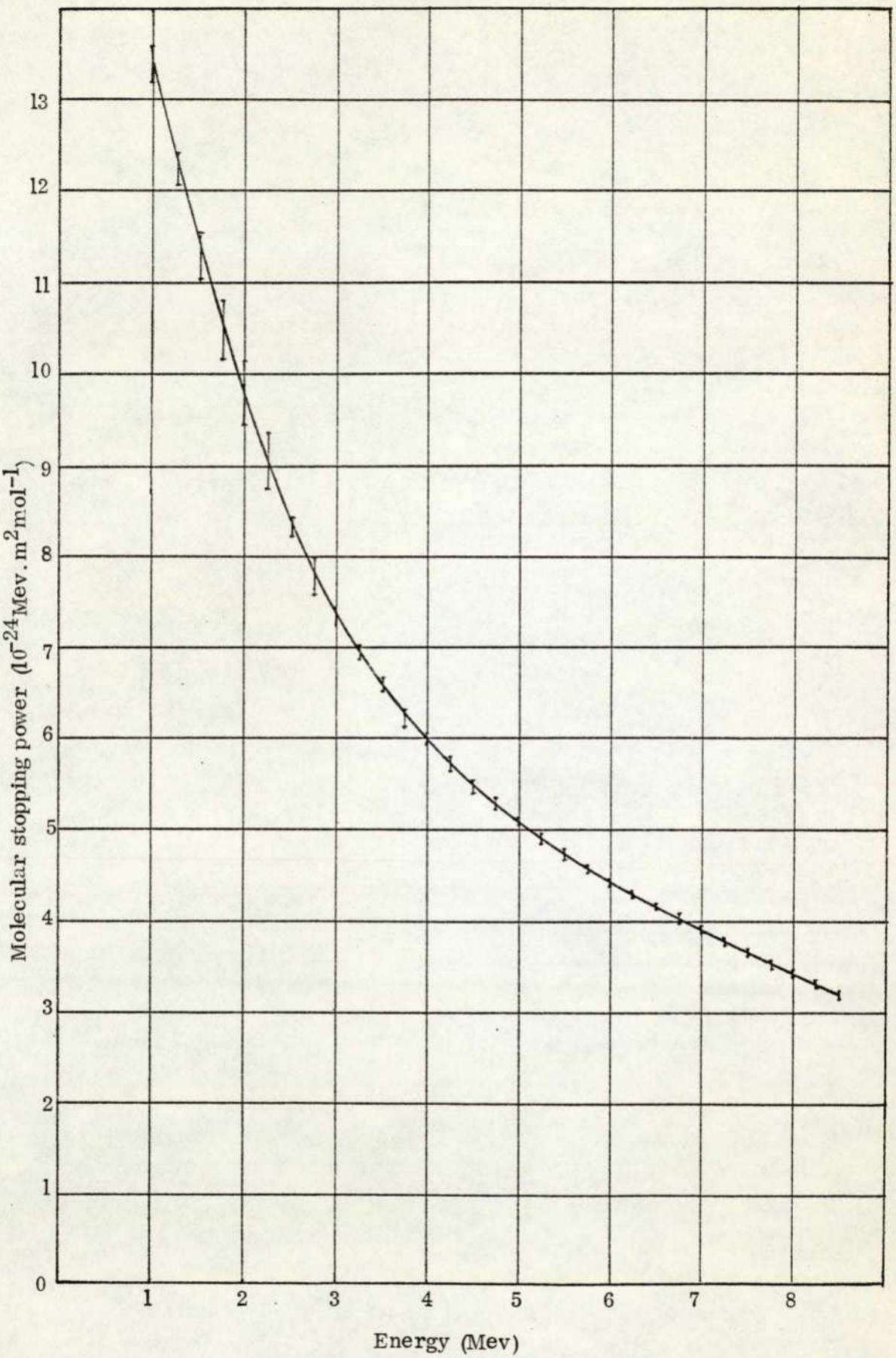

Graph 4.6 Variation of molecular stopping power of methyl alcohol vapour with alpha-particle energy.

4.2 d Ethyl alcohol (C_2H_5OH) Vapour

For the ethyl alcohol vapour measurements the distance between the ^{212}Bi source and the detector was 45 cm and the gas temperature was about 24 ^{o}C, in this condition the pressure variation could be up to 7 cm. Hg but at about 5 cm.Hg pressure because of association of the C_2H_5OH molecules, the stopping power of the vapour for alpha-particles appeared to increase and therefore the range of alpha-particles showed a sharp decrease. This was overcome by using thin metal foils of uniform thickness 6 - 18 μm in a manner similar to that described in Section 4.2 b for water vapour.

The range energy relation for alpha-particles in C_2H_5OH vapour is shown in graph 4.7 and represents the results of all separate sets of vapour measurements with overlapping energy ranges obtained by the use of different foils and sources.

The stopping powers, molecular stopping powers and molecular stopping powers calculated from the uncorrected Bethe formula at various alpha-particle energies for ethyl alcohol vapour are shown in table 4.6.

Graph 4.8 shows the molecular stopping power of C_2H_5OH vapour as a function of alpha-particle energy.

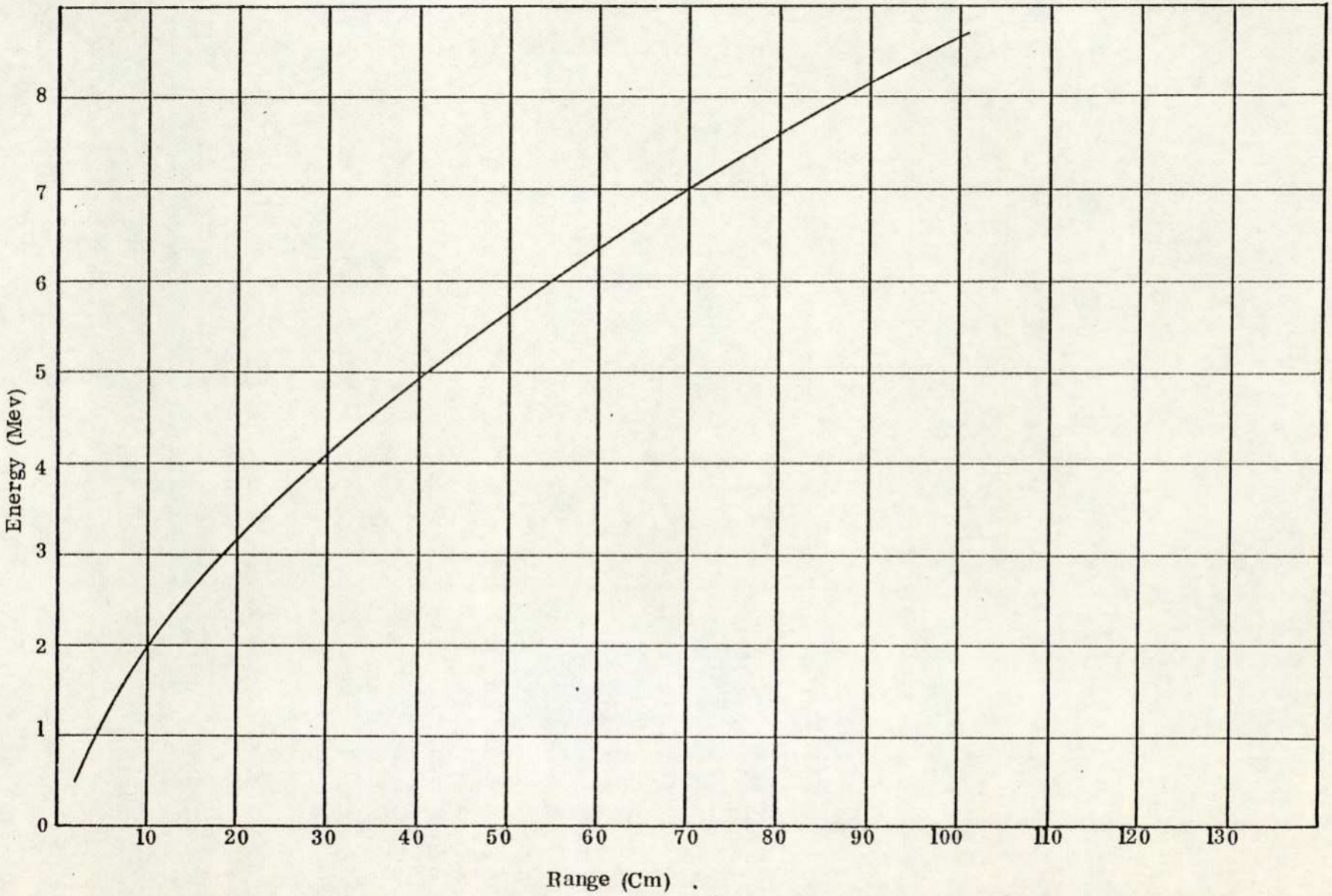

Graph 4.7 Range energy relation for alpha-particles in ethyl alcohol vapour at 3 cm. Hg pressure and 15°C.

Energy (Mev)	$\frac{dE}{dx} \times 10^2$ Mev/cm	10^{-24} Mev m^2 mol^{-1} $\frac{dE}{dx}/N$ experimental	$\frac{dE}{dx}/N$ calculated
1.00	19.97 ± 0.18	19.84 ± 0.18	22.03
1.25	18.59 ± 0.28	18.46 ± 0.28	19.40
1.50	16.55 ± 0.41	16.44 ± 0.41	17.38
1.75	15.01 ± 0.29	14.91 ± 0.29	15.77
2.00	14.04 ± 0.35	13.95 ± 0.35	14.47
2.25	12.96 ± 0.25	12.87 ± 0.25	13.38
2.50	11.89 ± 0.23	11.81 ± 0.23	12.46
2.75	11.18 ± 0.19	11.10 ± 0.19	11.68
3.00	10.59 ± 0.21	10.52 ± 0.21	10.99
3.25	10.09 ± 0.28	10.02 ± 0.22	10.39
3.50	9.58 ± 0.31	9.52 ± 0.31	9.86
3.75	9.25 ± 0.26	9.19 ± 0.25	9.39
4.00	8.82 ± 0.29	8.76 ± 0.29	8.96
4.25	8.50 ± 0.34	8.44 ± 0.34	8.57
4.50	8.22 ± 0.29	8.16 ± 0.29	8.23
4.75	8.02 ± 0.30	7.97 ± 0.30	7.91
5.00	7.80 ± 0.30	7.75 ± 0.30	7.63
5.25	7.67 ± 0.25	7.62 ± 0.25	7.34
5.50	7.53 ± 0.20	7.48 ± 0.20	7.09
5.75	7.35 ± 0.15	7.30 ± 0.15	6.85
6.00	7.12 ± 0.10	7.07 ± 0.10	6.65
6.25	6.93 ± 0.05	6.88 ± 0.05	6.45
6.50	6.68 ± 0.01	6.63 ± 0.01	6.26
6.75	6.40 ± 0.05	6.36 ± 0.05	6.08
7.00	6.19 ± 0.05	6.15 ± 0.05	5.92
7.25	5.94 ± 0.01	5.90 ± 0.01	5.76
7.50	5.76 ± 0.02	5.72 ± 0.02	5.61
7.75	5.54 ± 0.05	5.50 ± 0.05	5.47
8.00	5.35 ± 0.12	5.31 ± 0.12	5.34

Table 4.6 Ethyl alcohol (C_2H_5OH) Vapour

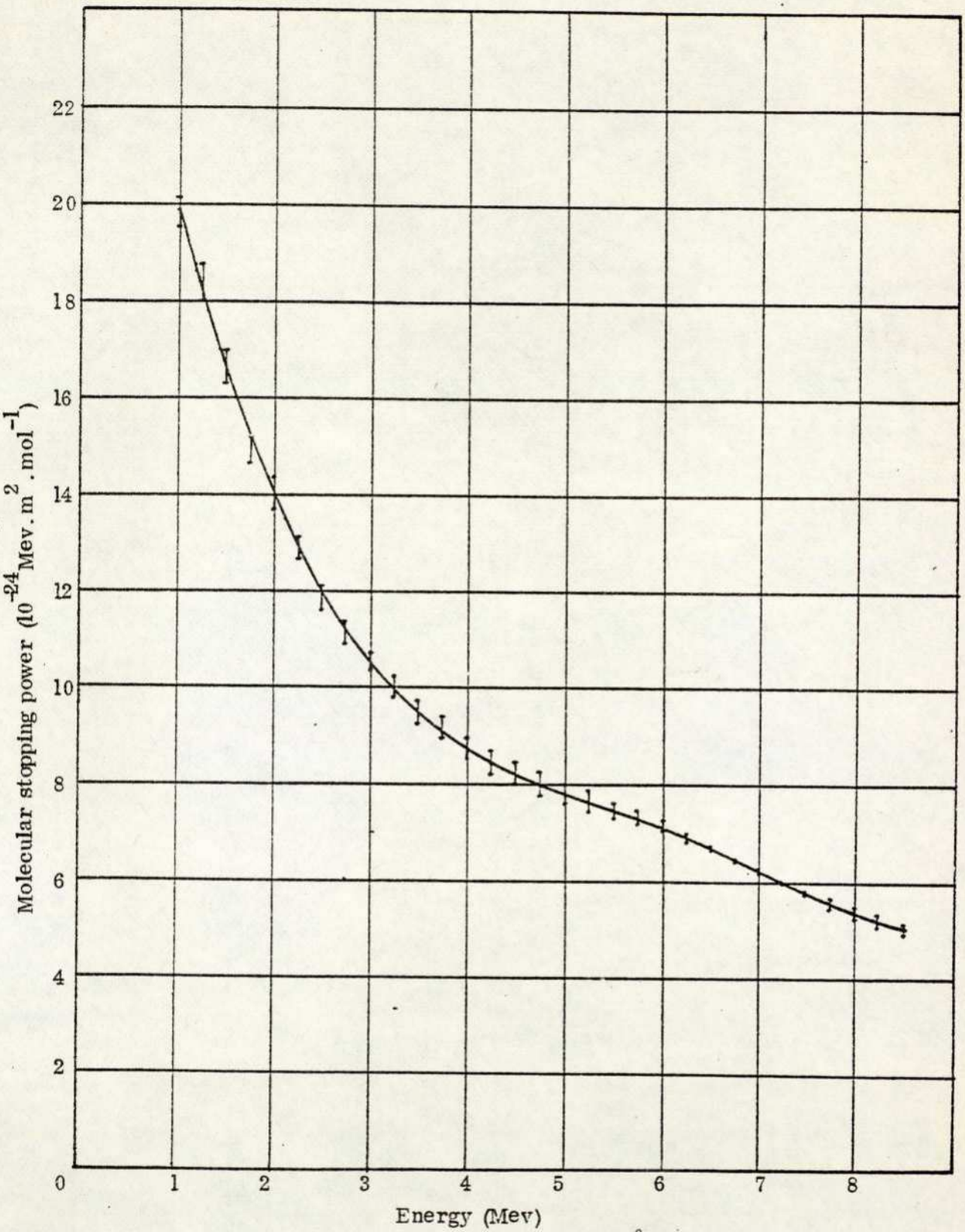

Graph 4.8 Variation of molecular stopping power of ethyl alcohol vapour with alpha-particle energy.

4.2 e Propyl alcohol $(CH_3)_2CHOH$ vapour

For the propyl alcohol vapour measurements the distance between the ^{212}Bi source and detector was 47 cm and the vapour temperature was $27^{o}C$. The vapour pressure was insufficient completely to stop the 8.78 Mev alpha-particles. However by combining measurements with the 8.78 Mev particles and the 6.05 Mev particles a complete range-energy relation could be derived.

The range-energy relation for alpha-particles in propyl alcohol vapour is shown in graph 4.9, and representsthe results of all separate sets of vapour measurements by using different sources.

The stopping powers, molecular stopping powers and molecular stopping powers calculated from the uncorrected Bethe formula at various alpha-particle energies for propyl alcohol vapour are shown in table 4.7.

Graph 4.10 shows the molecular stopping power of $(CH_3)_2CHOH$ vapour as a function of alpha-particle energy.

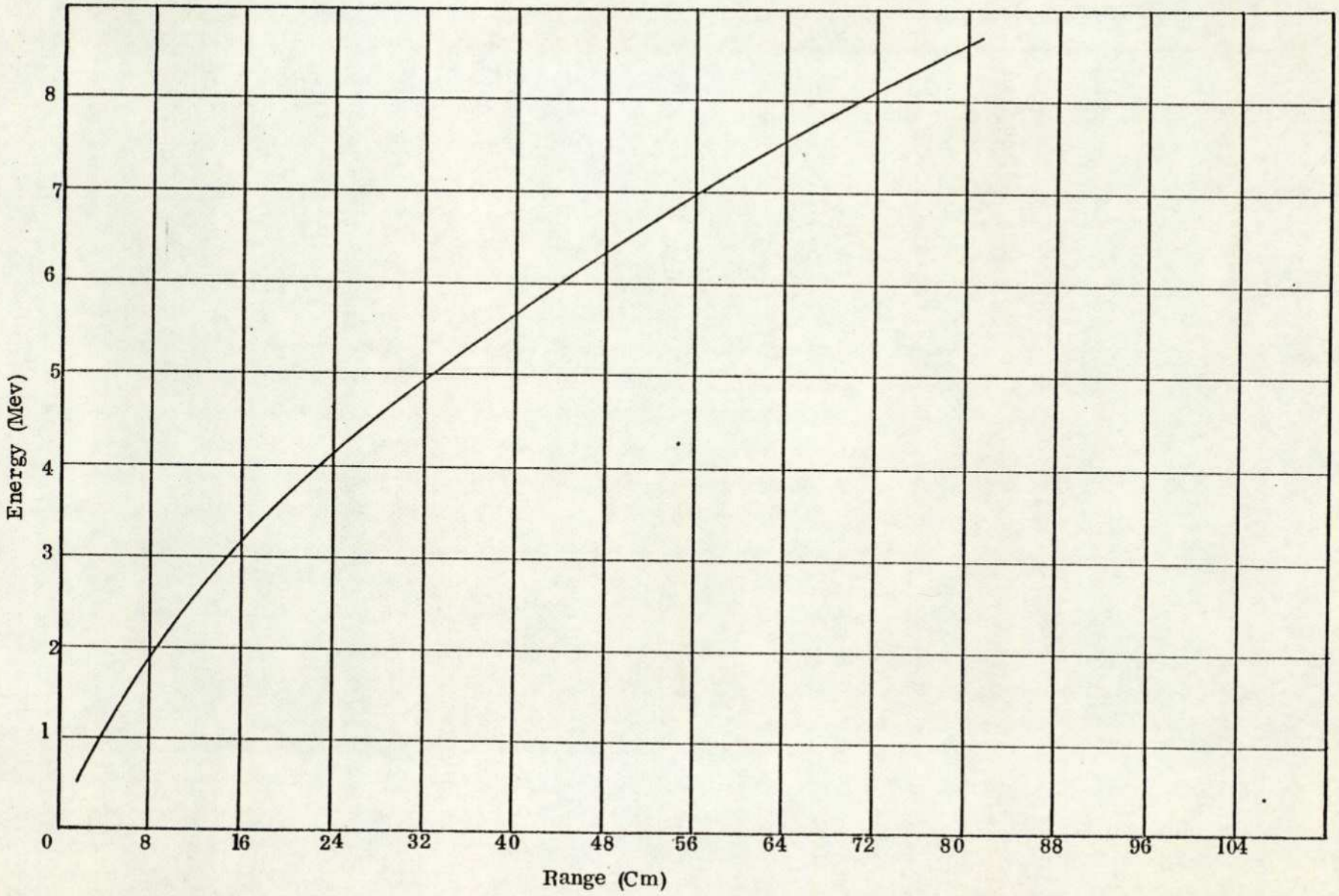

Graph 4.9 Range energy relation for alpha-particles in propyl alcohol vapour at 3cm.Hg pressure and 15 ^{o}C.

Energy (Mev)	$\frac{dE}{dx} \times 10^2$ Mev/cm	10^{-24} Mev m^2 mol^{-1} $\frac{dE}{dx}$ experimental $\frac{}{N}$	$\frac{dE}{dx}$ calculated $\frac{}{N}$
1.00	24.61 ± 0.19	24.44 ± 0.19	28.72
1.25	22.76 ± 0.15	22.61 ± 0.15	25.54
1.50	21.06 ± 0.22	20.92 ± 0.22	22.86
1.75	19.55 ± 0.24	19.42 ± 0.24	20.74
2.00	18.22 ± 0.03	18.10 ± 0.03	19.02
2.25	17.07 ± 0.09	16.95 ± 0.09	17.59
2.50	16.05 ± 0.24	15.94 ± 0.24	16.38
2.75	14.91 ± 0.20	14.81 ± 0.20	15.34
3.00	13.97 ± 0.15	13.88 ± 0.15	14.44
3.25	13.10 ± 0.13	13.01 ± 0.13	13.65
3.50	12.39 ± 0.22	12.31 ± 0.22	12.95
3.75	11.79 ± 0.22	11.71 ± 0.22	12.32
4.00	11.40 ± 0.28	11.32 ± 0.28	11.77
4.25	11.04 ± 0.25	10.97 ± 0.25	11.26
4.50	10.62 ± 0.22	10.55 ± 0.22	10.80
4.75	9.94 ± 0.20	9.87 ± 0.20	10.38
5.00	9.65 ± 0.25	9.58 ± 0.25	9.99
5.25	9.37 ± 0.15	9.31 ± 0.15	9.64
5.50	9.16 ± 0.21	9.10 ± 0.21	9.31
5.75	8.94 ± 0.25	8.88 ± 0.25	9.01
6.00	8.68 ± 0.22	8.62 ± 0.22	8.72
6.25	8.46 ± 0.13	8.40 ± 0.13	8.46
6.50	8.25 ± 0.10	8.19 ± 0.10	8.21
6.75	8.00 ± 0.16	7.95 ± 0.16	7.98
7.00	7.75 ± 0.08	7.70 ± 0.08	7.75
7.25	7.47 ± 0.06	7.42 ± 0.06	7.56
7.50	7.20 ± 0.05	7.15 ± 0.05	7.37
7.75	6.95 ± 0.01	6.90 ± 0.01	7.18
8.00	6.73 ± 0.10	6.68 ± 0.10	7.01

Table 4.7 Propyl alcohol $(CH_3)_2$ CHOH Vapour

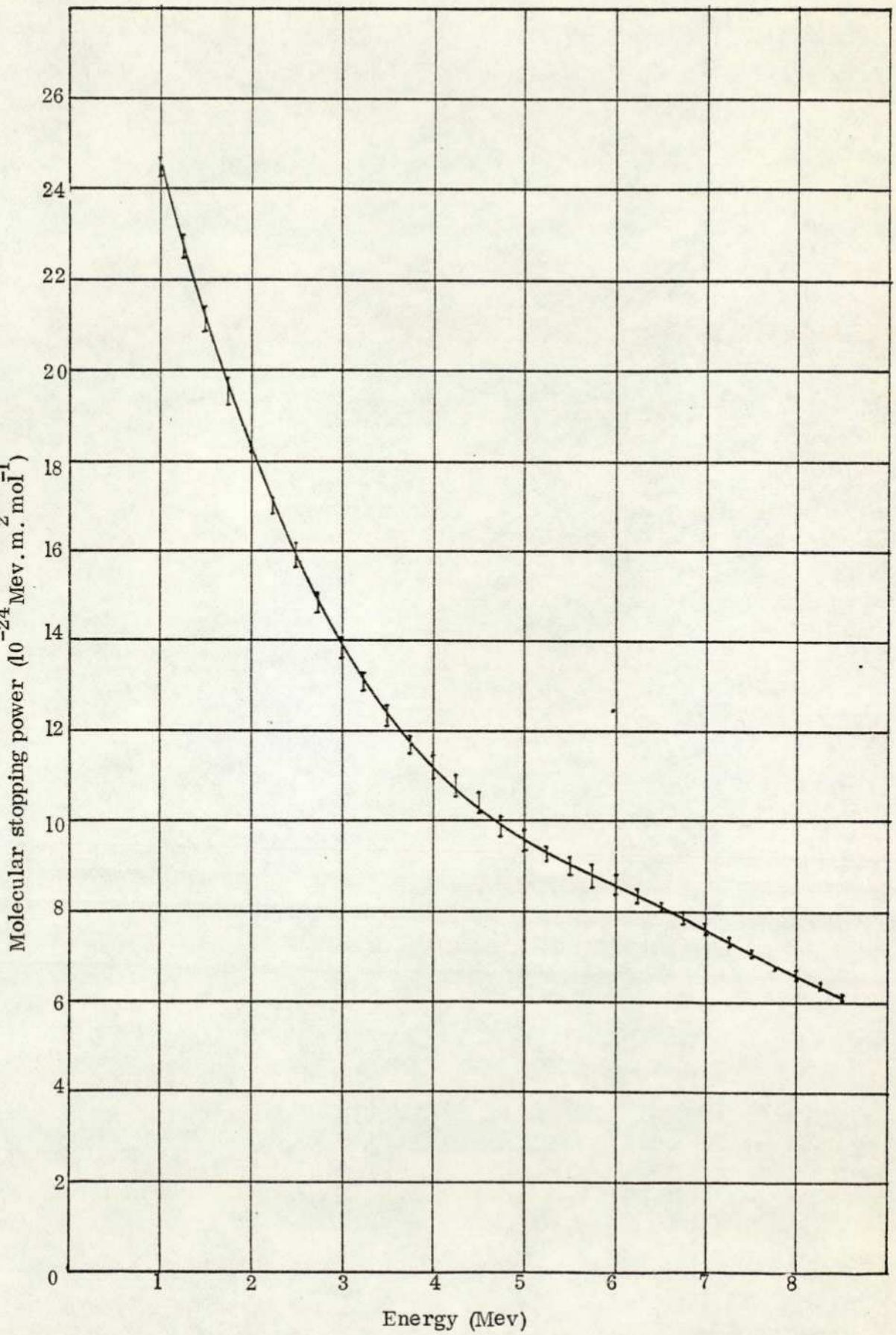

Graph 4.10 Variation of molecular stopping power of propyl alcohol vapour with alpha-particle energy.

4.2 f Dichloromethane (CH_2Cl_2) Vapour

The range-energy relation for alpha-particles in dichloromethane vapour is shown in graph 4.11, and represents the results of all separate sets of vapour measurements by using different sources.

The stopping powers, molecular stopping powers and molecular stopping powers calculated from the uncorrected Bethe formula are shown in table 4.8.

Graph 4.12, shows the molecular stopping power of CH_2Cl_2 vapour as a function of alpha-particle energy.

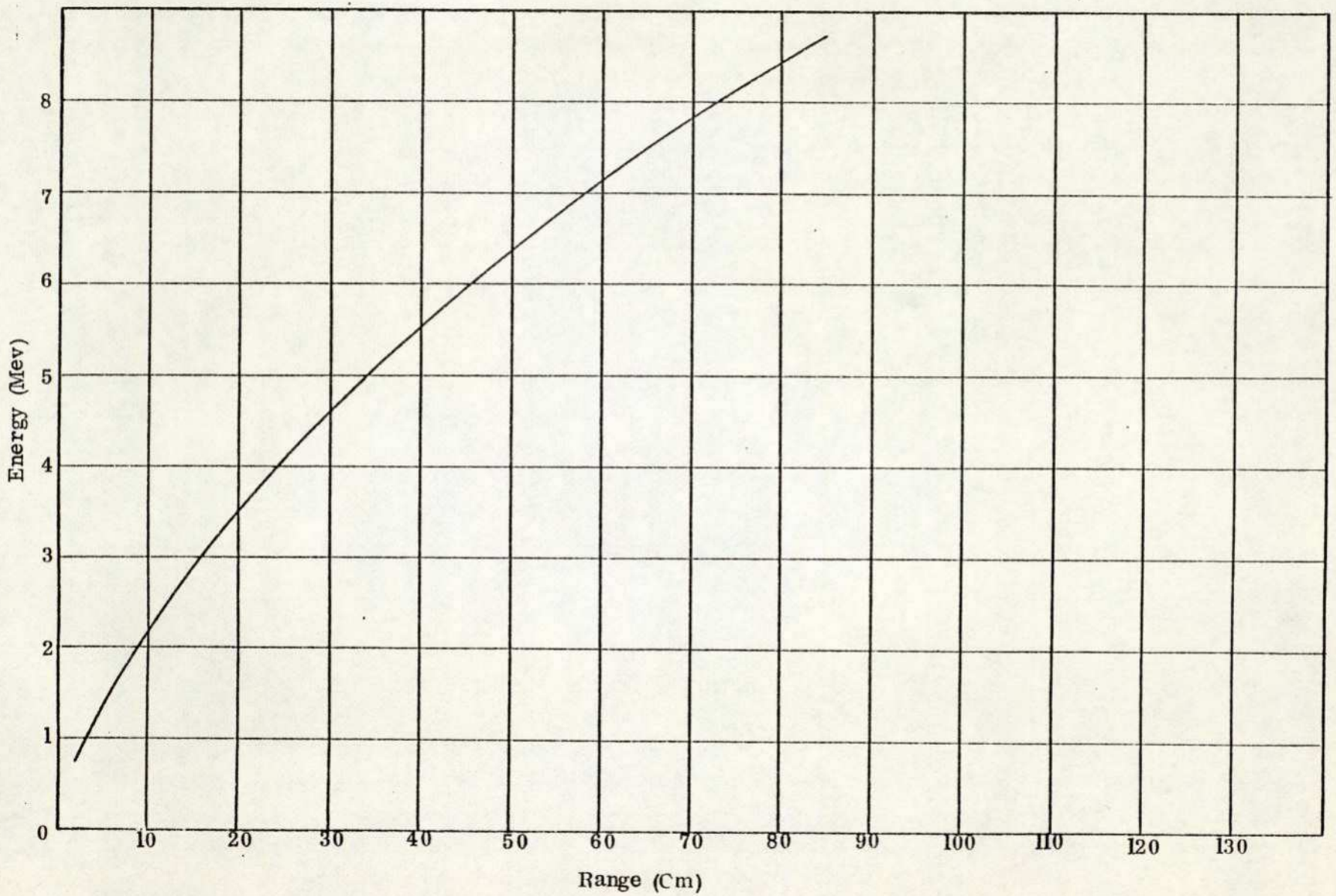

Graph 4.11 Range energy relation for alpha-particles in dichloromethane vapour at 3 cmHg. pressure and 15 ^{o}C.

Energy (Mev)	$\frac{dE}{dx}$ x 10^2 Mev/cm	$\frac{\frac{dE}{dx}}{N}$ experimental 10^{-24} Mev m^2 mol^{-1}	$\frac{\frac{dE}{dx}}{N}$ calculated
1.00	21.45 ± 0.32	21.31 ± 0.32	21.58
1.25	20.19 ± 0.28	20.05 ± 0.28	20.14
1.50	18.93 ± 0.30	18.80 ± 0.30	18.74
1.75	17.51 ± 0.19	17.39 ± 0.19	17.48
2.00	16.22 ± 0.24	16.11 ± 0.24	16.37
2.25	15.27 ± 0.15	15.17 ± 0.15	15.39
2.50	14.36 ± 0.11	14.26 ± 0.11	14.53
2.75	13.55 ± 0.07	13.46 ± 0.07	13.77
3.00	12.89 ± 0.12	12.80 ± 0.12	13.09
3.25	12.38 ± 0.06	12.30 ± 0.06	12.48
3.50	11.79 ± 0.17	11.71 ± 0.17	11.92
3.75	11.30 ± 0.12	11.22 ± 0.12	11.43
4.00	10.83 ± 0.08	10.76 ± 0.08	10.97
4.25	10.46 ± 0.07	10.39 ± 0.07	10.56
4.50	10.12 ± 0.02	10.05 ± 0.02	10.17
4.75	9.79 ± 0.06	9.72 ± 0.06	9.82
5.00	9.42 ± 0.07	9.36 ± 0.07	9.50
5.25	9.16 ± 0.07	9.10 ± 0.07	9.19
5.50	8.88 ± 0.05	8.82 ± 0.05	8.91
5.75	8.59 ± 0.06	8.53 ± 0.06	8.65
6.00	8.33 ± 0.06	8.27 ± 0.06	8.40
6.25	8.09 ± 0.02	8.04 ± 0.02	8.17
6.50	7.86 ± 0.01	7.81 ± 0.01	7.95
6.75	7.63 ± 0.02	7.58 ± 0.02	7.75
7.00	7.40 ± 0.01	7.35 ± 0.01	7.56
7.25	7.20 ± 0.02	7.15 ± 0.02	7.37
7.50	6.97 ± 0.04	6.92 ± 0.04	7.20
7.75	6.73 ± 0.04	6.68 ± 0.04	7.04
8.00	6.54 ± 0.05	6.50 ± 0.05	6.88

Table 4.8 Dichloromethane (CH_2Cl_2) vapour.

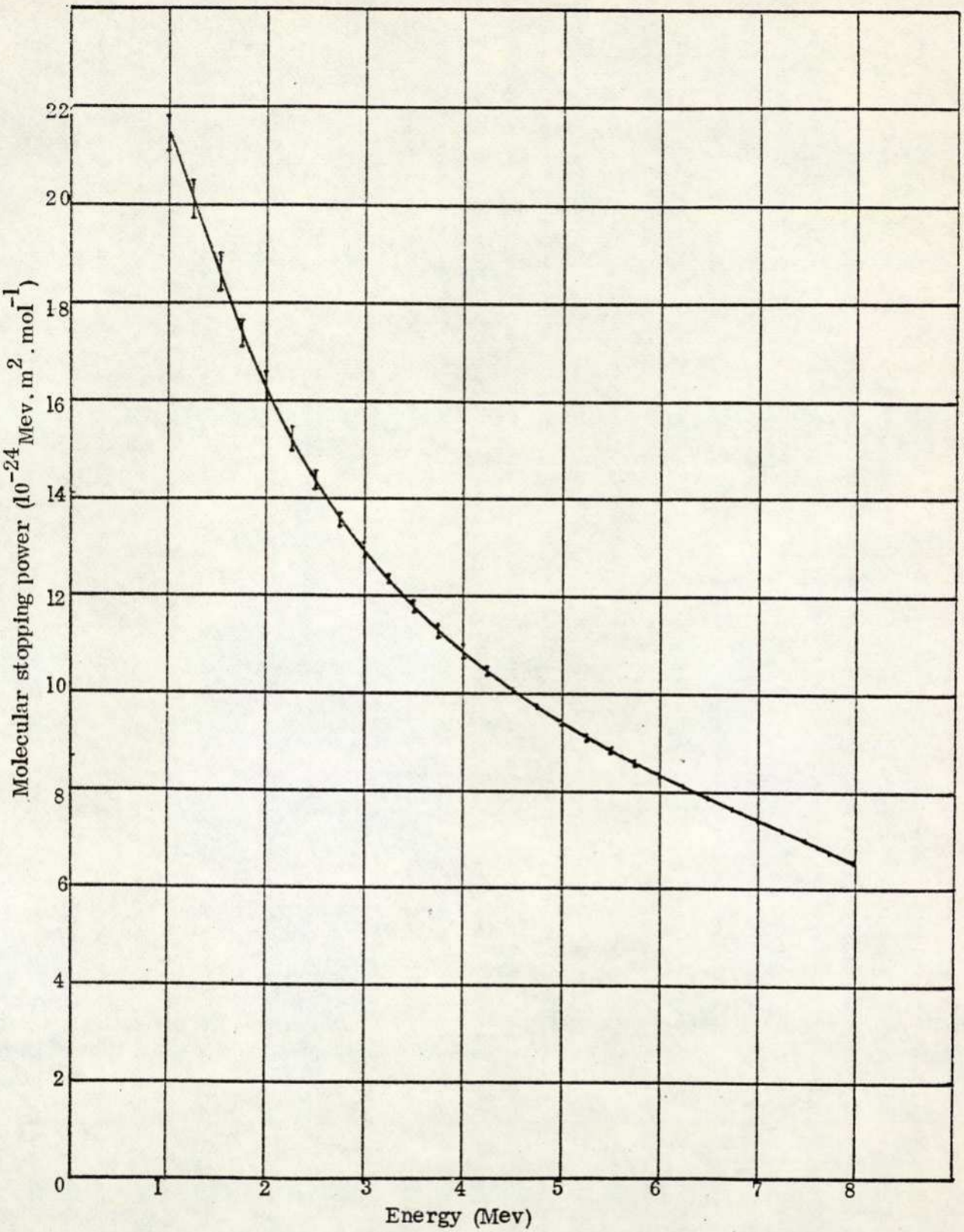

Graph 4.12 Variation of molecular stopping power of dichloromethane vapour with alpha-particle energy.

4.2 g Trichloromethane ($CHCl_3$) vapour

The range-energy relation for alpha-particles in trichloromethane vapour is shown in graph 4.13, and represent the results of all separate sets of vapour measurements by using different sources.

The stopping powers, molecular stopping powers and molecular stopping powers calculated from the uncorrected Bethe formula are shown in table 4.9.

Graph 4.14 shows the molecular stopping power of $CHCl_3$ vapour as a function of alpha-particle energy.

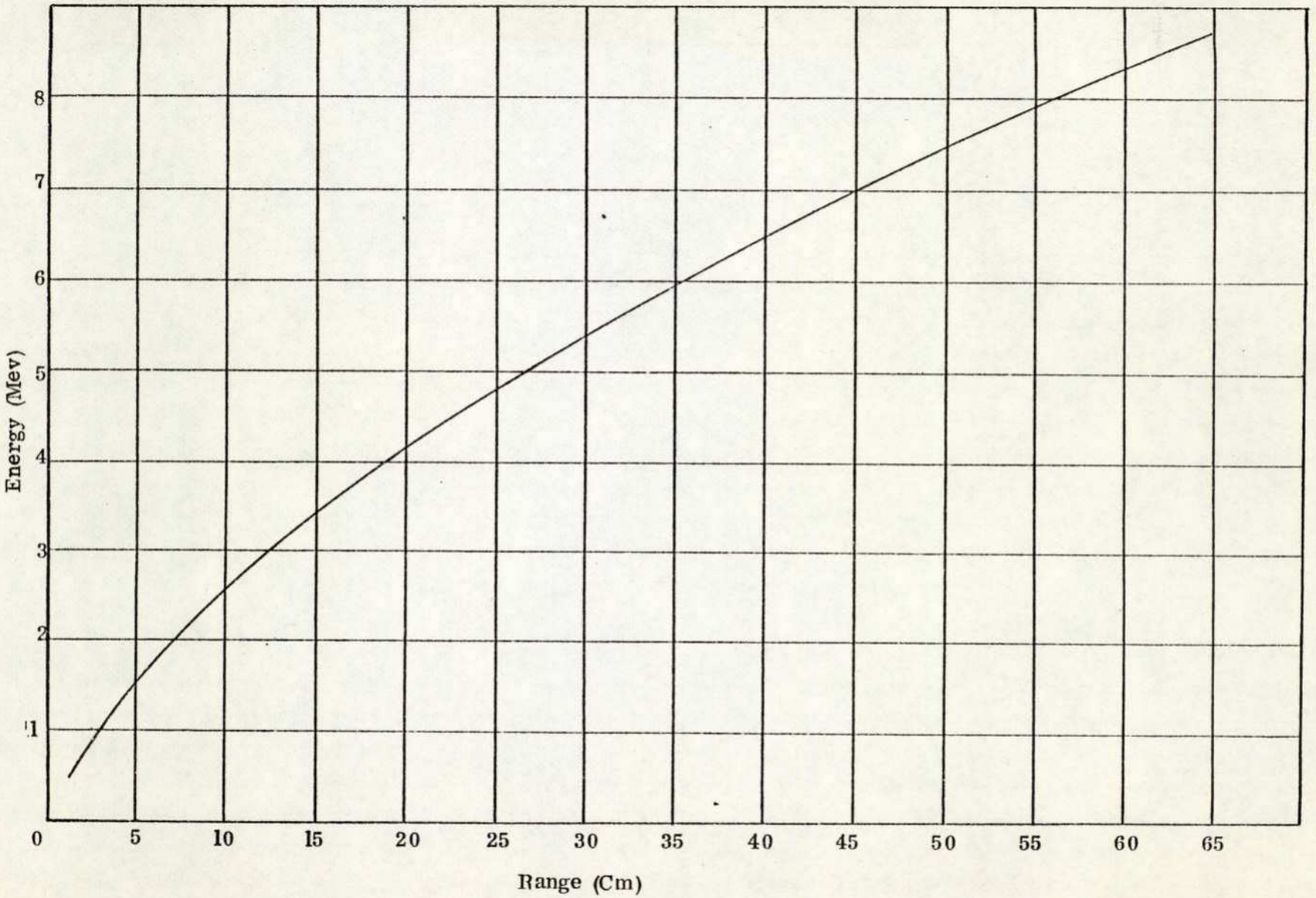

Graph 4.13 Range energy relation for alpha-particles in trichloromethane vapour at 3 cm.Hg. pressure and 15^{o}C.

Energy (Mev)	$\frac{dE}{dx} \times 10^2$ Mev/cm	$\frac{dE}{dx}\frac{1}{N}$ experimental (10^{-14} Mev m^2 mol^{-1})	$\frac{dE}{dx}\frac{1}{N}$ calculated (10^{-14} Mev m^2 mol^{-1})
1.00	27.58 ± 0.40	27.39 ± 0.40	27.57
1.25	26.35 ± 0.70	26.17 ± 0.70	26.02
1.50	24.41 ± 0.50	24.25 ± 0.50	24.38
1.75	22.73 ± 0.22	22.57 ± 0.22	22.86
2.00	21.07 ± 0.28	20.93 ± 0.28	21.48
2.25	19.83 ± 0.30	19.70 ± 0.30	20.26
2.50	18.43 ± 0.19	18.31 ± 0.19	19.17
2.75	17.54 ± 0.29	17.42 ± 0.29	18.20
3.00	16.67 ± 0.18	16.56 ± 0.18	17.33
3.25	15.86 ± 0.28	15.75 ± 0.28	16.54
3.50	14.91 ± 0.23	14.81 ± 0.23	15.83
3.75	14.30 ± 0.27	14.20 ± 0.27	15.18
4.00	13.67 ± 0.28	13.58 ± 0.28	14.59
4.25	13.33 ± 0.08	13.24 ± 0.08	14.05
4.50	12.90 ± 0.13	12.81 ± 0.13	13.55
4.75	12.57 ± 0.07	12.49 ± 0.07	13.09
5.00	12.27 ± 0.03	12.19 ± 0.03	12.67
5.25	11.97 ± 0.03	11.89 ± 0.03	12.27
5.50	11.65 ± 0.03	11.57 ± 0.03	11.90
5.75	11.31 ± 0.04	11.23 ± 0.04	11.55
6.00	10.97 ± 0.04	10.90 ± 0.04	11.23
6.25	10.64 ± 0.07	10.57 ± 0.07	10.93
6.50	10.32 ± 0.12	10.25 ± 0.12	10.64
6.75	10.05 ± 0.15	9.98 ± 0.15	10.37
7.00	9.74 ± 0.21	9.67 ± 0.21	10.11
7.25	9.45 ± 0.25	9.39 ± 0.25	9.87
7.50	9.19 ± 0.25	9.13 ± 0.25	9.64
7.75	8.93 ± 0.24	8.87 ± 0.24	9.43
8.00	8.73 ± 0.17	8.67 ± 0.17	9.22

Table 4.9 Trichloromethane ($CHCl_3$) vapour.

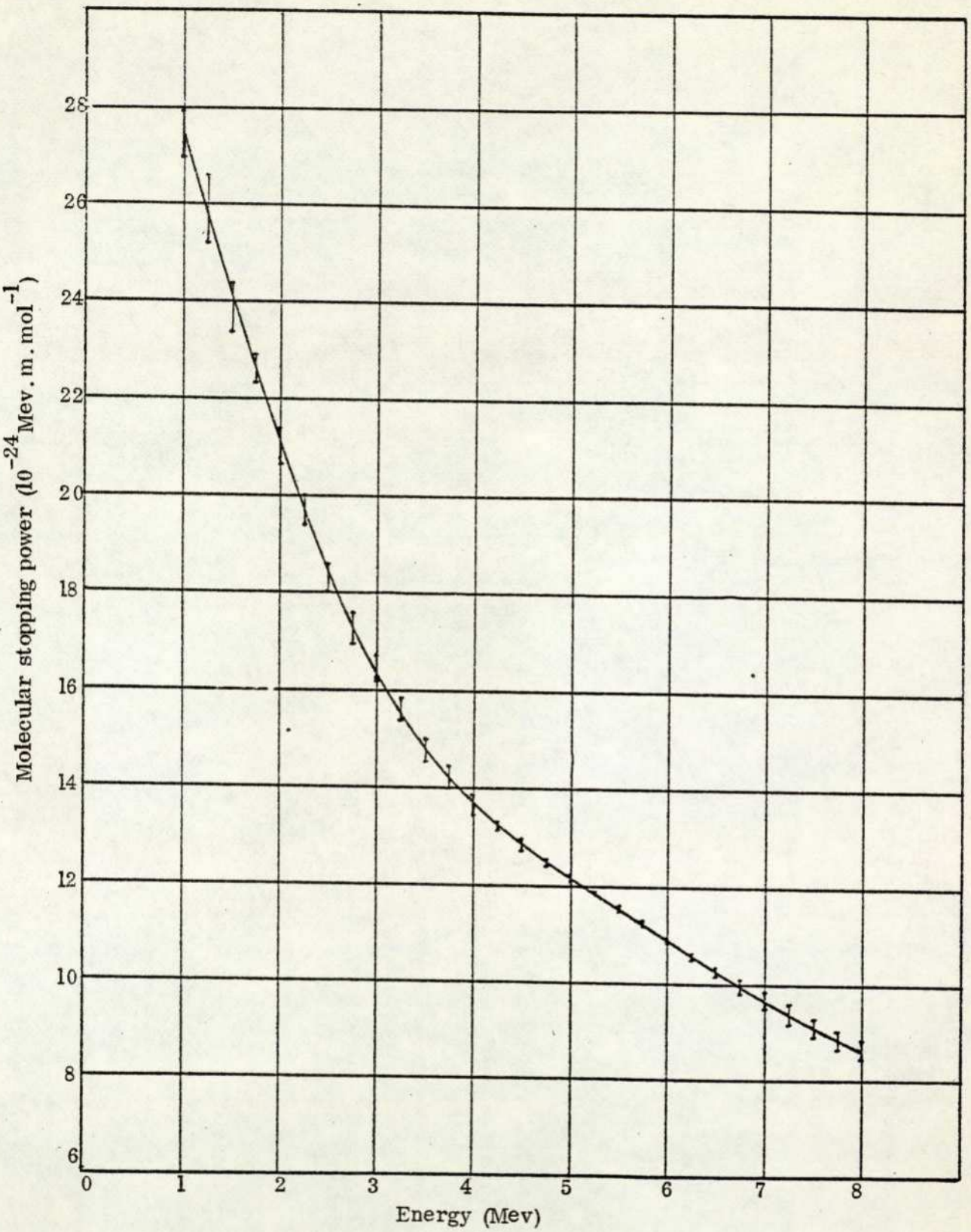

Graph 4.14 Variation of molecular stopping power of trichloromethane vapour with alpha-particle energy.

4.2 h Carbontetrachloride (CCl_4) Vapour

The range-energy relation for alpha-particles in carbontetrachloride vapour is shown in graph 4.15 and represents the results of all separate sets of vapour measurements by using different sources.

The stopping powers, molecular stopping powers and molecular stopping powers calculated from the uncorrected Bethe formula are shown in table 4.10.

Graph 4.16, shows the molecular stopping power of CCl_4 vapour as a function of alpha-particle energy.

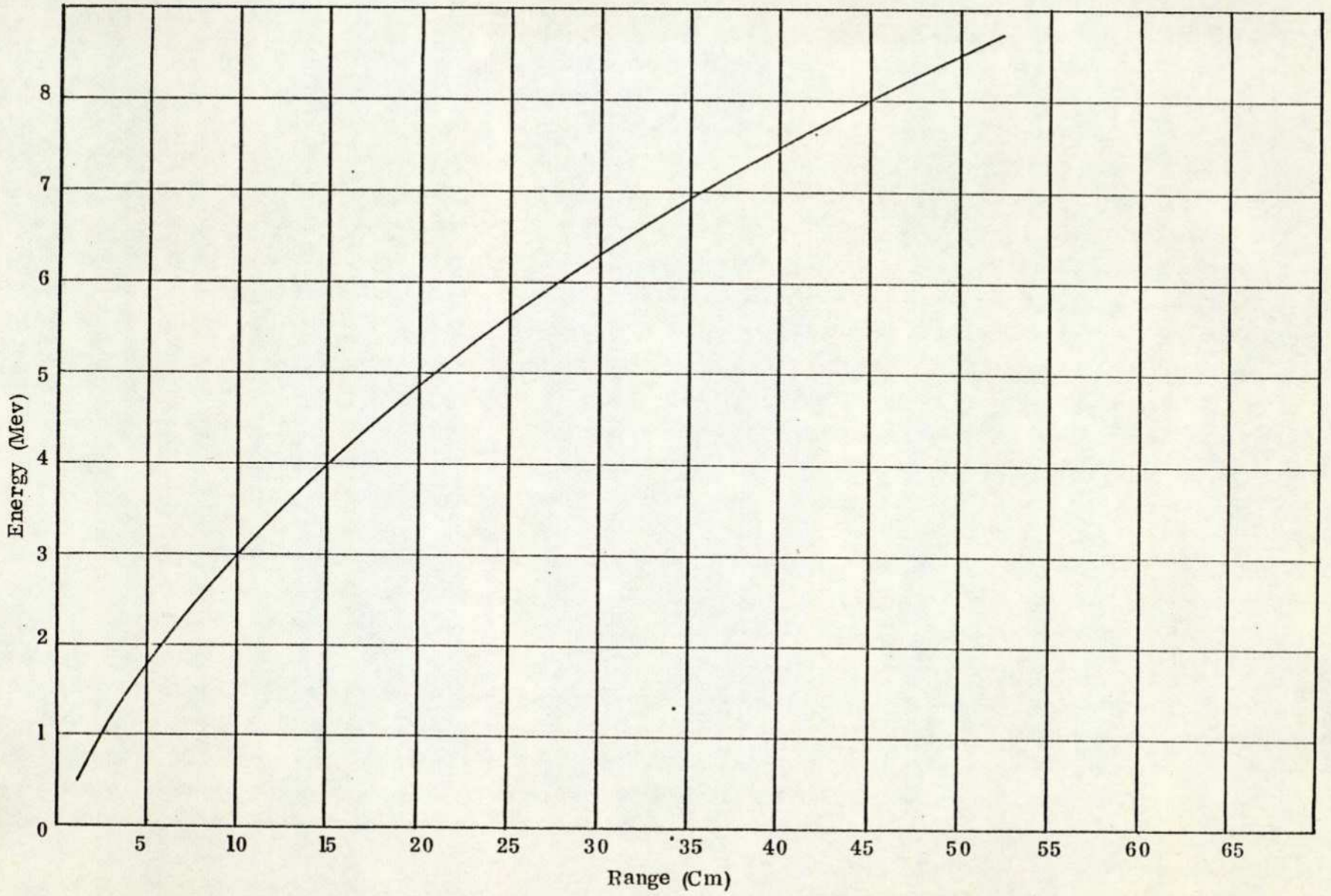

Graph 4.15 Range energy relation for alpha-particles in carbontetrachloride vapour at 3 cm.Hg pressure and 15 ^{o}C.

Energy (Mev)	$\frac{dE}{dx}$ x 10^2 Mev/cm	$\frac{dE}{dx}$ experimental	$\frac{dE}{dx}$ calculated
		10^{-24} Mev m^2 mol^{-1}	
		N	N
1.00	33.71 ± 0.35	33.48 ± 0.35	33.62
1.25	31.95 ± 0.28	31.73 ± 0.28	31.95
1.50	30.05 ± 0.30	29.85 ± 0.30	30.07
1.75	28.18 ± 0.22	27.99 ± 0.22	28.27
2.00	26.47 ± 0.25	26.29 ± 0.25	26.63
2.25	24.84 ± 0.14	24.67 ± 0.14	25.16
2.50	23.55 ± 0.20	23.39 ± 0.20	23.84
2.75	22.37 ± 0.24	22.22 ± 0.24	22.65
3.00	21.32 ± 0.12	21.18 ± 0.12	21.59
3.25	20.34 ± 0.21	20.20 ± 0.21	20.62
3.50	19.47 ± 0.15	19.34 ± 0.15	19.75
3.75	18.72 ± 0.20	18.59 ± 0.20	18.96
4.00	18.03 ± 0.08	17.91 ± 0.08	18.23
4.25	17.46 ± 0.12	17.34 ± 0.12	17.56
4.50	16.87 ± 0.09	16.76 ± 0.09	16.95
4.75	16.30 ± 0.10	16.19 ± 0.10	16.38
5.00	15.75 ± 0.14	15.64 ± 0.14	15.85
5.25	15.20 ± 0.08	15.10 ± 0.08	15.36
5.50	14.72 ± 0.08	14.62 ± 0.08	14.90
5.75	14.25 ± 0.05	14.15 ± 0.05	14.47
6.00	13.80 ± 0.15	13.71 ± 0.15	14.07
6.25	13.38 ± 0.12	13.29 ± 0.12	13.69
6.50	13.04 ± 0.10	12.95 ± 0.10	13.34
6.75	12.79 ± 0.05	12.70 ± 0.06	13.00
7.00	12.52 ± 0.08	12.44 ± 0.08	12.68
7.25	12.26 ± 0.11	12.18 ± 0.11	12.38
7.50	11.98 ± 0.15	11.90 ± 0.15	12.10
7.75	11.73 ± 0.22	11.65 ± 0.22	11.83
8.00	11.56 ± 0.23	11.48 ± 0.23	11.57

Table 4.10 Carbontetrachloride (CCl_4) Vapour

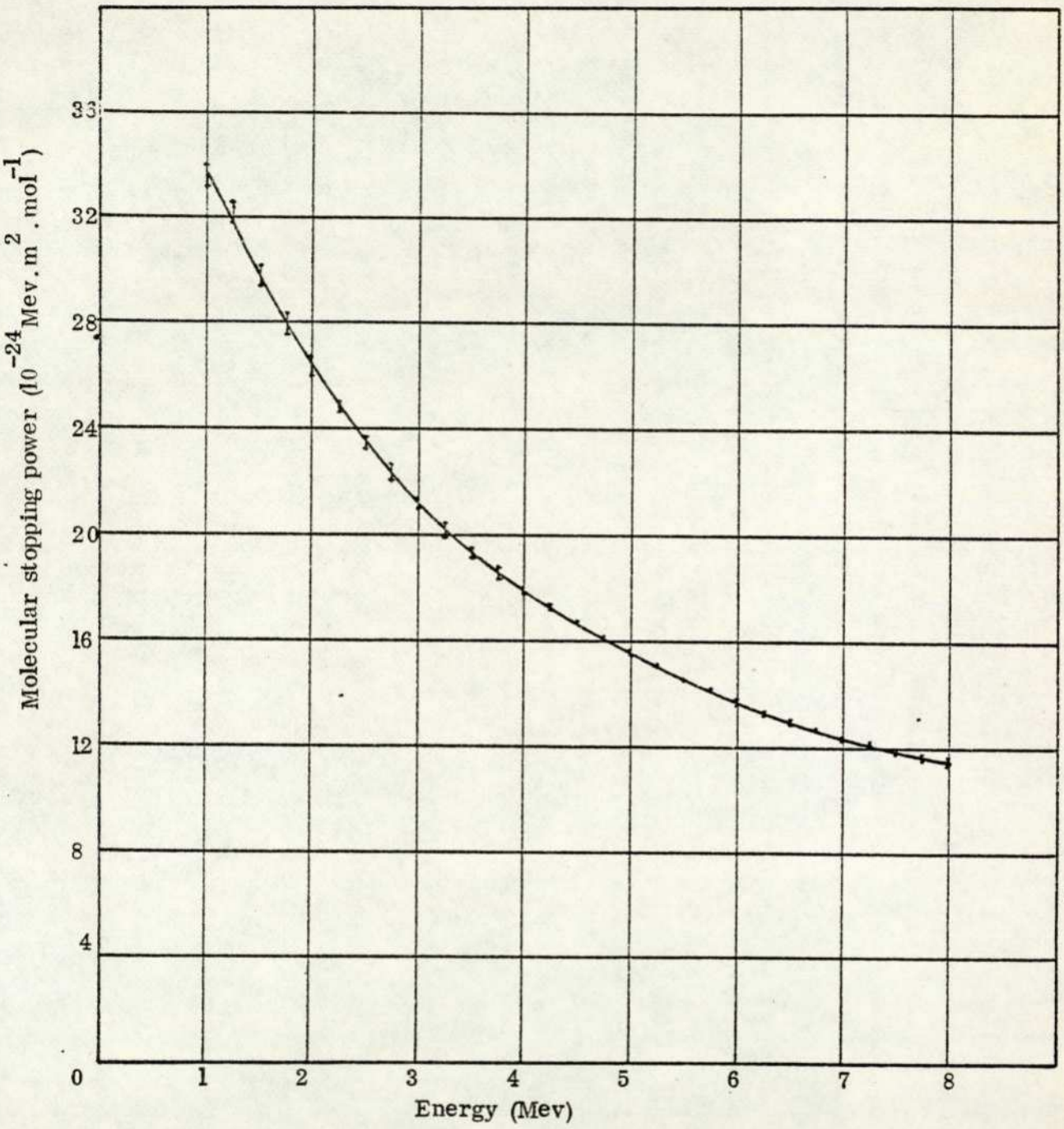

Graph 4.16 Variation of molecular stopping power of carbontetrachloride vapour with alpha-particle energy.

4.3 The results of experimental measurements with liquid (method I)

4.3a Water (H_2O) liquid

For the water liquid measurements with method I, graph 4.18 the molecular stopping power values in the energy region 4-6 Mev do not appear to be showing a consistently smooth decrease with increasing energy. This does not agree with the form of the vapour curve nor with other published work and since this does not occur either with other liquids this may not be a real effect. Initially difficulties were experienced in using this method with water due to bubble formation within the steps. This problem seemed to be overcome, but there may still have been irregularities in the liquid-solid interface at the corners of the steps which could have led to inconsistencies.

The range-energy relation for alpha-particles in water liquid is shown in graph 4.17 and represents the results of all separate sets of liquid measurements with ^{212}Bi source.

The stopping powers, molecular stopping powers and molecular stopping powers calculated from the uncorrected Bethe formula at various alpha-particle energies for water liquid are shown in table 4.11.

Graph 4.18 shows the molecular stopping power of water liquid as a function of alpha-particle energy.

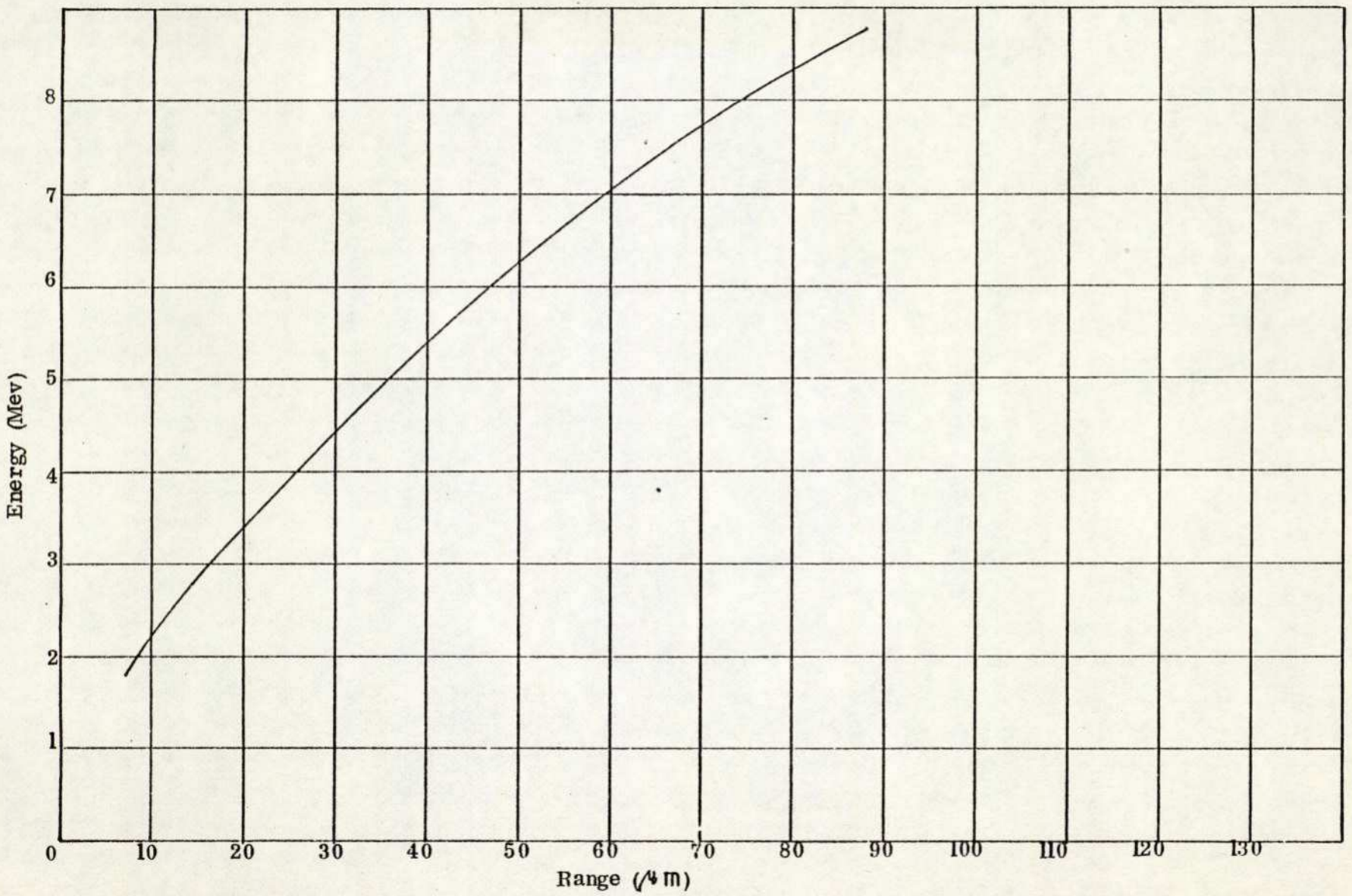

Graph 4.17 Range-energy relation for alpha-particles in water liquid (method I).

Energy (Mev)	$\frac{dE}{dx} \times 10^2$ Mev/μ	10^{-24} Mev m^2 mol^{-1} $\frac{dE}{dx}/N$ experimental	$\frac{dE}{dx}/N$ calculated
1.00			7.97
1.25			7.06
1.50			6.34
1.75			5.77
2.00	16.48 ± 0.27	4.93 ± 0.08	5.29
2.25	15.34 ± 0.72	4.59 ± 0.22	4.93
2.50	14.24 ± 0.72	4.26 ± 0.22	4.57
2.25	12.97 ± 0.40	3.88 ± 0.12	4.30
3.00	12.03 ± 0.36	3.68 ± 0.11	4.06
3.25	11.37 ± 0.16	3.44 ± 0.05	3.85
3.50	10.93 ± 0.03	3.27 ± 0.01	3.64
3.75	10.70 ± 0.07	3.20 ± 0.02	3.46
4.00	10.53 ± 0.07	3.15 ± 0.02	3.31
4.25	10.33 ± 0.07	3.09 ± 0.02	3.19
4.50	10.10 ± 0.10	3.02 ± 0.03	3.04
4.75	9.90 ± 0.03	2.96 ± 0.01	2.93
5.00	9.59 ± 0.03	2.87 ± 0.01	2.82
5.25	9.29 ± 0.07	2.78 ± 0.02	2.72
5.50	8.89 ± 0.03	2.66 ± 0.01	2.63
5.75	8.56 ± 0.10	2.56 ± 0.03	2.54
6.00	8.19 ± 0.03	2.45 ± 0.03	2.46
6.25	7.96 ± 0.03	2.38 ± 0.01	2.39
6.50	7.79 ± 0.03	2.33 ± 0.01	2.32
6.75	7.56 ± 0.03	2.26 ± 0.01	2.26
7.00	7.39 ± 0.03	2.21 ± 0.01	2.20
7.25	7.15 ± 0.03	2.14 ± 0.01	2.14
7.50	6.92 ± 0.03	2.07 ± 0.01	2.09
7.75	6.62 ± 0.03	1.98 ± 0.01	2.03
8.00	6.28 ± 0.03	1.88 ± 0.01	1.99
8.25	5.95 ± 0.07	1.78 ± 0.02	1.95
8.50	5.62 ± 0.07	1.68 ± 0.02	1.91

Table 4.11 Water (H_2O) Liquid

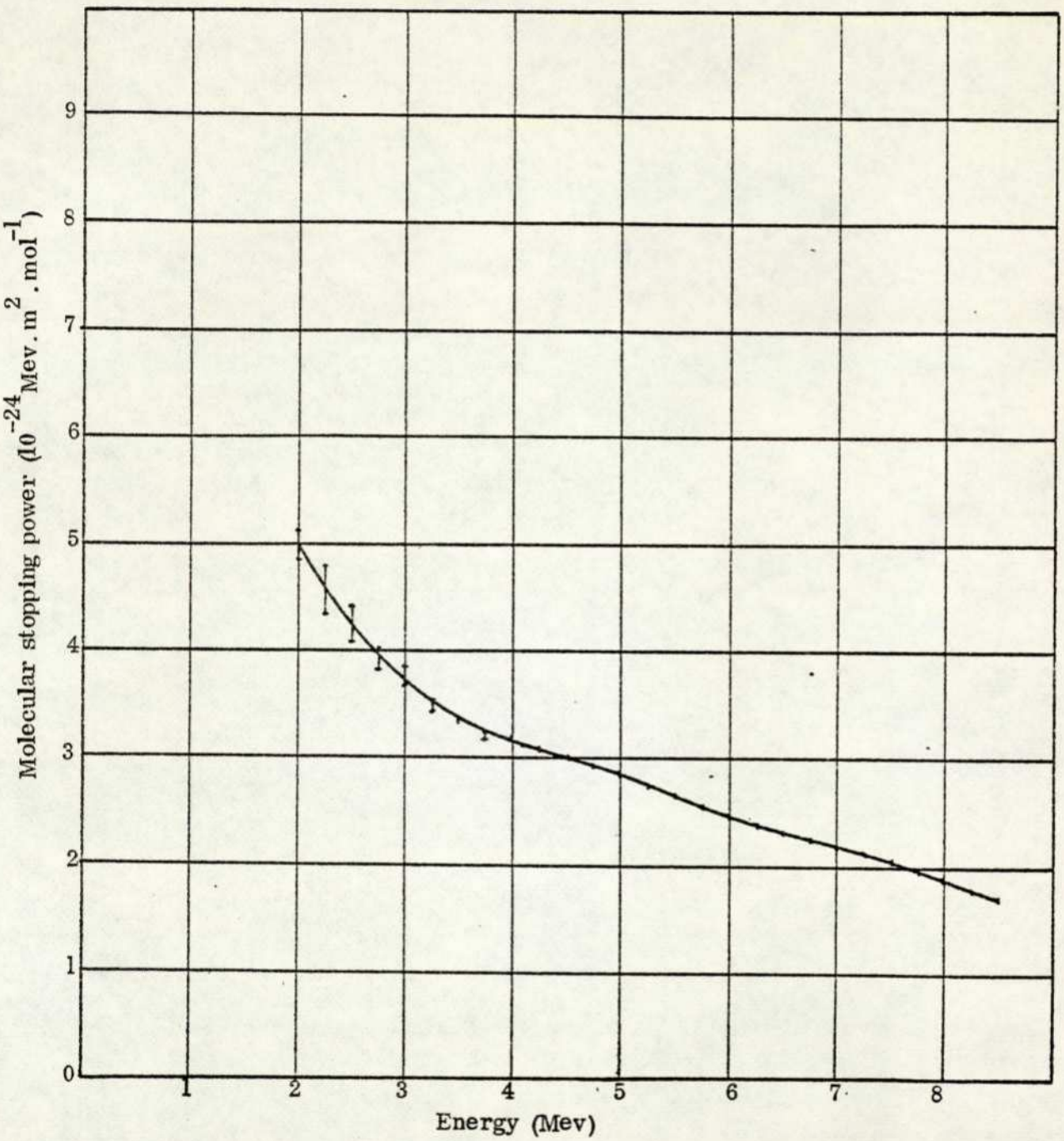

Graph 4.18 Variation of molecular stopping power of water liquid (method I) with alpha-particle energy.

4.3b Methyl alcohol (CH_3OH) liquid

The range-energy relation for alpha-particles in methyl alcohol liquid is shown in graph 4.19 and represents the results of all separate sets of liquid measurements with ^{212}Bi source.

The stopping powers, molecular stopping powers and molecular stopping powers calculated from the uncorrected Bethe formula at various alpha-particle energies for methyl alcohol liquid are shown in table 4.12.

Graph 4.20 shows the molecular stopping power of methyl alcohol liquid as a function of alpha-particle energy.

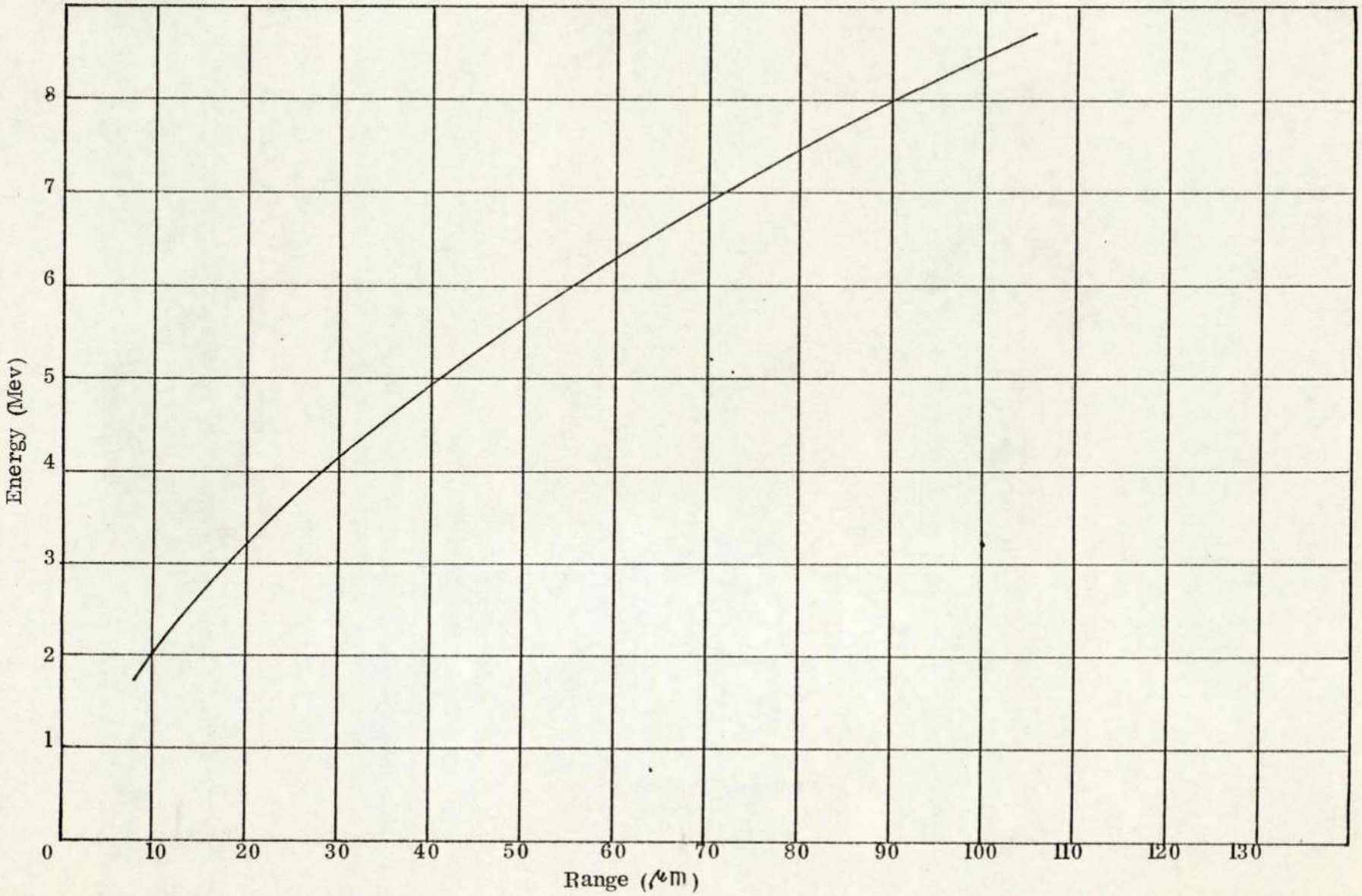

Graph 4.19 Range-energy relation for alpha-particles in methyl alcohol liquid (method I)

Energy (Mev)	$\frac{dE}{dx} \times 10^2$ Mev/μ	10^{-24} Mev m^2 mol^{-1} $\frac{dE}{dx}/N$ experimental	$\frac{dE}{dx}/N$ calculated
1.00			15.01
1.25			13.24
1.50			11.87
1.75			10.78
2.00	14.33 ± 0.74	9.63 ± 0.50	9.89
2.25	13.48 ± 0.52	9.06 ± 0.35	9.16
2.50	12.08 ± 0.13	8.12 ± 0.09	8.53
2.75	11.47 ± 0.27	7.71 ± 0.18	7.99
3.00	10.56 ± 0.12	7.10 ± 0.08	7.53
3.25	9.88 ± 0.21	6.64 ± 0.14	7.12
3.50	9.30 ± 0.34	6.25 ± 0.23	6.76
3.75	8.90 ± 0.06	5.98 ± 0.04	6.43
4.00	8.49 ± 0.03	5.71 ± 0.02	6.14
4.25	8.23 ± 0.03	5.53 ± 0.02	5.88
4.50	8.03 ± 0.06	5.40 ± 0.04	5.64
4.75	7.80 ± 0.03	5.24 ± 0.02	5.42
5.00	7.51 ± 0.09	5.05 ± 0.06	5.22
5.25	7.36 ± 0.04	4.95 ± 0.03	5.04
5.50	7.14 ± 0.06	4.80 ± 0.04	4.87
5.75	6.89 ± 0.06	4.63 ± 0.04	4.71
6.00	6.65 ± 0.03	4.47 ± 0.02	4.56
6.25	6.49 ± 0.09	4.36 ± 0.06	4.42
6.50	6.26 ± 0.01	4.21 ± 0.01	4.29
6.75	6.07 ± 0.01	4.08 ± 0.01	4.17
7.00	5.89 ± 0.03	3.96 ± 0.02	4.06
7.25	5.70 ± 0.01	3.83 ± 0.01	3.95
7.50	5.50 ± 0.03	3.70 ± 0.02	3.85
7.75	5.28 ± 0.06	3.55 ± 0.04	3.76
8.00	5.09 ± 0.09	3.42 ± 0.06	3.67

Table 4.12 Methyl alcohol (CH_3OH) Liquid

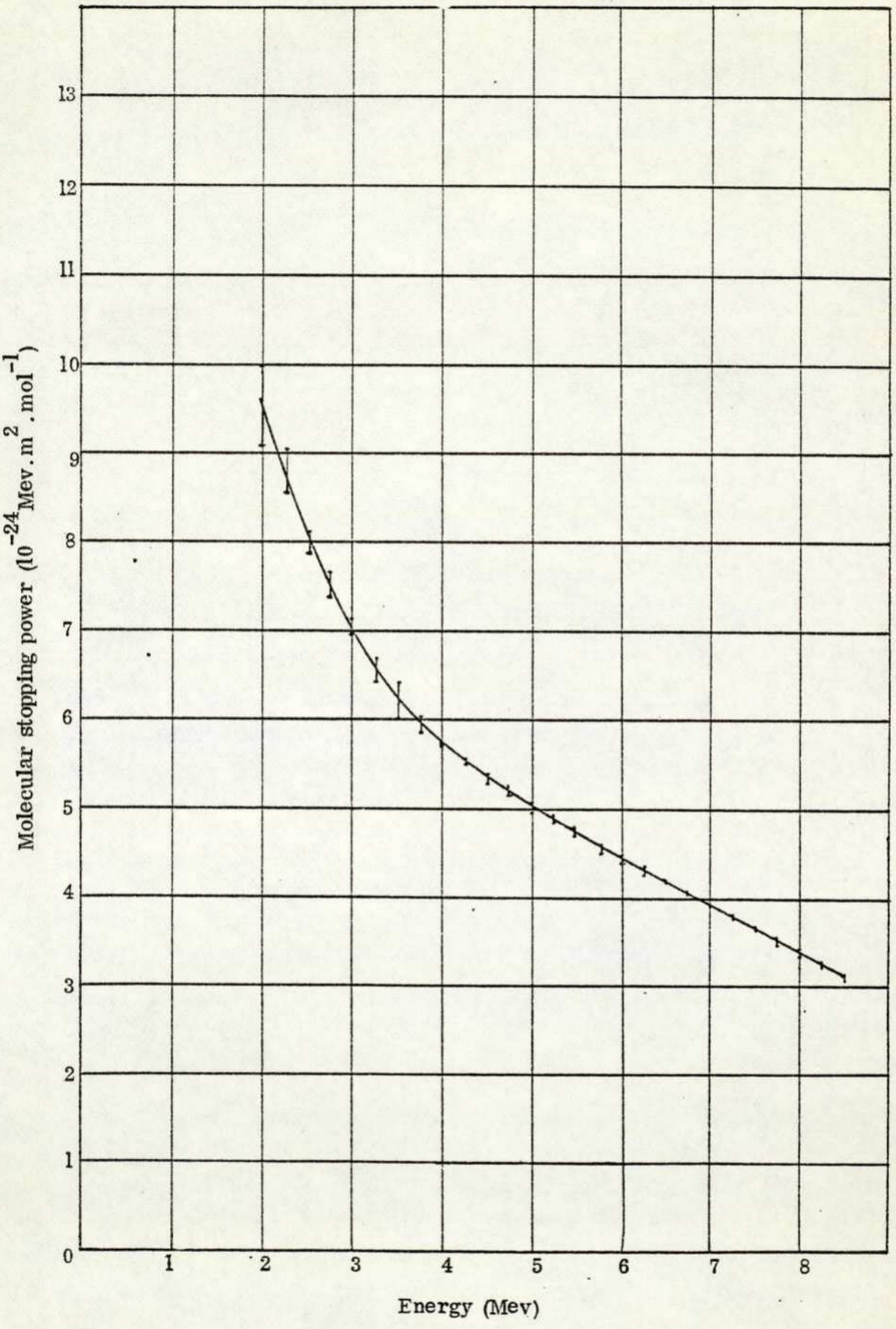

Graph 4.20 Variation of molecular stopping power of methyl alcohol liquid (method I) with alpha-particle energy.

4.3c Ethyl alcohol (C_2H_5OH) liquid.

The range-energy relation for alpha-particles in ethyl alcohol liquid is shown in graph 4.21 and represents the results of all separate sets of liquid measurements with ^{212}Bi source.

The stopping powers, molecular stopping powers and molecular stopping powers calculated from the uncorrected Bethe formula at various alpha-particle energies for ethyl alcohol liquid are shown in table 4.13.

Graph 4.22 shows the molecular stopping power of C_2H_5OH liquid as a function of alpha-particle energy.

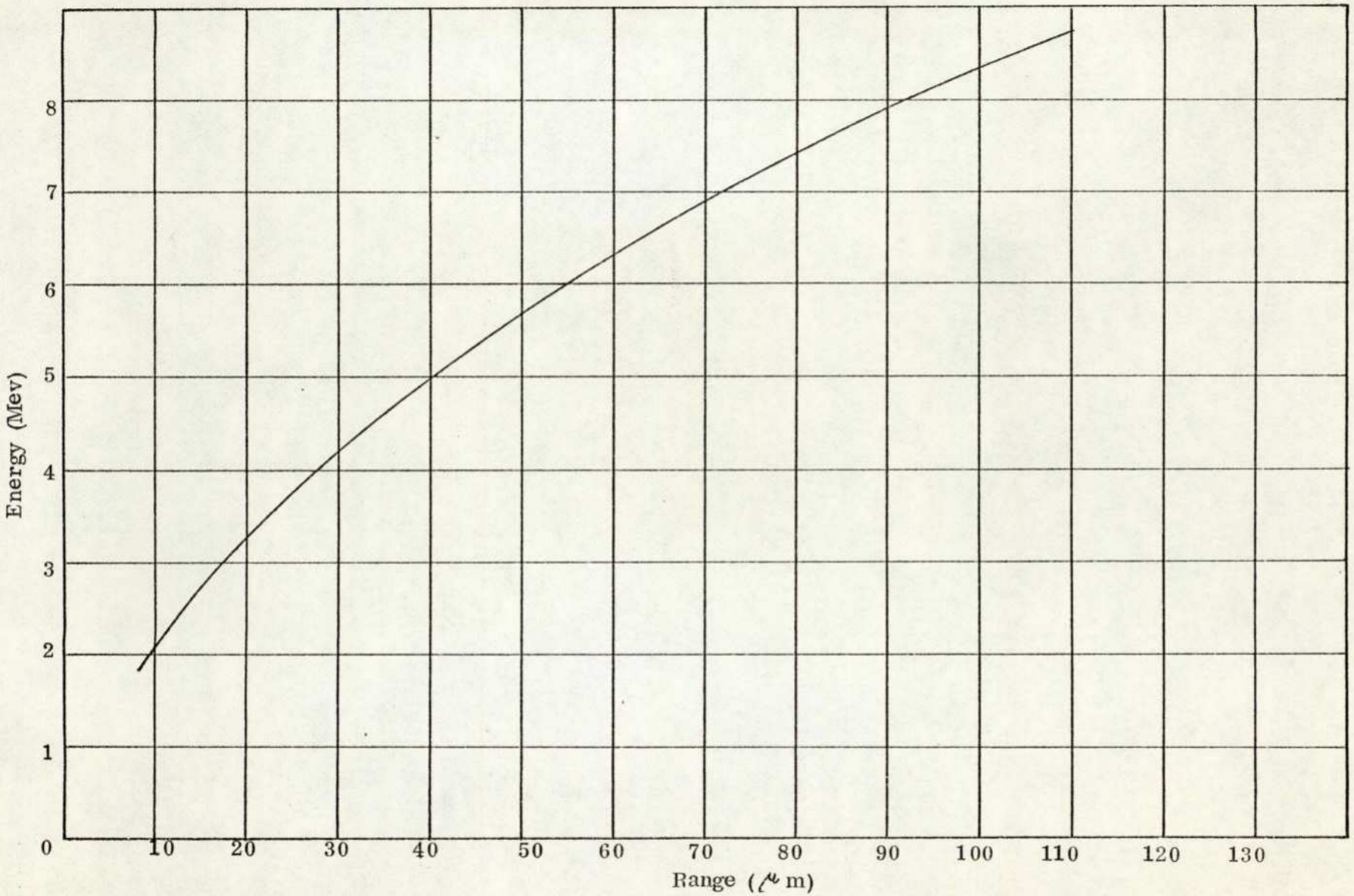

Graph 4.21. Range-energy relation for alpha-particles in ethyl alcohol liquid (method I).

Energy (Mev)	$\frac{dE}{dx} \times 10^2$ Mev/μ	10^{-24} Mev m^2 mol^{-1} $\frac{dE}{dx}\frac{1}{N}$ experimental	$\frac{dE}{dx}\frac{1}{N}$ calculated
2.00	13.71 ± 0.41	13.29 ± 0.40	14.47
2.25	12.81 ± 0.52	12.41 ± 0.50	13.38
2.50	12.00 ± 0.52	11.63 ± 0.50	12.46
2.75	11.14 ± 0.40	10.80 ± 0.39	11.68
3.00	10.50 ± 0.27	10.18 ± 0.26	10.99
3.25	10.03 ± 0.22	9.72 ± 0.21	10.39
3.50	9.55 ± 0.12	9.25 ± 0.12	9.86
3.75	9.18 ± 0.12	8.90 ± 0.12	9.39
4.00	8.79 ± 0.20	8.52 ± 0.20	8.96
4.25	8.44 ± 0.15	8.18 ± 0.15	8.57
4.50	8.12 ± 0.10	7.87 ± 0.10	8.23
4.75	7.83 ± 0.08	7.59 ± 0.08	7.91
5.00	7.53 ± 0.09	7.30 ± 0.09	7.63
5.25	7.24 ± 0.12	7.02 ± 0.12	7.34
5.50	6.94 ± 0.09	6.73 ± 0.09	7.09
5.75	6.70 ± 0.10	6.49 ± 0.10	6.85
6.00	6.45 ± 0.12	6.25 ± 0.12	6.65
6.25	6.23 ± 0.10	6.04 ± 0.10	6.45
6.50	6.07 ± 0.10	5.88 ± 0.10	6.26
6.75	5.87 ± 0.07	5.69 ± 0.07	6.08
7.00	5.68 ± 0.06	5.50 ± 0.06	5.92
7.25	5.48 ± 0.06	5.31 ± 0.06	5.76
7.50	5.29 ± 0.05	5.13 ± 0.05	5.61
7.75	5.12 ± 0.10	4.96 ± 0.10	5.47
8.00	4.97 ± 0.11	4.82 ± 0.11	5.34

Table 4.13 Ethyl alcohol (C_2H_5OH) Liquid

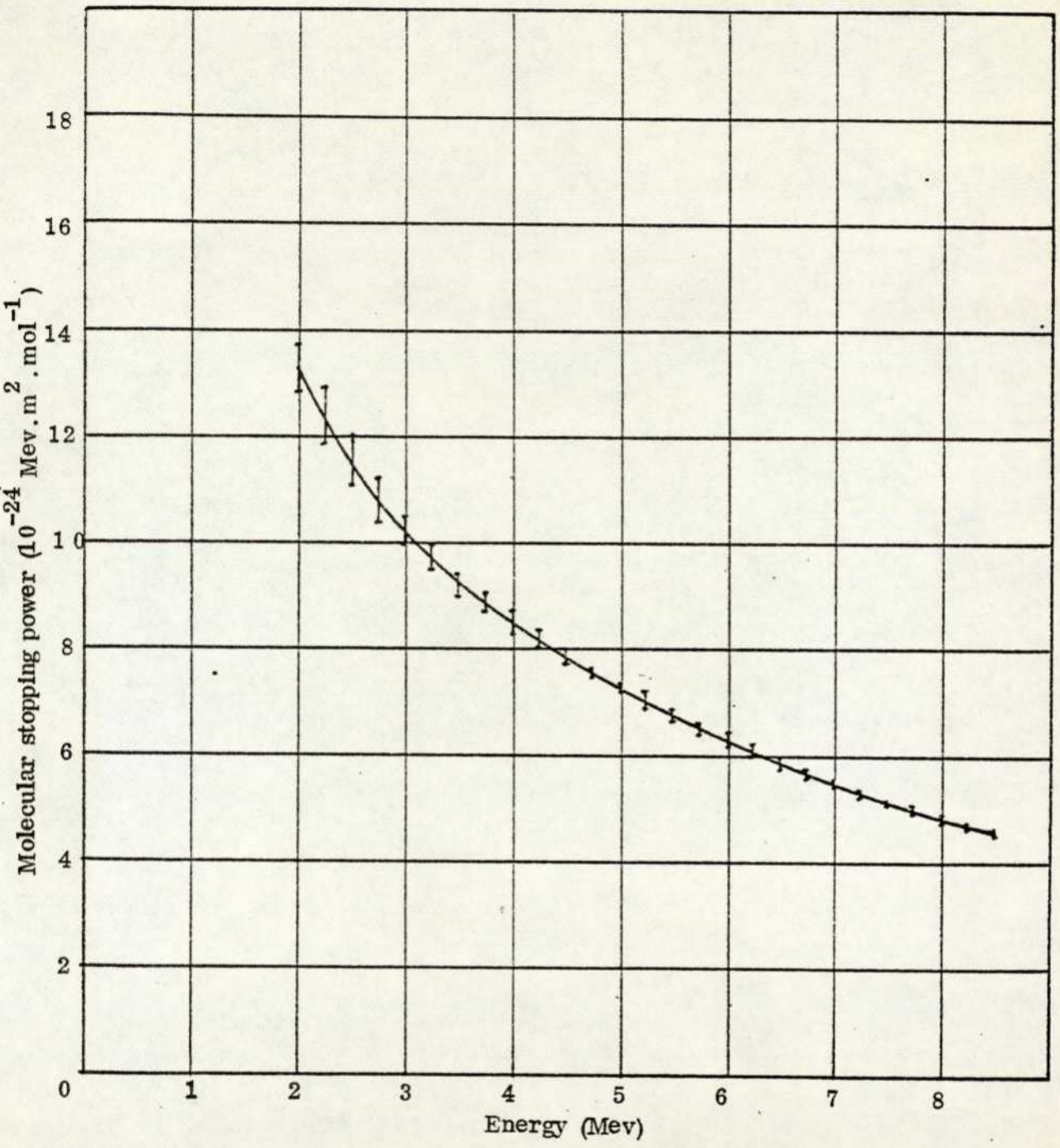

Graph 4.22. Variation of molecular stopping power of ethyl alcohol liquid (method I) with alpha-particle energy.

4.3d Propyl alcohol $(CH_3)_2CHOH$ liquid.

The range-energy relation for alpha-particles in propyl alcohol liquid is shown in graph 4.23 and represents the results of all separate sets of liquid measurements with ^{212}Bi source.

The stopping powers, molecular stopping powers and molecular stopping powers calculated from the uncorrected Bethe formula at various alpha-particle energies for propyl alcohol liquid are shown in table 4.14.

Graph 4.24 shows the molecular stopping power of $(CH_3)_2$ CHOH liquid as a function of alpha-particle energy.

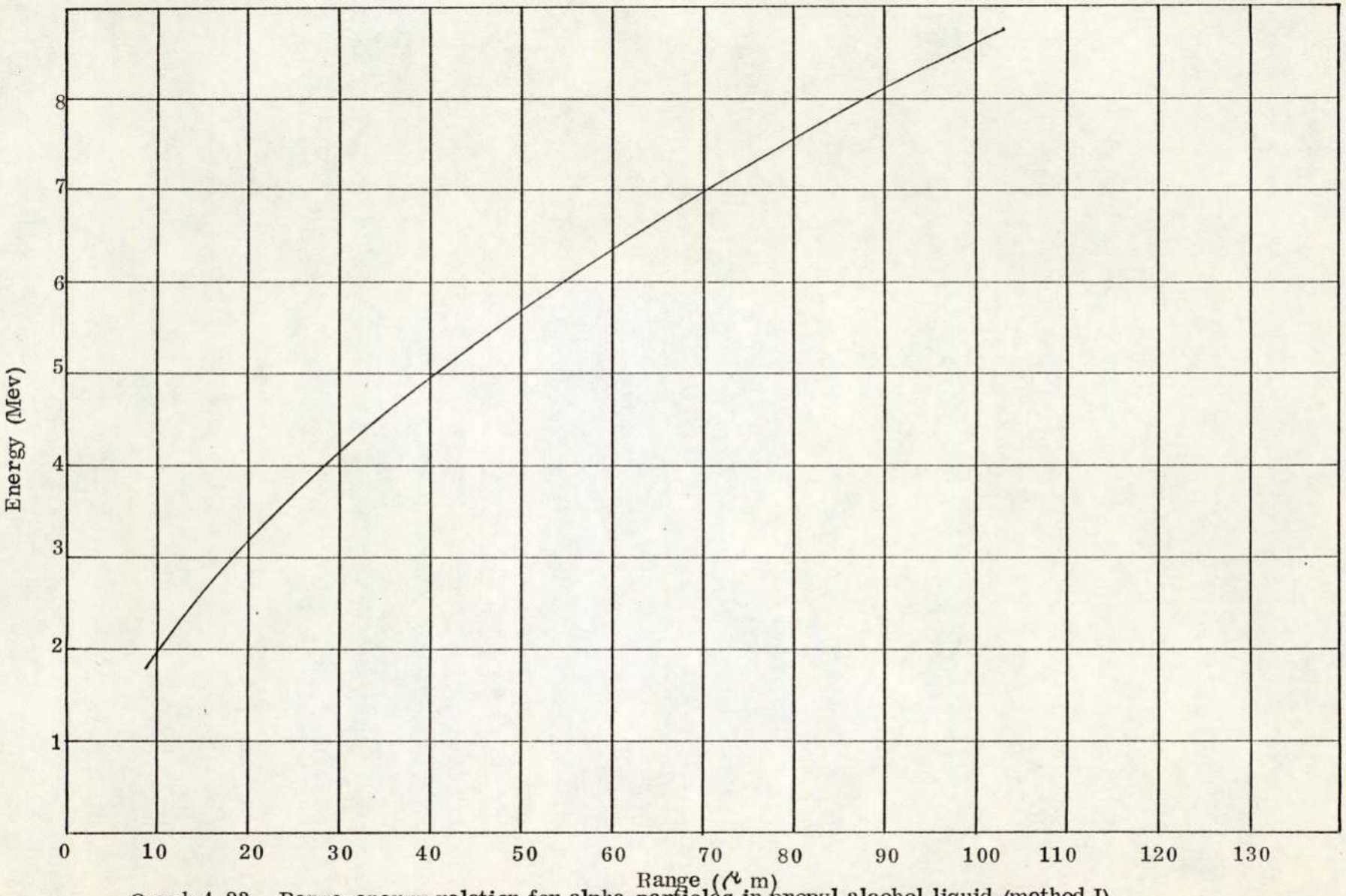

Graph 4.23. Range-energy relation for alpha-particles in propyl alcohol liquid (method I).

Energy (Mev)	$\frac{dE}{dx} \times 10^2$ Mev/μ	10^{-24} Mev m^2 mol^{-1} $\frac{dE}{dx}\frac{1}{N}$ experimental	$\frac{dE}{dx}\frac{1}{N}$ calculated
2.00	14.01 ± 0.24	17.81 ± 0.31	19.02
2.25	13.14 ± 0.12	16.70 ± 0.15	17.59
2.50	12.38 ± 0.20	15.74 ± 0.26	16.38
2.75	11.57 ± 0.07	14.70 ± 0.09	15.34
3.00	10.79 ± 0.16	13.71 ± 0.20	14.44
3.25	10.17 ± 0.10	12.93 ± 0.13	13.65
3.50	9.71 ± 0.08	12.34 ± 0.10	12.95
3.75	9.32 ± 0.15	11.84 ± 0.19	12.33
4.00	8.93 ± 0.17	11.35 ± 0.21	11.77
4.25	8.62 ± 0.14	10.95 ± 0.18	11.26
4.50	8.28 ± 0.14	10.52 ± 0.18	10.80
4.75	7.91 ± 0.08	10.05 ± 0.10	10.38
5.00	7.64 ± 0.17	9.71 ± 0.22	9.99
5.25	7.42 ± 0.16	9.43 ± 0.20	9.64
5.50	7.23 ± 0.13	9.19 ± 0.17	9.31
5.75	7.08 ± 0.15	9.00 ± 0.19	9.01
6.00	6.86 ± 0.16	8.72 ± 0.20	8.72
6.25	6.69 ± 0.13	8.50 ± 0.16	8.46
6.50	6.49 ± 0.17	8.25 ± 0.21	8.21
6.75	6.22 ± 0.10	7.90 ± 0.13	7.98
7.00	6.08 ± 0.18	7.73 ± 0.23	7.75
7.25	5.86 ± 0.19	7.45 ± 0.19	7.56
7.50	5.62 ± 0.13	7.14 ± 0.17	7.37
7.75	5.37 ± 0.16	6.82 ± 0.20	7.18
8.00	5.16 ± 0.17	6.56 ± 0.21	7.01

Table 4.14 Propyl alcohol $(CH_3)_2CHOH$ Liquid

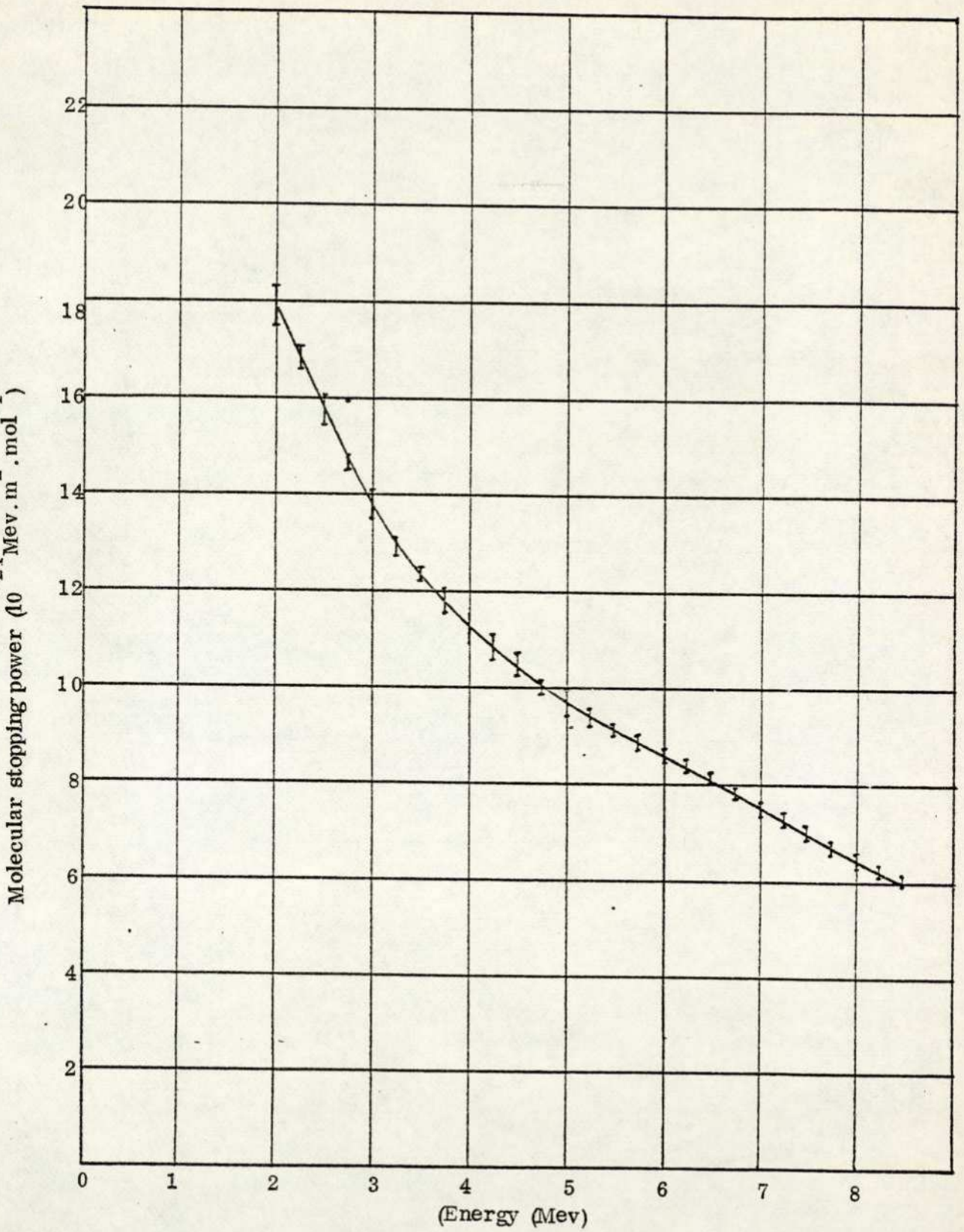

Graph 4.24. Variation of molecular stopping power of propyl alcohol liquid (method I) with alpha-particle energy.

4.4 The results of experimental measurements with liquid (method II)

4.4a Methyl alcohol (CH_3OH) liquid

The range-energy relation for alpha-particles in methyl alcohol liquid is shown in graph 4.25 and represent the results of all separate sets of liquid measurements by using different sources.

The stopping powers, molecular stopping powers and molecular stopping powers calculated from the uncorrected Bethe formula at various alpha-particle energies for methyl alcohol liquid are shown in table 4.15.

Graph 4.26 shows the molecular stopping power of CH_3OH liquid as a function of alpha-particle energy.

Graph 4.25. Range-energy relation for alpha-particles in methyl alcohol liquid (method II).

Energy (Mev)	$\frac{dE}{dx} \times 10^2$ Mev/μ	$\frac{dE}{dx}$ experimental / N (10^{-24} Mev m^2 mol^{-1})	$\frac{dE}{dx}$ calculated / N (10^{-24} Mev m^2 mol^{-1})
1.00	19.19 ± 0.60	12.90 ± 0.40	15.01
1.25	17.90 ± 0.25	12.03 ± 0.17	13.24
1.50	16.65 ± 0.12	11.19 ± 0.08	11.87
1.75	15.35 ± 0.36	10.32 ± 0.24	10.78
2.00	14.47 ± 0.37	9.73 ± 0.25	9.89
2.25	13.55 ± 0.30	9.11 ± 0.20	9.16
2.50	12.44 ± 0.30	8.36 ± 0.20	8.53
2.75	11.71 ± 0.22	7.87 ± 0.15	7.99
3.00	10.93 ± 0.15	7.35 ± 0.10	7.53
3.25	10.35 ± 0.07	6.96 ± 0.05	7.12
3.50	9.76 ± 0.10	6.56 ± 0.07	6.76
3.75	9.34 ± 0.12	6.28 ± 0.08	6.43
4.00	8.84 ± 0.10	5.94 ± 0.07	6.14
4.25	8.45 ± 0.10	5.68 ± 0.07	5.88
4.50	8.11 ± 0.09	5.45 ± 0.06	5.64
4.75	7.81 ± 0.12	5.25 ± 0.08	5.42
5.00	7.47 ± 0.10	5.02 ± 0.07	5.22
5.25	7.17 ± 0.07	4.82 ± 0.05	5.04
5.50	6.90 ± 0.06	4.64 ± 0.04	4.87
5.75	6.68 ± 0.05	4.49 ± 0.03	4.71
6.00	6.44 ± 0.06	4.33 ± 0.04	4.56
6.25	6.26 ± 0.06	4.21 ± 0.04	4.42
6.50	6.05 ± 0.06	4.07 ± 0.04	4.29
6.75	5.89 ± 0.06	3.96 ± 0.04	4.17
7.00	5.70 ± 0.07	3.83 ± 0.05	4.06
7.25	5.50 ± 0.04	3.70 ± 0.03	3.95
7.50	5.31 ± 0.04	3.57 ± 0.03	3.85
7.75	5.12 ± 0.04	3.44 ± 0.03	3.76
8.00	4.91 ± 0.04	3.30 ± 0.03	3.67

Table 4.15 Methyl alcohol (CH_3OH) Liquid

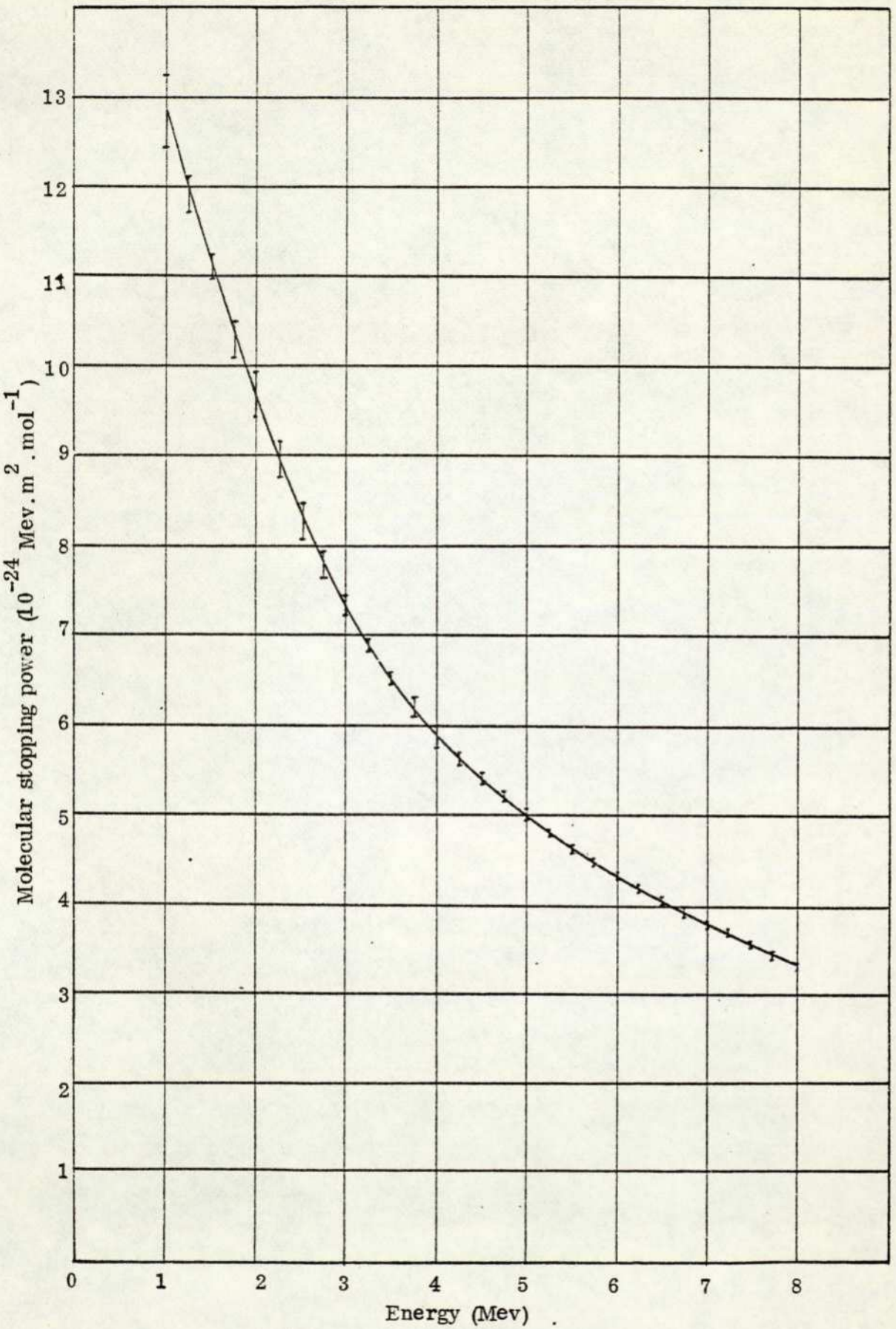

Graph 4.26. Variation of molecular stopping power of methyl alcohol liquid (method II) with alpha-particle energy.

4.4b Ethyl alcohol (C_2H_5OH) liquid

The range-energy relation for alpha-particles in ethyl alcohol liquid is shown in graph 4.27 and represents the results of all separate sets of liquid measurements by using different sources.

The stopping powers, molecular stopping powers and molecular stopping powers calculated from the uncorrected Bethe formula at various alpha-particle energies for ethyl alcohol liquid are shown in table 4.16.

Graph 4.28 shows the molecular stopping power of C_2H_5OH liquid as a function of alpha-particle energy.

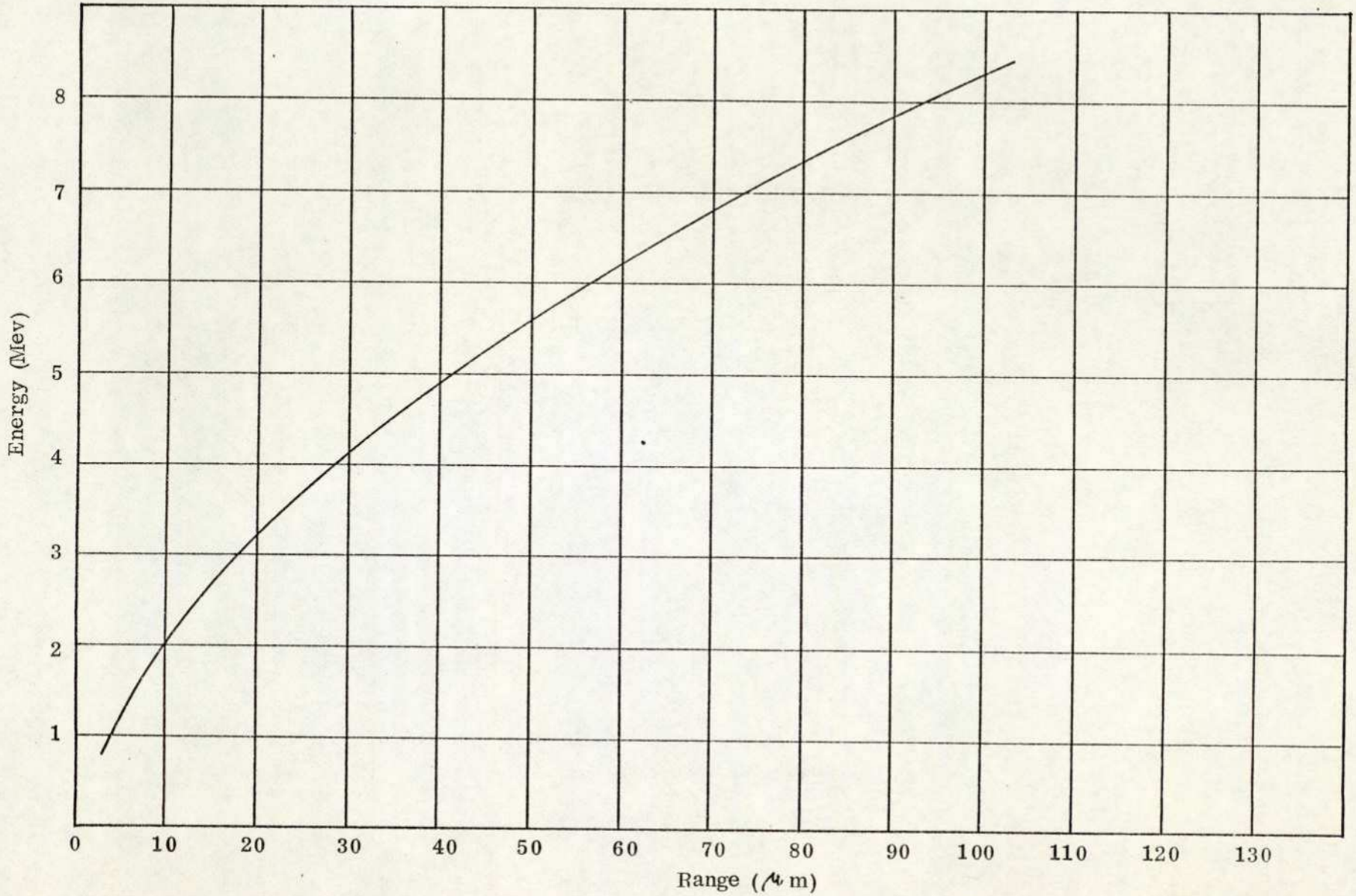

Graph 4.27. Range-energy relation for alpha-particles in ethyl alcohol liquid (method II).

Energy (Mev)	$\frac{dE}{dx} \times 10^{-2}$ Mev/μ	$\frac{\frac{dE}{dx}}{N}$ experimental (10^{-24} Mev m^2 mol^{-1})	$\frac{\frac{dE}{dx}}{N}$ calculated (10^{-24} Mev m^2 mol^{-1})
1.00	18.91 ± 0.83	18.33 ± 0.80	22.03
1.25	17.57 ± 0.42	17.03 ± 0.41	19.40
1.50	16.26 ± 0.45	15.76 ± 0.44	17.38
1.75	15.03 ± 0.44	14.57 ± 0.43	15.77
2.00	13.73 ± 0.29	13.31 ± 0.28	14.47
2.25	12.84 ± 0.17	12.44 ± 0.16	13.38
2.50	11.90 ± 0.20	11.53 ± 0.19	12.46
2.75	11.04 ± 0.08	10.70 ± 0.08	11.68
3.00	10.47 ± 0.04	10.15 ± 0.04	10.99
3.25	10.00 ± 0.08	9.69 ± 0.08	10.39
3.50	9.49 ± 0.06	9.20 ± 0.06	9.86
3.75	9.09 ± 0.08	8.81 ± 0.08	9.39
4.00	8.67 ± 0.08	8.40 ± 0.08	8.96
4.25	8.30 ± 0.09	8.04 ± 0.09	8.57
4.50	8.00 ± 0.11	7.75 ± 0.11	8.23
4.75	7.71 ± 0.13	7.47 ± 0.13	7.91
5.00	7.40 ± 0.15	7.17 ± 0.15	7.63
5.25	7.10 ± 0.12	6.88 ± 0.12	7.34
5.50	6.83 ± 0.11	6.62 ± 0.11	7.09
5.75	6.55 ± 0.08	6.35 ± 0.08	6.85
6.00	6.35 ± 0.07	6.15 ± 0.07	6.65
6.25	6.14 ± 0.07	5.95 ± 0.07	6.45
6.50	5.96 ± 0.06	5.78 ± 0.06	6.26
6.75	5.78 ± 0.03	5.60 ± 0.03	6.08
7.00	5.57 ± 0.04	5.40 ± 0.04	5.92
7.25	5.37 ± 0.05	5.20 ± 0.05	5.76
7.50	5.16 ± 0.06	5.00 ± 0.06	5.61
7.75	4.95 ± 0.05	4.80 ± 0.05	5.47
8.00	4.64 ± 0.05	4.50 ± 0.05	5.34

Table 4.16 Ethyl alcohol (C_2H_5OH) Liquid

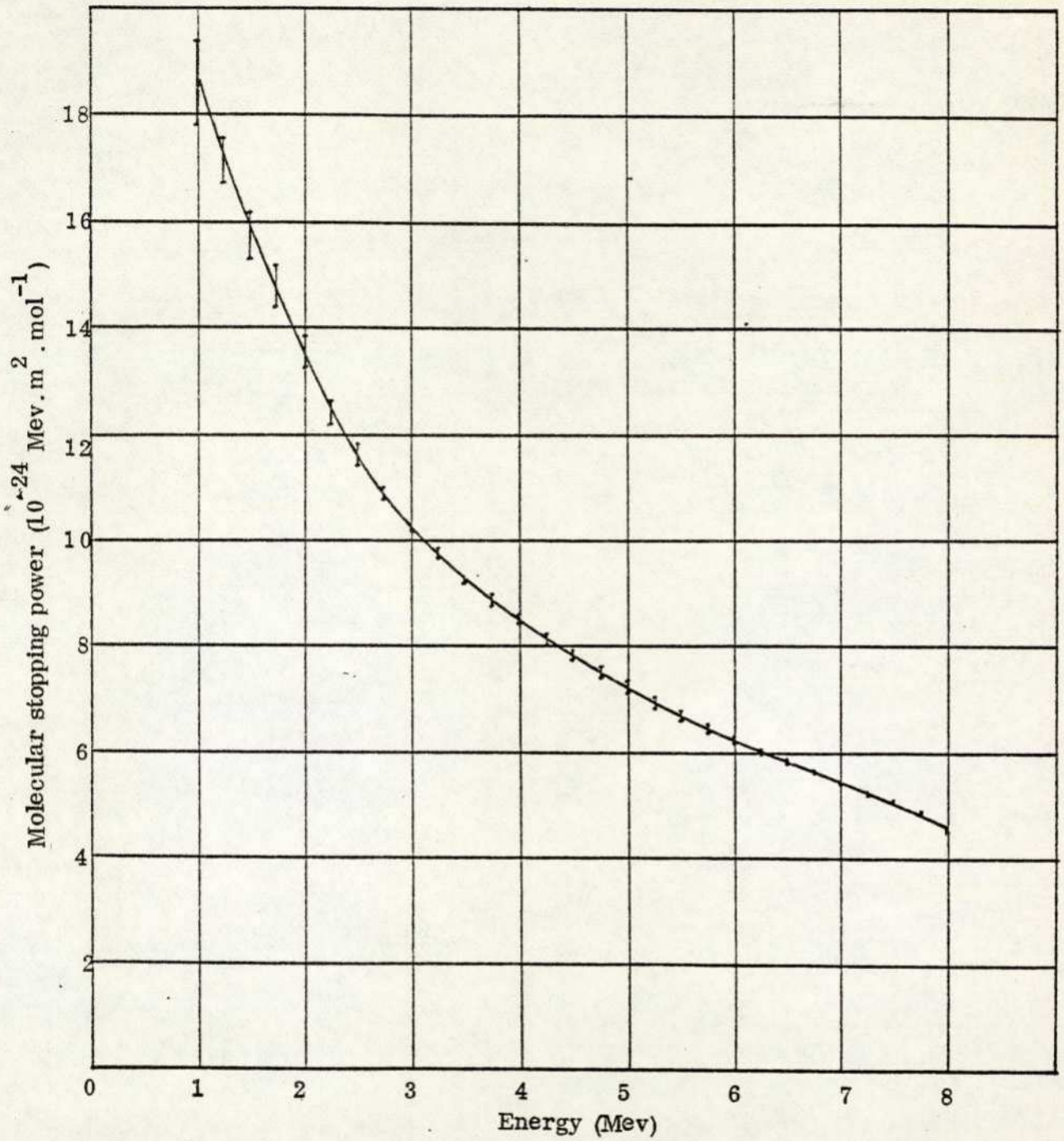

Graph 4.28. Variation of molecular stopping power of ethyl alcohol liquid (method II) with alpha-particle energy.

4.4c Propyl alcohol $(CH_3)_2CHOH$ liquid

The range-energy relation for alpha-particles in propyl alcohol liquid is shown in graph 4.29 and representsthe results of all separate sets of liquid measurements by using different sources.

The stopping powers, molecular stopping powers and molecular stopping powers calculated from the uncorrected Bethe formula at various alpha particle energies for propyl alcohol liquid are shown in table 4.17.

Graph 4.30 shows the molecular stopping power of $(CH_3)_2CHOH$ liquid as a function of alpha-particle energy.

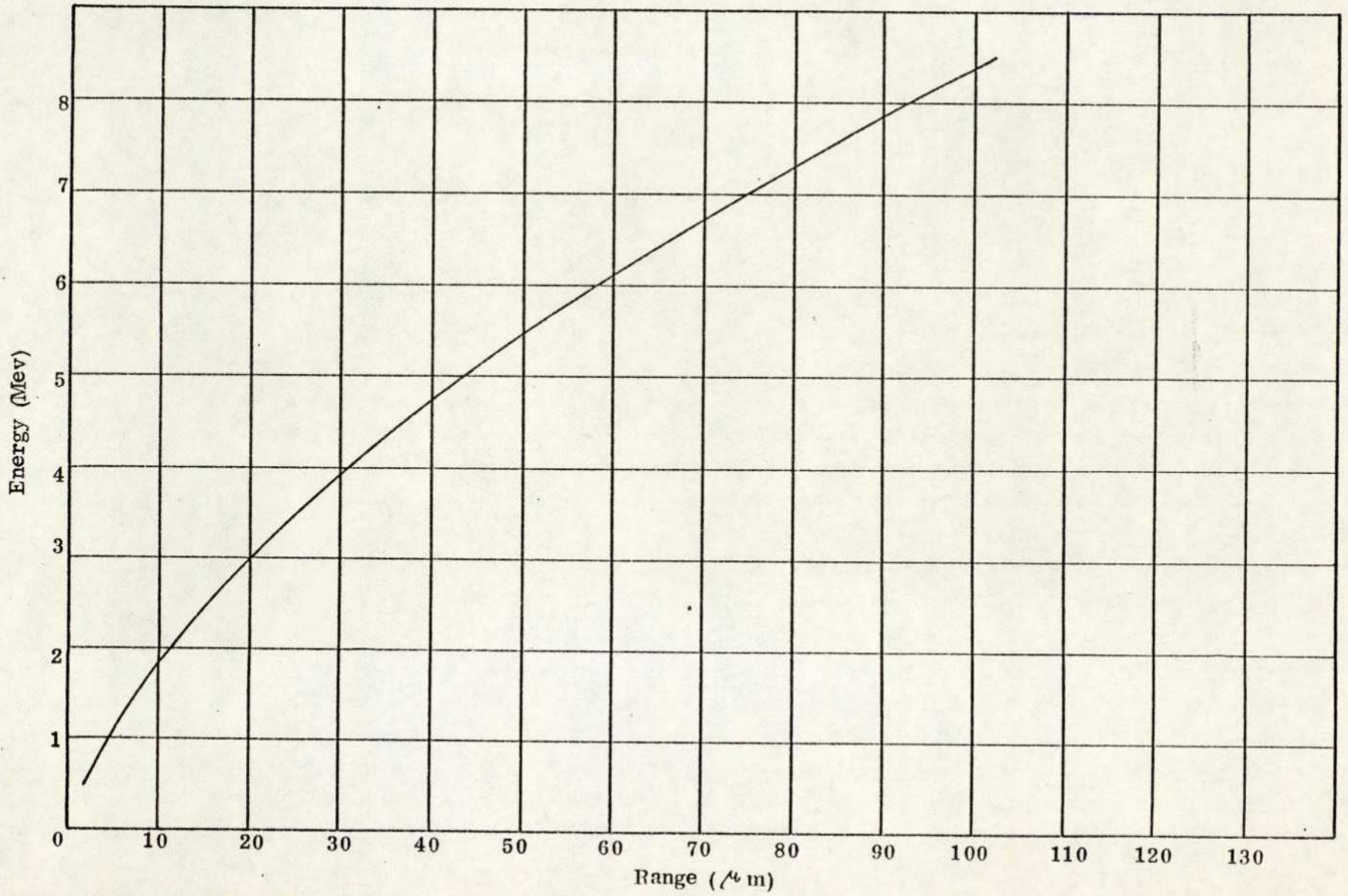

Graph 4.29. Range energy for alpha-particles in propyl alcohol liquid (method II).

Energy (mev)	$\frac{dE}{dx} \times 10^2$ Mev/μ	10^{-24} Mev m^2 mol^{-1} $\frac{dE}{dx}\frac{1}{N}$ experimental	$\frac{dE}{dx}\frac{1}{N}$ calculated
1.00	18.72 ± 0.41	23.79 ± 0.52	28.72
1.25	17.39 ± 0.35	22.10 ± 0.45	25.54
1.50	15.62 ± 0.31	19.85 ± 0.40	22.86
1.75	14.89 ± 0.30	18.92 ± 0.38	20.74
2.00	13.97 ± 0.21	17.76 ± 0.27	19.02
2.25	13.06 ± 0.27	16.60 ± 0.34	17.59
2.50	12.19 ± 0.32	15.49 ± 0.41	16.38
2.75	11.52 ± 0.16	14.64 ± 0.20	15.34
3.00	10.68 ± 0.17	13.57 ± 0.22	14.44
3.25	10.09 ± 0.14	12.83 ± 0.18	13.65
3.50	9.66 ± 0.17	12.28 ± 0.21	12.95
3.75	9.13 ± 0.24	11.61 ± 0.30	12.33
4.00	8.75 ± 0.09	11.12 ± 0.11	11.77
4.25	8.43 ± 0.17	10.72 ± 0.22	11.26
4.50	8.12 ± 0.11	10.32 ± 0.14	10.80
4.75	7.87 ± 0.20	10.00 ± 0.25	10.38
5.00	7.45 ± 0.16	9.47 ± 0.20	9.99
5.25	7.16 ± 0.15	9.10 ± 0.19	9.64
5.50	6.97 ± 0.19	8.86 ± 0.24	9.31
5.75	6.81 ± 0.09	8.65 ± 0.12	9.01
6.00	6.57 ± 0.12	8.35 ± 0.15	8.72
6.25	6.37 ± 0.18	8.10 ± 0.23	8.46
6.50	6.18 ± 0.20	7.85 ± 0.26	8.21
6.75	5.96 ± 0.24	7.58 ± 0.31	7.98
7.00	5.73 ± 0.16	7.28 ± 0.20	7.75
7.25	5.48 ± 0.11	6.96 ± 0.14	7.56
7.50	5.22 ± 0.09	6.64 ± 0.12	7.37
7.75	4.99 ± 0.08	6.34 ± 0.10	7.18
8.00	4.82 ± 0.09	6.13 ± 0.12	7.01

Table 4.17 Propyl alcohol $(CH_3)_2CHOH$ liquid.

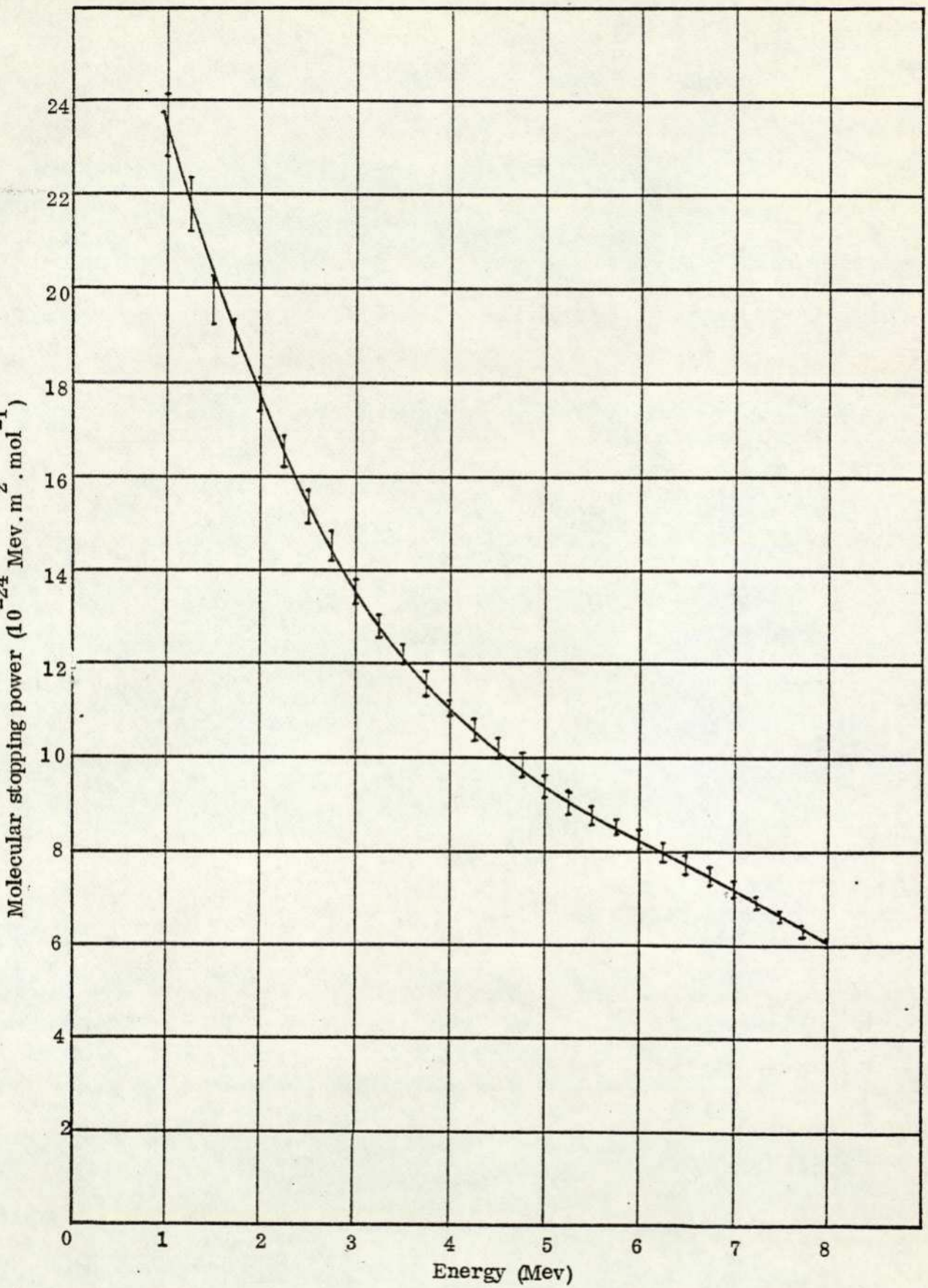

Graph 4.30. Variation of molecular stopping power of propyl alcohol liquid (method II) with alpha-particle energy.

4.4d Dichloromethane (CH_2Cl_2) liquid

The range-energy relation for alpha-particles in dichloromethane liquid is shown in graph 4.31 and represents the results of all separate sets of liquid measurements by using different sources.

The stopping powers, molecular stopping powers and molecular stopping powers calculated from the uncorrected Bethe formula at various alpha-particle energies for dichloromethane liquid are shown in table 4.18.

Graph 4.32 shows the molecular stopping power of CH_2Cl_2 liquid as a function of alpha-particle energy.

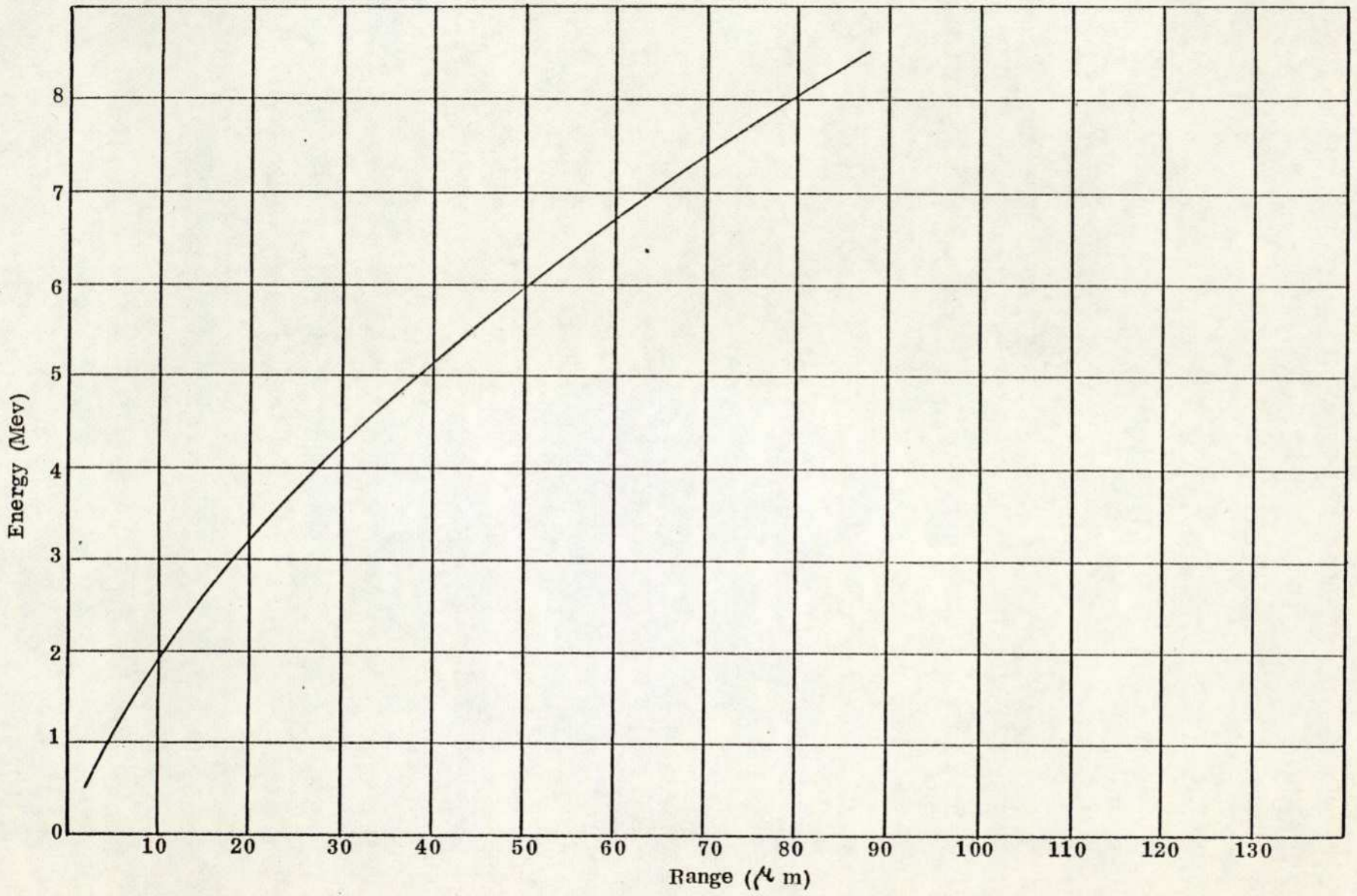

Graph 4.31. Range-energy relation for alpha-particles in dichloromethane liquid (method II).

Energy (Mev)	$\frac{dE}{dx} \times 10^2$ Mev/μ	$\frac{\frac{dE}{dx}}{N}$ experimental	$\frac{\frac{dE}{dx}}{N}$ calculated
		10^{-24} Mev m^2 mol^{-1}	
1.00	18.76 ± 0.17	19.82 ± 0.18	21.58
1.25	17.55 ± 0.20	18.54 ± 0.21	20.14
1.50	16.73 ± 0.11	17.67 ± 0.12	18.74
1.75	15.91 ± 0.14	16.81 ± 0.15	17.48
2.00	15.00 ± 0.13	15.84 ± 0.14	16.37
2.25	14.17 ± 0.14	14.97 ± 0.15	15.39
2.50	13.36 ± 0.09	14.11 ± 0.10	14.53
2.75	21.59 ± 0.11	13.30 ± 0.12	13.77
3.00	11.99 ± 0.21	12.66 ± 0.22	13.09
3.25	11.44 ± 0.19	12.08 ± 0.20	12.48
3.50	10.90 ± 0.08	11.51 ± 0.09	11.92
3.75	10.42 ± 0.09	11.01 ± 0.10	11.43
4.00	10.09 ± 0.05	10.66 ± 0.05	10.97
4.25	9.71 ± 0.06	10.26 ± 0.06	10.56
4.50	9.41 ± 0.05	9.94 ± 0.05	10.17
4.75	9.10 ± 0.05	9.61 ± 0.05	9.82
5.00	8.76 ± 0.05	9.25 ± 0.05	9.50
5.25	8.48 ± 0.05	8.96 ± 0.05	9.19
5.50	8.26 ± 0.05	8.72 ± 0.05	8.91
5.75	8.05 ± 0.03	8.50 ± 0.03	8.65
6.00	7.86 ± 0.09	8.30 ± 0.10	8.40
6.25	7.68 ± 0.08	8.11 ± 0.08	8.17
6.50	7.43 ± 0.12	7.85 ± 0.12	7.95
6.75	7.19 ± 0.24	7.60 ± 0.25	7.75
7.00	6.95 ± 0.24	7.34 ± 0.25	7.56
7.25	6.73 ± 0.21	7.11 ± 0.22	7.37
7.50	6.48 ± 0.19	6.84 ± 0.20	7.20
7.75	6.19 ± 0.19	6.54 ± 0.20	7.04
8.00	6.06 ± 0.11	6.40 ± 0.12	6.88

Table 4.18 Dichloromethane (CH_2Cl_2) liquid.

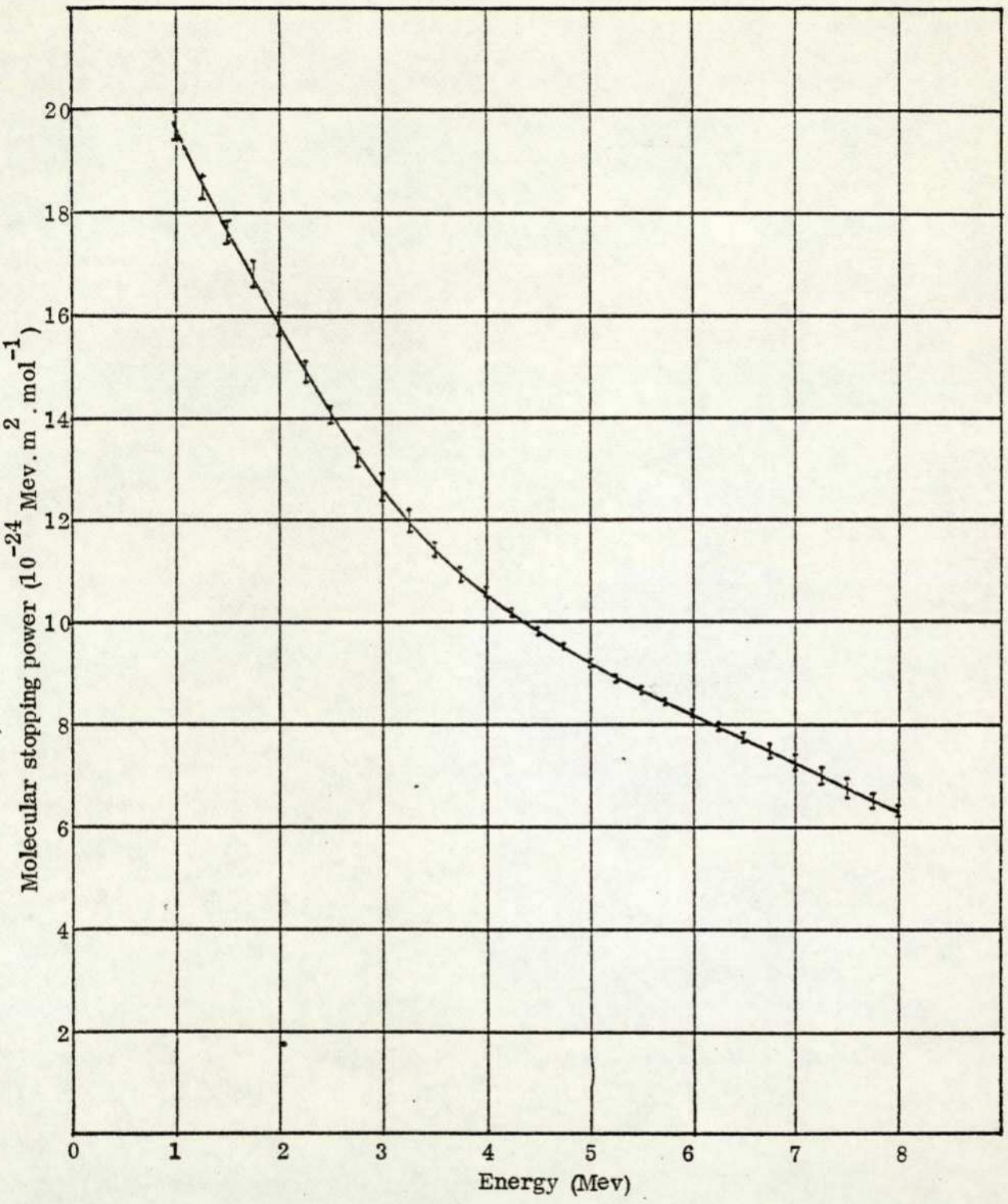

Graph 4.32. Variation of molecular stopping power of dichloromethane liquid with alpha-particle energy.

4.4e Trich loromethane $CHCl_3$ liquid

The range-energy relation for alpha-particles in tricholoromethane liquid is shown in graph 4.33 and representsthe results of separate sets of liquid measurements by using different sources.

The stopping powers, molecular stopping powers and molecular stopping powers calculated from the uncorrected Bethe formula at various alpha-particle energies for tricholoromethane liquid are shown in table 4.19.

Graph 4.34 shows the molecular stopping power of $CHCl_3$ liquid as a function of alpha-particle energy.

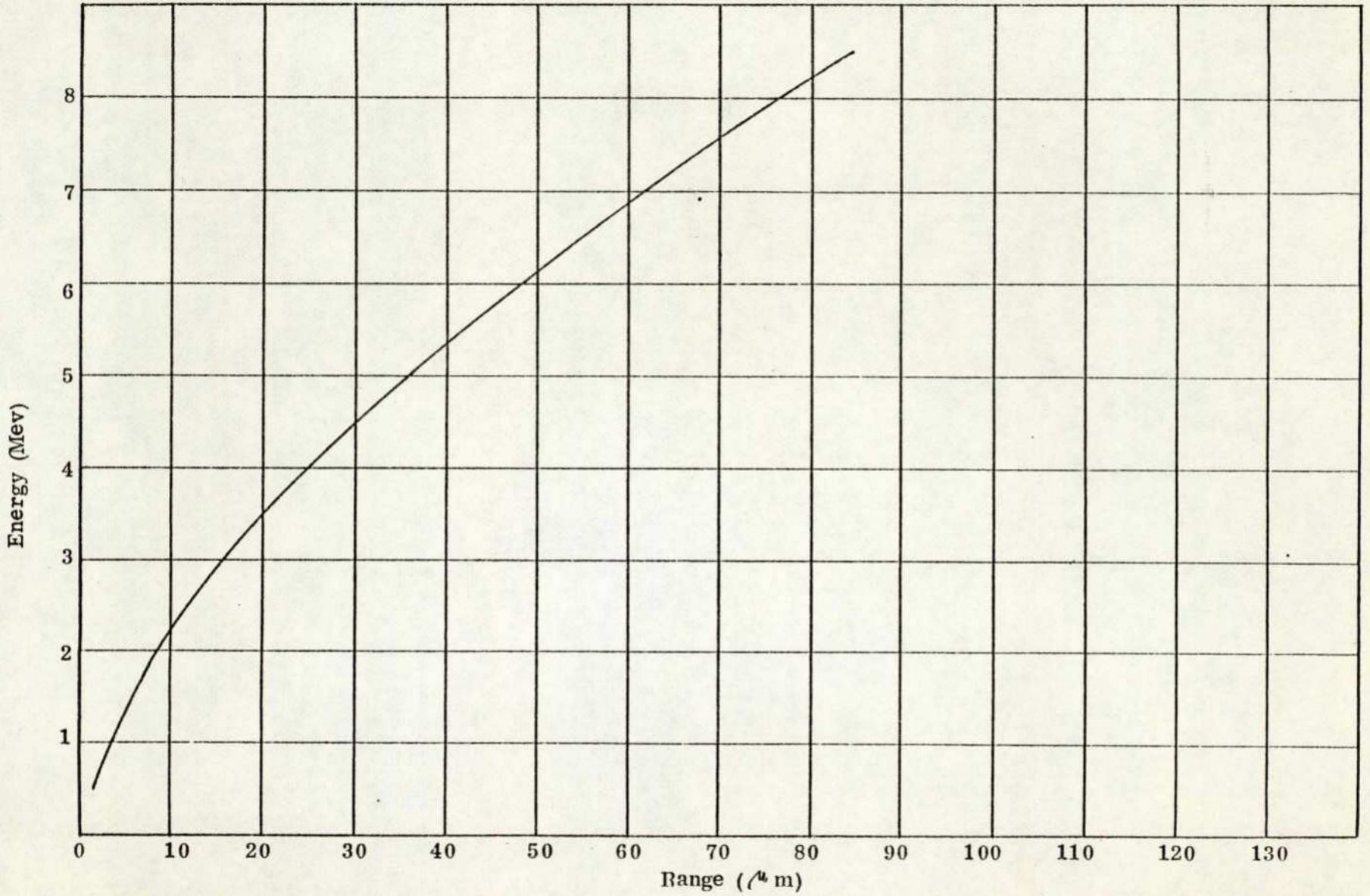

Graph 4.33. Range-energy relation for alpha-particles in trichloromethane liquid (method II).

Energy (Mev)	$\frac{dE}{dx} \times 10^2$ Mev/ρ	10^{-24} Mev m^2 mol^{-1} $\frac{dE}{dx}/N$ experimental	$\frac{dE}{dx}/N$ calculated
1.00	20.21 ± 0.28	26.85 ± 0.37	27.57
1.25	19.36 ± 0.32	25.72 ± 0.42	26.02
1.50	17.92 ± 0.27	23.81 ± 0.36	24.38
1.75	16.66 ± 0.23	22.13 ± 0.31	22.86
2.00	15.49 ± 0.17	20.58 ± 0.22	21.48
2.25	14.44 ± 0.11	19.19 ± 0.15	20.26
2.50	13.52 ± 0.09	17.97 ± 0.12	19.17
2.75	12.96 ± 0.15	17.22 ± 0.20	18.20
3.00	12.31 ± 0.08	16.35 ± 0.11	17.33
3.25	11.67 ± 0.13	15.50 ± 0.17	16.54
3.50	10.98 ± 0.17	14.59 ± 0.22	15.83
3.75	10.54 ± 0.08	14.00 ± 0.10	15.18
4.00	10.13 ± 0.07	13.46 ± 0.09	14.59
4.25	9.88 ± 0.11	13.13 ± 0.15	14.05
4.50	9.51 ± 0.09	12.64 ± 0.12	13.55
4.75	9.19 ± 0.08	12.21 ± 0.10	13.09
5.00	8.87 ± 0.11	11.78 ± 0.14	12.67
5.25	8.61 ± 0.11	11.44 ± 0.15	12.27
5.50	8.48 ± 0.05	11.27 ± 0.06	11.90
5.75	8.31 ± 0.07	11.04 ± 0.09	11.55
6.00	8.15 ± 0.06	10.83 ± 0.08	11.23
6.25	7.95 ± 0.04	10.57 ± 0.05	10.93
6.50	7.71 ± 0.06	10.24 ± 0.08	10.64
6.75	7.44 ± 0.04	9.89 ± 0.05	10.37
7.00	7.29 ± 0.05	9.68 ± 0.06	10.11
7.25	7.11 ± 0.09	9.45 ± 0.12	9.87
7.50	6.92 ± 0.11	9.20 ± 0.14	9.64
7.75	6.74 ± 0.15	8.96 ± 0.20	9.43
8.00	6.54 ± 0.08	8.69 ± 0.10	9.22

Table 4.19 Tricholoromethane ($CHCl_3$) liquid.

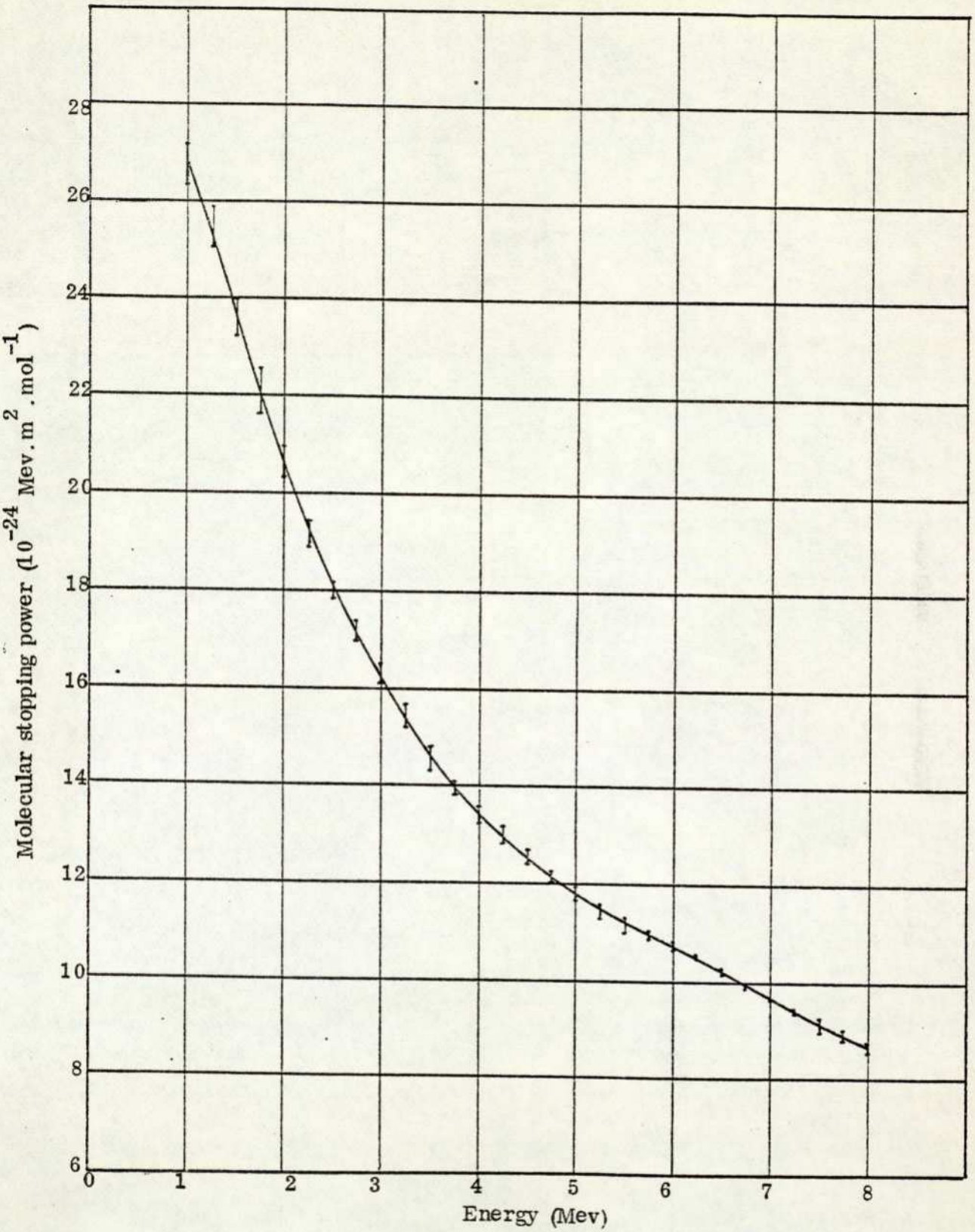

Graph 4.34. Variation of molecular stopping power of trichloromethane liquid with alpha-particle.

4.4f Carbontetrachloride (CCl_4) liquid

The range-energy relation for alpha-particles in carbontetrachloride liquid is shown in graph 4.35 and represents the results of separate sets of liquid measurements by using different sources.

The stopping powers, molecular stopping powers and molecular stopping powers calculated from the uncorrected Bethe formula at various alpha-particle energies for carbontetrachloride liquid are shown in table 4.20.

Graph 4.36 shows the molecular stopping power of CCl_4 liquid as a function of alpha-particle energy.

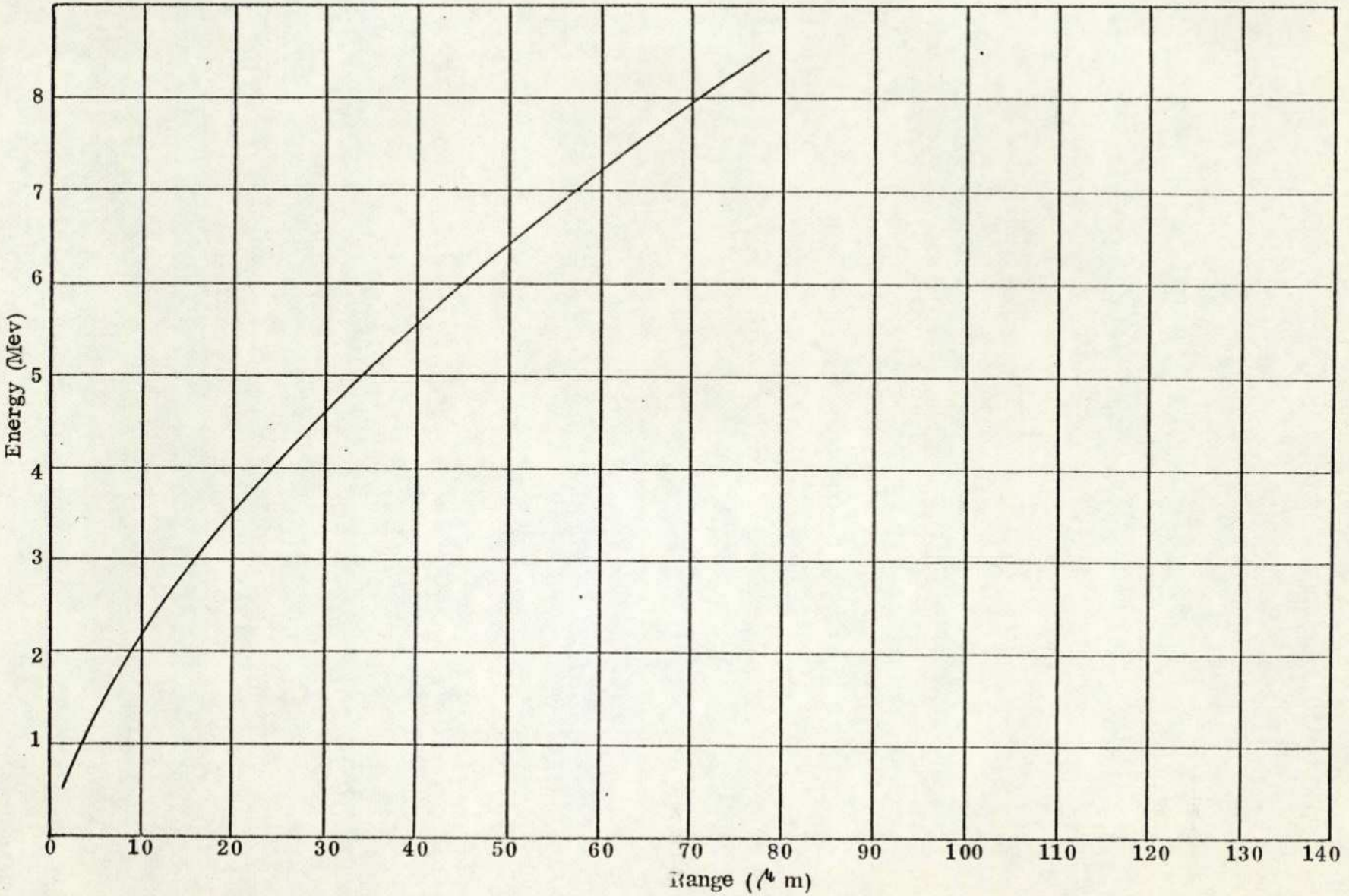

Graph 4.35. Range-energy relation for alpha-particles in carbontetrachloride liquid (method II).

Energy (Mev)	$\frac{dE}{dX}$ x 10^2 Mev/μ	10^{-24} Mev m^2 mol^{-1} $\frac{dE}{dx}_N$ experimental	$\frac{dE}{dx}_N$ calculated
1.00	20.28 ± 0.44	32.49 ± 0.70	33.62
1.25	19.37 ± 0.46	31.03 ± 0.73	31.95
1.50	18.36 ± 0.21	29.41 ± 0.33	30.07
1.75	17.40 ± 0.33	27.88 ± 0.53	28.27
2.00	16.27 ± 0.21	26.07 ± 0.34	26.63
2.25	15.27 ± 0.25	24.46 ± 0.40	25.16
2.50	14.44 ± 0.11	23.14 ± 0.17	23.84
2.75	13.78 ± 0.12	22.07 ± 0.20	22.65
3.00	13.11 ± 0.17	21.00 ± 0.28	21.59
3.25	12.52 ± 0.24	20.05 ± 0.38	20.62
3.50	12.02 ± 0.26	19.25 ± 0.41	19.75
3.75	11.53 ± 0.23	18.47 ± 0.37	18.96
4.00	11.07 ± 0.15	17.73 ± 0.24	18.23
4.25	10.80 ± 0.12	17.30 ± 0.20	17.56
4.50	10.40 ± 0.11	16.66 ± 0.18	16.95
4.75	10.06 ± 0.03	16.12 ± 0.05	16.38
5.00	9.69 ± 0.05	15.52 ± 0.08	15.85
5.25	9.35 ± 0.08	14.98 ± 0.13	15.36
5.50	9.01 ± 0.10	14.43 ± 0.16	14.90
5.75	8.71 ± 0.10	13.96 ± 0.16	14.47
6.00	8.47 ± 0.11	13.57 ± 0.18	14.07
6.25	8.24 ± 0.11	13.20 ± 0.18	13.69
6.50	8.02 ± 0.07	12.85 ± 0.12	13.34
6.75	7.84 ± 0.06	12.56 ± 0,10	13.00
7.00	7.68 ± 0.06	12.31 ± 0.10	12.68
7.25	7.54 ± 0.09	12.08 ± 0.14	12.38
7.50	7.38 ± 0.11	11.83 ± 0.18	12.10
7.75	7.24 ± 0.16	11.60 ± 0.26	11.83
8.00	7.13 ± 0.16	11.42 ± 0.25	11.57

Table 4.20 Carbontetrachloride (CCl_4) liquid.

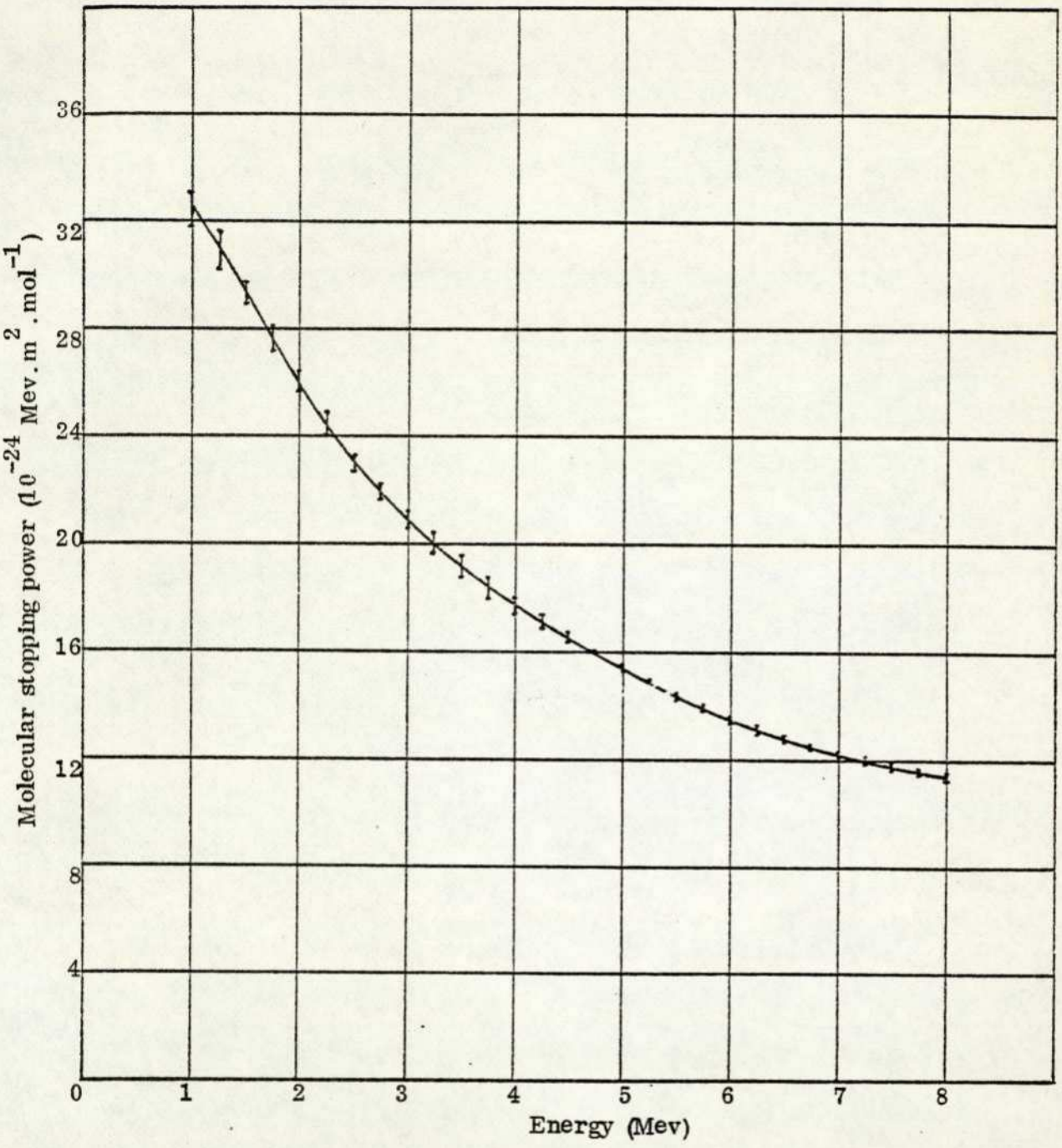

Graph 4.36. Variation of molecular stopping power of carbontetrachloride liquid (method II) with alpha-particle energy.

5. A Critical appraisal of the Stopping power measurements in vapour and liquid phases and also comparison of the present work with other workers results.

5.1 Water H_2O.

The molecular stopping powers of water and water vapour as a function of energy are plotted in graph 5.1. These results are compared with recent calculated stopping powers (Walsh 1970, Venkataraman et al 1975 and Palmer and Akhavan-Rezayat 1978).

The liquid water results are significantly different from those reported by Palmer and Akhavan-Rezayat using method II, between energies $4 < E < 6$ Mev. This could be due to difficulties in the present measurements (method I) with bubble formations as described in section 4.3a. On the other hand, as will be discussed later, it can be seen from table 5.1 that at these energies the present water results agree well with the calculated values assuming an effective Z_1 value of 2.

In table 5.1 the molecular stopping powers of water vapour and water are shown in columns (1) and (2) respectively in comparison with calculated values in columns (3)-(5).

Column (3) gives the calculated molecular stopping powers of water obtained from the uncorrected Bethe formula. In column (4) the values in column (3) have been corrected for the anomalous stopping contribution of the K Shell electrons in oxygen in accordance with the C_k corrections calculated by Walske (1952). In column (5) a further correction has been made due to the Z_1^3 effect as suggested by Ashley et al (1973). This is a

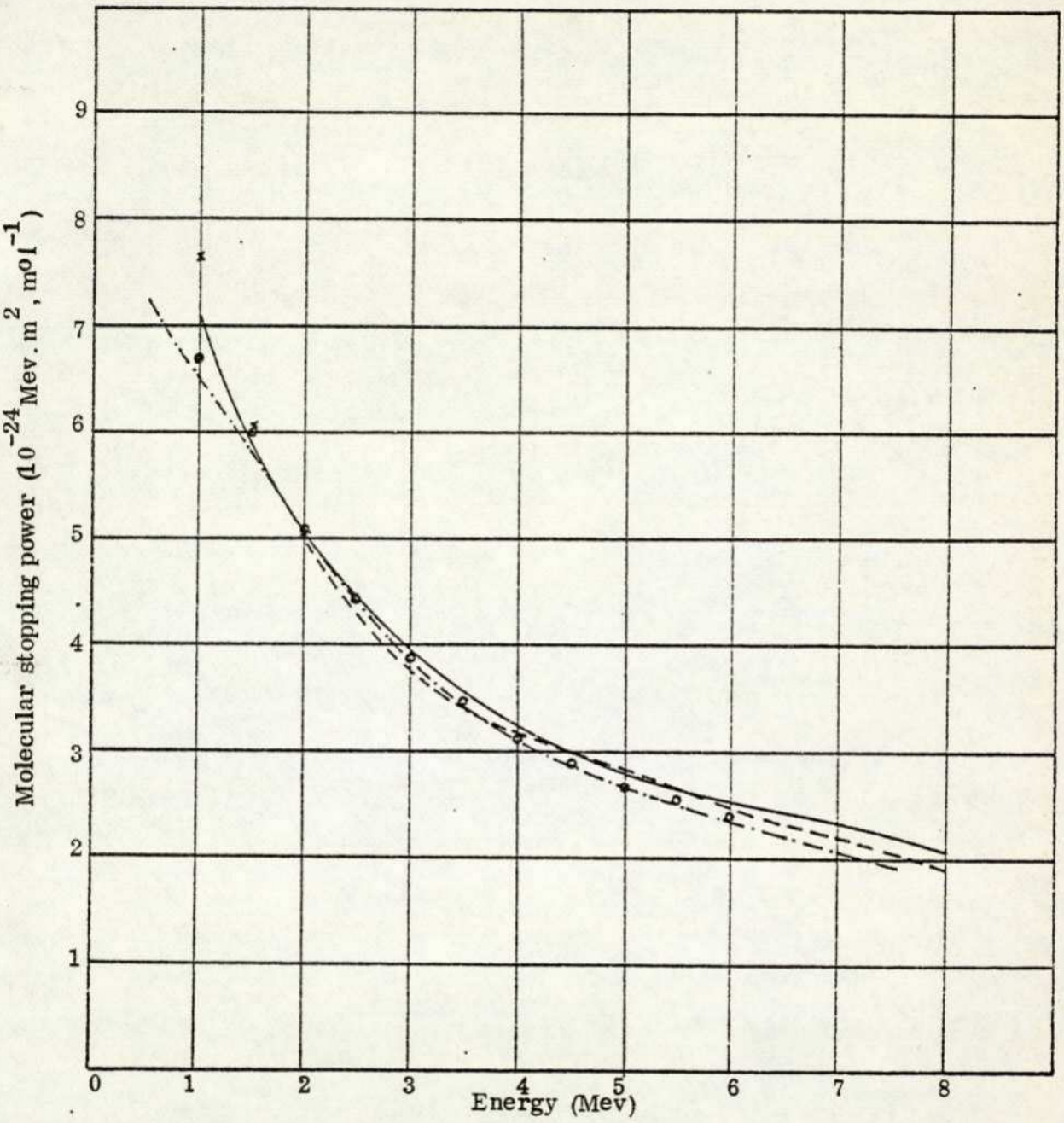

Graph 5.1. Variation of molecular stopping power of —— water vapour and - - - liquid water (method I) with energy: —·——— liquid water (method II Palmer and Akhavan Rezayat 1978); O Venkataraman et al (1975) (calculated from atomic data); x Walsh (1974).

Table 5.1 Comparison of experimental and calculated stopping powers (10^{-24} Mev.m^2.mol^{-1})

Energy (Mev)	(1)	(2)	(3)	(4)	(5)
1.00	7.05		7.97	8.10	9.15
1.25	6.65		7.06	7.10	7.87
1.50	5.85		6.34	6.35	6.95
1.75	5.49		5.77	5.76	6.24
2.00	5.08	4.93	5.29	5.25	5.63
2.25	4.74	4.59	4.93	4.85	5.17
2.50	4.48	4.26	4.57	4.51	4.78
2.75	4.23	3.88	4.30	4.22	4.45
3.00	3.97	3.68	4.06	3.97	4.16
3.25	3.79	3.44	3.85	3.75	3.92
3.50	3.63	3.27	3.64	3.55	3.70
3.75	3.44	3.20	3.46	3.38	3.51
4.00	3.31	3.15	3.31	3.23	3.35
4.25	3.17	3.09	3.19	3.09	3.20
4.50	3.05	3.02	3.04	2.96	3.05
4.75	2.95	2.96	2.93	2.85	2.94
5.00	2.83	2.87	2.82	2.74	2.82
5.25	2.75	2.78	2.72	2.65	2.72
5.50	2.68	2.66	2.63	2.56	2.62
5.75	2.61	2.56	2.54	2.48	2.54
6.00	2.55	2.45	2.46	2.40	2.46
6.25	2.50	2.38	2.39	2.33	2.38
6.50	2.45	2.33	2.32	2.26	2.31
6.75	2.39	2.26	2.26	2.20	2.24
7.00	2.34	2.21	2.20	2.14	2.18
7.25	2.28	2.14	2.14	2.08	2.12
7.50	2.22	2.07	2.09	2.03	2.07
7.75	2.15	1.98	2.03	1.98	2.01
8.00	2.07	1.88	1.99	1.94	1.97

Columns (1) and (2) list experimental stopping powers of water vapour and liquid respectively.

Columns (3) - (5) list calculated stopping powers.

positive correction factor i.e. increasing the stopping power. The accuracy of these corrections, as previously discussed, is markedly dependent upon the value of Z_1 assumed for the alpha-particles.

It is of interest to compare the magnitude of these corrections with the experimental stopping power values of water and water vapour. The C_k correction increases the molecular stopping power values calculated from the uncorrected Bethe formula by about 1.6% at 1 Mev but decreases to zero at 1.5 Mev. At energies above 3 Mev it decreases the value in column (3) by 2-3%. The Z_1^3 correction increases the stopping power by nearly 15% at the lowest energy but falls to less than 2% at high energies.

The calculated stopping power values are significantly higher than the experimental values at low energies for both water and water vapour. The mean excitation energy I is one of the important parameters needed to characterize the Bethe formula. The problem, however, becomes very involved when one tries to estimate I or to extend the formula to the lower-velocity region by applying the inner-shell corrections.

The experimental stopping power values in water vapour are higher than those in water especially at lower energies, (apart from the energy region $4.75 < E < 5.5$ Mev which is described previously).

It is assumed that the mean effective charge Z_{1eff} carried by alpha-particles is different in the different phases of water. The probability of electron capture is almost certain to increase with increasing electron density, which would reduce the mean charge of the alpha-particles and reduce the stopping power. Therefore it is reasonable to suppose that the reduced value of the alpha-particle mean charge is

mainly responsible for the difference in stopping of water and water vapour at lower energies. Table 5.1a gives the values of Z_{1eff} which would bring the experimental stopping power values from different phases into agreement with the calculated value in column (5). These values could be compared with the values of Z_{1eff} quoted by Evans and Barkas which were shown in table 4.3a. The value for Z_{1eff} for energies above 5 Mev is significantly greater than 2, which is physically impossible. For water liquid as already stated the value for Z_1 is consistently equal to 2 at energies greater than 4.5 Mev, but for water vapour no explanation could be found account for value of Z_1 at higher energies.

Energy (Mev)	(1)	(2)	Energy (Mev)	(1)	(2)
1.00	1.76		4.75	2.00	2.00
1.25	1.84		5.00	2.00	2.02
1.50	1.84		5.25	2.01	2.02
1.75	1.88		5.50	2.02	2.02
2.00	1.90	1.87	5.75	2.03	2.01
2.25	1.92	1.88	6.00	2.04	2.00
2.50	1.94	1.89	6.25	2.05	2.00
2.75	1.95	1.87	6.50	2.05	2.01
3.00	1.95	1.88	6.75	2.06	2.01
3.25	1.97	1.87	7.00	2.07	2.01
3.50	1.98	1.88	7.25	2.07	2.01
3.75	1.98	1.91	7.50	2.07	2.00
4.00	1.99	1.94	7.75	2.07	1.99
4.25	1.99	1.97	8.00	2.05	1.95
4.50	2.00	1.99			

Table 5.1a The value of Z_{1eff}

Colums (1) and (2) give the value of Z_{1eff} for water vapour and liquid water respectively.

5.2. Methyl alcohol (CH_3OH).

The molecular stopping powers of methyl alcohol vapour and liquid (methods I and II) as a function of energy are plotted in graph 5.2.

In table 5.2 the molecular stopping powers of CH_3OH vapour and liquid (methods I and II) are shown in columns (1)-(3) respectively in comparison with calculated values in columns (4)-(6).

Column (4) gives the calculated molecular stopping powers of methyl alcohol obtained from the uncorrected Bethe formula. In column (5) the values in column (4) have been corrected for the K shell electrons in carbon and oxygen in accordance with the C_K corrections calculated by Walske (1952). In column (6) a further correction has been made due to the Z_1^3 effect as suggested by Ashley eh al (1973).

The C_K correction may be seen to increase the molecular stopping power values calculated from the uncorrected Bethe formula by about 1-4% below 1.5 Mev. At energies above 1.5 Mev it decreases the value in column (4) by about 1-2%. The combined effect of the Z_1^3 correction increases the stopping power by about 16% at the lowest energy. The corrections effectively fall to zero at 4 Mev and then give rise to a decrease in stopping power of about 0.8% above 4 Mev.

The experimental stopping power values in methyl alcohol vapour show a general tendency to be higher than those in the liquid at all energies for method II and for energies lower than 5 Mev for method I. However these differences in most cases lie within the limits of experimental error which are given in tables 4.5, 4.12 and 4.15.

To bring the experimental stopping power values for different

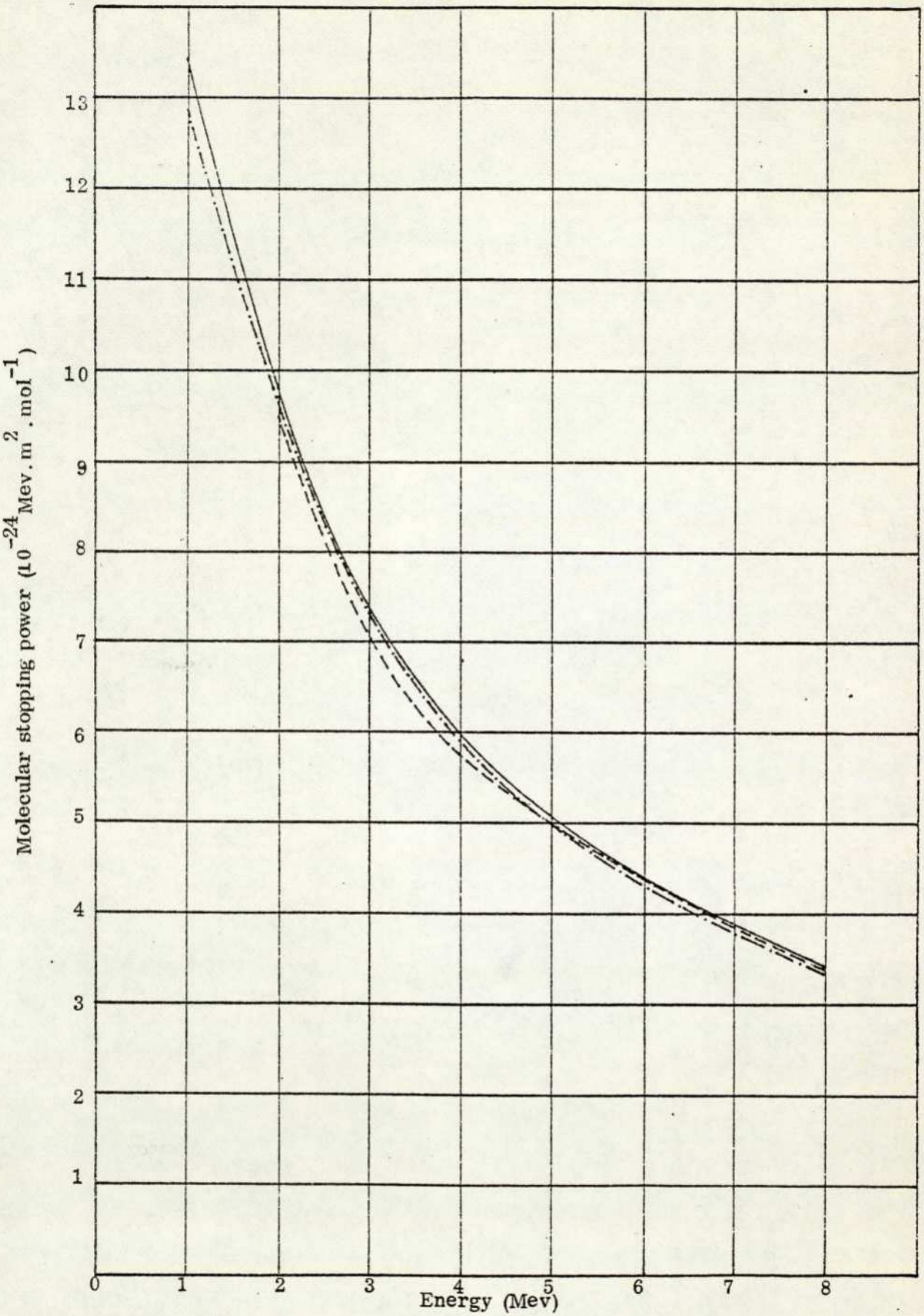

Graph 5.2. Variation of molecular stopping power of —— methyl alcohol vapour; - - - methyl alcohol liquid (method I) and; —·—·—methyl alcohol liquid (method II) with energy.

Table 5.2 Comparison of experimental and calculated stopping powers (10^{-24} . Mev. m^2 . mol^{-1})

Energy (Mev)	(1)	(2)	(3)	(4)	(5)	(6)
1.00	13.38		12.90	15.01	15.63	17.45
1.25	12.42		12.03	13.24	13.57	14.88
1.50	11.52		11.19	11.87	12.01	12.99
1.75	10.58		10.32	10.78	10.69	11.45
2.00	9.82	9.63	9.73	9.89	9.74	10.34
2.25	9.19	9.06	9.11	9.16	9.00	9.50
2.50	8.38	8.12	8.36	8.53	8.35	8.76
2.75	7.90	7.71	7.87	7.99	7.79	8.14
3.00	7.35	7.10	7.35	7.53	7.34	7.64
3.25	6.97	6.64	6.96	7.12	6.93	7.19
3.50	6.58	6.25	6.56	6.76	6.58	6.80
3.75	6.30	5.98	6.28	6.43	6.26	6.46
4.00	5.98	5.71	5.94	6.14	5.97	6.14
4.25	5.74	5.53	5.68	5.88	5.72	5.88
4.50	5.52	5.40	5.45	5.64	5.49	5.63
4.75	5.28	5.24	5.25	5.42	5.27	5.40
5.00	5.09	5.05	5.02	5.22	5.08	5.20
5.25	4.89	4.95	4.82	5.04	4.91	5.02
5.50	4.73	4.80	4.64	4.87	4.74	4.84
5.75	4.59	4.63	4.49	4.71	4.59	4.68
6.00	4.45	4.47	4.33	4.56	4.44	4.52
6.25	4.32	4.36	4.21	4.42	4.31	4.36
6.50	4.19	4.21	4.07	4.29	4.18	4.25
6.75	4.06	4.08	3.96	4.17	4.07	4.13
7.00	3.92	3.96	3.83	4.06	3.96	4.02
7.25	3.78	3.83	3.70	3.95	3.86	3.92
7.50	3.66	3.70	3.57	3.85	3.76	3.81
7.75	3.54	3.55	3.44	3.76	3.67	3.72
8.00	3.44	3.42	3.30	3.67	3.59	3.64

Columns (1) - (3) list experimental stopping powers of methyl alcohol, ie. (CH_3OH) Vapour and liquid (methods I and II) respectively.

Columns (4) -(6) list calculated stopping powers.

phases into agreement with the calculated values in column (6), Z_{1eff} has been calculated and is shown in table 5.2a.

Energy Mev	(1)	(2)	(3)	Energy Mev	(1)	(2)	(3)
1.00	1.75		1.72	4.75	1.98	1.97	1.97
1.25	1.83		1.80	5.00	1.98	1.97	1.97
1.50	1.88		1.86	5.25	1.97	1.99	1.96
1.75	1.92		1.90	5.50	1.98	1.99	1.96
2.00	1.95	1.93	1.94	5.75	1.98	1.99	1.96
2.25	1.97	1.95	1.96	6.00	1.98	1.99	1.96
2.50	1.96	1.93	1.95	6.25	1.99	2.00	1.97
2.75	1.97	1.95	1.97	6.50	1.99	1.99	1.96
3.00	1.96	1.93	1.96	6.75	1.98	1.99	1.96
3.25	1.97	1.92	1.97	7.00	1.97	1.99	1.98
3.50	1.97	1.92	1.96	7.25	1.96	1.98	1.94
3.75	1.98	1.92	1.97	7.50	1.96	1.97	1.94
4.00	1.97	1.93	1.97	7.75	1.95	1.95	1.92
4.25	1.98	1.94	1.97	8.00	1.94	1.94	1.91
4.50	1.98	1.96	1.97				

Table 5.2a The Value of Z_{1eff}

Columns (1)-(3) give the value of Z_{1eff} of methyl alcohol, i.e. CH_3OH vapour and liquid (methods I and II) respectively.

5.3 Ethyl alcohol (C_2H_5OH)

The molecular stopping power of ethyl alcohol vapour and liquid (methods I and II) as a function of energy are plotted in graph 5.3. These results are compared with the stopping power measurement (Palmer 1961), and are seen to be lower by between 2 to 12% below 5 Mev. The result obtained by Palmer used nuclear emulsions for alpha-particle detection and energy measurement; this is inherently less accurate than methodsusing solid state detectors and therefore the present measurement can be considered to be more reliable.

In table 5.3 the molecular stopping power of C_2H_5OH vapour and liquid (methods I and II) are shown in columns (1) - (3) respectively in comparison with calculated valuesin columns (4) - (6).

Column (4) gives the calculated molecular stopping powers of ethyl alcohol obtained from the uncorrected Bethe formula. In column (5) these values have been modified in accordance with the C_k corrections for carbon and oxygen suggested by Walske (1952). In column (6) a further correction has been made due to the Z_1^3 effect as suggested by Ashley et al (1973).

The C_k correction increases the molecular stopping power values calculated from the uncorrected Bethe formula by about 3% at 1 Mev. At energies above 1.5 Mev it decreases the value in column (4) by about 1.4 - 3%. The combined effect of the latter together with the Z_1^3 correction increases the stopping power by about 0.7 - 16.5% at energies below 3.5 Mev. The combined corrections effectively fall to Zero at 4.5 Mev and then give rise to a decrease in stopping power of about 0.9% above 4.5 Mev.

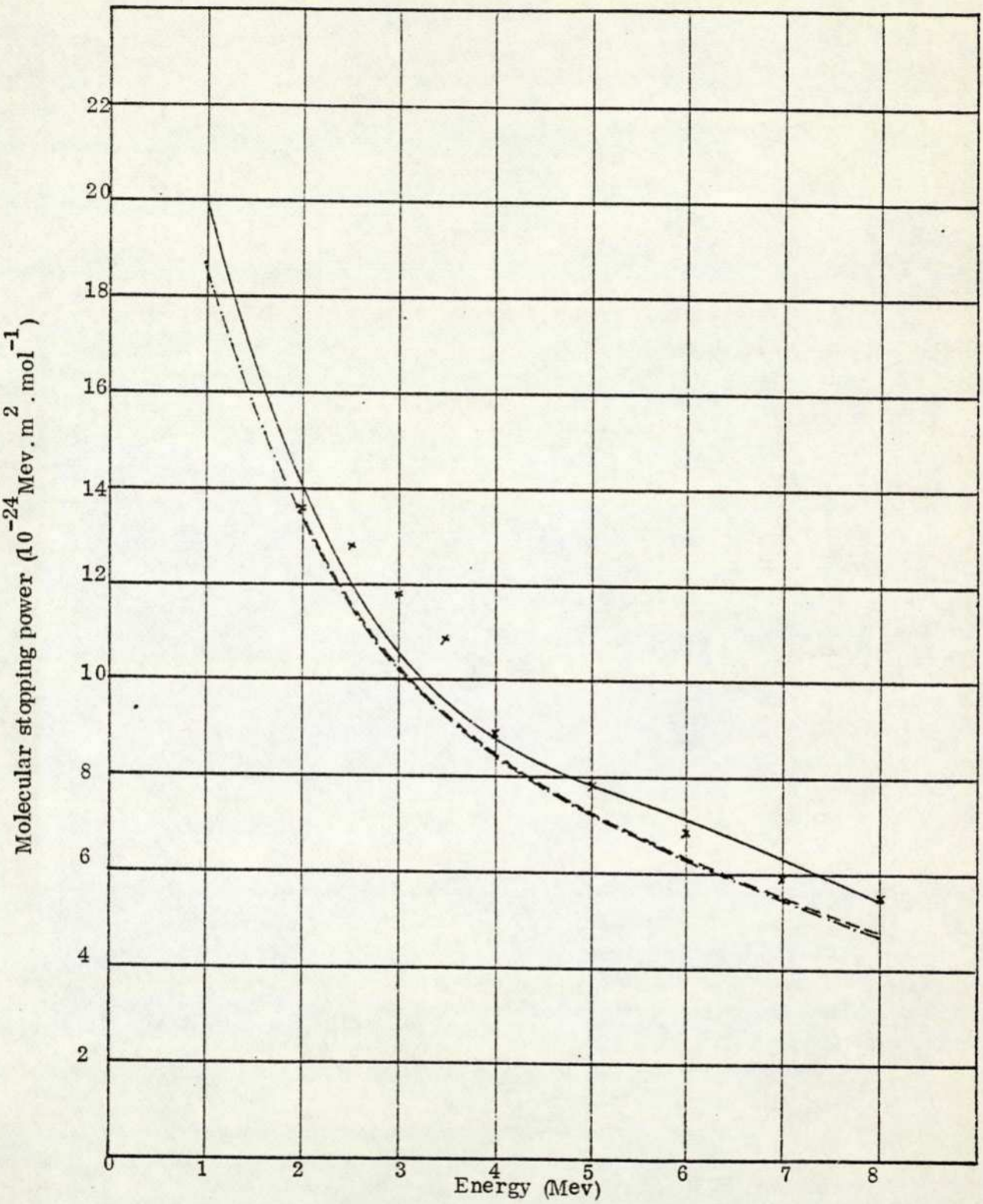

Graph 5.3. Variation of molecular stopping power of —— ethyl alcohol vapour; - - - ethyl alcohol liquid (method I) and; —·—·— ethyl alcohol liquid (method II) with energy: x Palmer (1961).

Table 5.3 Comparison of experimental and calculated stopping powers (10^{-24} Mev.m^2.mol^{-1})

Energy	(1)	(2)	(3)	(4)	(5)	(6)
1.00	19.84		18.33	22.03	22.70	25.67
1.25	18.46		17.03	19.40	19.66	21.78
1.50	16.44		15.76	17.38	17.40	18.98
1.75	14.91		14.57	15.77	15.55	16.77
2.00	13.95	13.29	13.31	14.47	14.18	15.15
2.25	12.87	12.41	12.44	13.38	13.09	13.88
2.50	11.81	11.63	11.53	12.46	12.15	12.81
2.75	11.10	10.80	10.70	11.68	11.35	11.91
3.00	10.52	10.18	10.15	10.99	10.68	11.16
3.25	10.02	9.72	9.69	10.39	10.09	10.54
3.50	9.52	9.25	9.20	9.86	9.57	9.93
3.75	9.19	8.90	8.81	9.39	9.12	9.44
4.00	8.76	8.52	8.40	8.96	8.70	8.98
4.25	8.44	8.18	8.04	8.57	8.33	8.54
4.50	8.16	7.87	7.75	8.23	8.00	8.23
4.75	7.97	7.59	7.47	7.91	7.69	7.89
5.00	7.75	7.30	7.17	7.63	7.42	7.61
5.25	7.62	7.02	6.88	7.34	7.14	7.31
5.50	7.48	6.73	6.62	7.09	6.90	7.05
5.75	7.30	6.49	6.35	6.85	6.67	6.81
6.00	7.07	6.25	6.15	6.65	6.48	6.61
6.25	6.88	6.04	5.95	6.45	6.29	6.41
6.50	6.63	5.88	5.78	6.26	6.11	6.22
6.75	6.36	5.69	5.60	6.08	5.93	6.03
7.00	6.15	5.50	5.40	5.92	5.78	5.88
7.25	5.90	5.31	5.20	5.76	5.62	5.71
7.50	5.72	5.13	5.00	5.61	5.48	5.56
7.75	5.50	4.96	4.80	5.47	5.35	5.43
8.00	5.31	4.82	4.50	5.34	5.22	5.29

Columns (1) - (3) list experimental stopping powers of ethyl alcohol, ie. (C_2H_5OH) vapour and liquid (methods I and II) respectively

Columns (4) - (6) list calculated stopping powers.

The experimental liquid stopping power values obtained by method I are higher than those obtained by method II by about 1-2% at energies below 7 Mev and by about 3% at higher energies. The values in C_2H_5OH vapour are higher than those in the liquid with both liquid stopping power methods. The difference between the vapour and liquid results (method I) at energies below 4 Mev is about 3%. At higher energies this difference increases, but it is possible that this is due to association of the C_2H_5OH molecules at higher vapour pressure as discussed in section 4.2d.

To bring the experimental stopping power values for different phases into agreement with the calculated values in column (6), Z_{1eff} has been calculated and is shown in table 5.3a.

Energy (Mev)	(1)	(2)	(3)	Energy (Mev)	(1)	(2)	(3)
1.00	1.76		1.69	4.75	2.01	1.96	1.95
1.25	1.84		1.77	5.00	2.02	1.96	1.94
1.50	1.86		1.82	5.25	2.04	1.96	1.94
1.75	1.89		1.86	5.50	2.06	1.95	1.94
2.00	1.92	1.87	1.87	5.75	2.07	1.95	1.93
2.25	1.93	1.89	1.89	6.00	2.07	1.94	1.93
2.50	1.92	1.91	1.90	6.25	2.07	1.94	1.93
2.75	1.93	1.90	1.90	6.50	2.06	1.94	1.93
3.00	1.94	1.91	1.91	6.75	2.05	1.94	1.93
3.25	1.95	1.92	1.92	7.00	2.05	1.93	1.92
3.50	1.96	1.93	1.93	7.25	2.03	1.93	1.91
3.75	1.97	1.94	1.93	7.50	2.03	1.92	1.90
4.00	1.98	1.95	1.93	7.75	2.01	1.91	1.88
4.25	1.99	1.96	1.94	8.00	2.00	1.91	1.84
4.50	1.99	1.96	1.94				

Table 5.3 a The Value of Z_{1eff}

Columns (1) - (3) give the value of Z_{1eff} of ethyl alcohol, ie. C_2H_5OH vapour and liquid (methods I and II) respectively.

5.4 Propyl alcohol $(CH_3)_2$ CHOH.

The molecular stopping powers of propyl alcohol vapour and liquid (methods I and II) as a function of energy are plotted in graph 5.4.

In table 5.4 the molecular stopping powers of $(CH_3)_2CHOH$ vapour and liquid (methods I and II) are shown in columns (1)-(3) respectively in comparison with calculated values in columns (4)-(6).

Column (4) gives the calculated molecular stopping powers of propyl alcohol obtained from the uncorrected Bethe formula. In column (5) these values have been modified in accordance with the C_k corrections for carbon and oxygen suggested by Walske (1952). In column (6) a further correction has been made due to the Z_1^3 effect as suggested by Ashley et al (1973).

The C_k correction increases the molecular stopping power values calculated from the uncorrected Bethe formula by about 2.5% at 1 Mev. At energies above 1.5 Mev it decreases the value in column (4) by about 0.7-3%. The combined effect of the latter together with the Z_1^3 correction increases the stopping power by about 0.5-10.5% at energies below 2.5 Mev. The combined corrections effectively fall to zero at 2.75 Mev and then give rise to a decrease in stopping power of about 1.4% above 2.5 Mev.

The experimental stopping power values in propyl alcohol vapour are higher than those in the liquid obtained by method I at energies below 3.5 Mev and above 7.5 Mev by 0.6-1.8%. At energies $4.5 < E < 6.5$ it is lower by 1-1.8%. These differences could be accountable to experimental error. The propyl alcohol vapour stopping power values are higher than those in

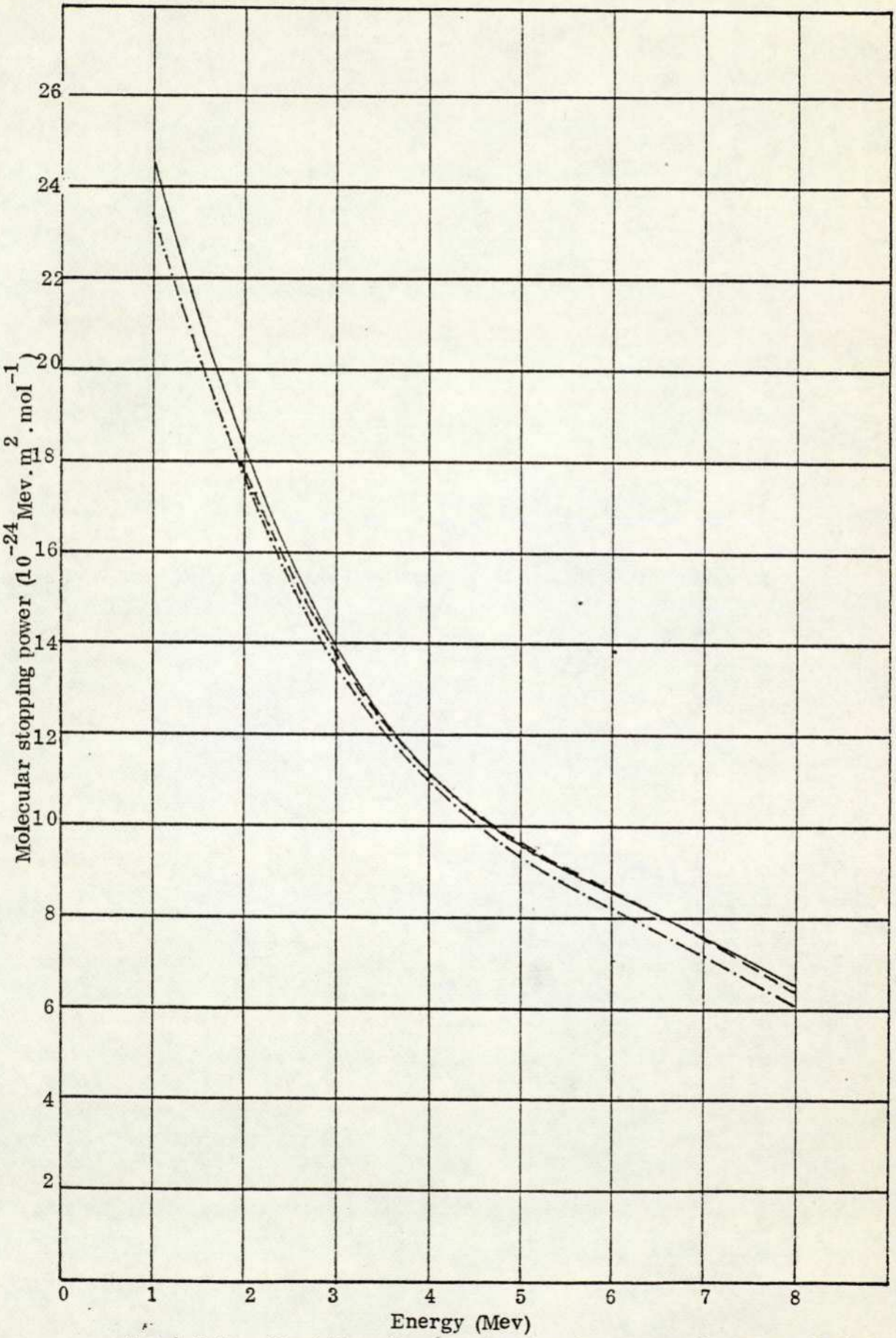

Graph 5.4. Variation of molecular stopping power of —— propyl alcohol vapour; - - - propyl alcohol liquid (method I) and —·—·— propyl alcohol liquid (method II) with energy.

Table 5.4 Comparison of experimental and calculated stopping powers

(10^{-24} Mev.m^2.mol^{-1})

Energy (Mev)	(1)	(2)	(3)	(4)	(5)	(6)
1.00	24.44		23.79	28.72	29.43	31.74
1.25	22.61		22.10	25.54	25.73	27.39
1.50	20.92		19.85	22.86	22.76	24.00
1.75	19.42		18.92	20.74	20.38	21.34
2.00	18.10	17.81	17.76	19.02	18.59	19.35
2.25	16.95	16.70	16.60	17.59	17.16	17.78
2.50	15.94	15.74	15.49	16.38	15.94	16.46
2.75	14.81	14.70	14.64	15.34	14.89	15.33
3.00	13.88	13.71	13.57	14.44	14.01	14.38
3.25	13.01	12.93	12.83	13.65	13.24	13.56
3.50	12.31	12.34	12.28	12.95	12.56	12.84
3.75	11.71	11.84	11.61	12.33	11.96	12.21
4.00	11.32	11.35	11.12	11.77	11.42	11.64
4.25	10.97	10.95	10.72	11.26	10.93	11.13
4.50	10.55	10.52	10.32	10.80	10.49	10.67
4.75	9.87	10.05	10.00	10.38	10.09	10.25
5.00	9.58	9.71	9.47	9.99	9.71	9.85
5.25	9.31	9.43	9.10	9.64	9.38	9.51
5.50	9.10	9.19	8.86	9.31	9.06	9.18
5.75	8.88	9.00	8.65	9.01	8.77	8.88
6.00	8.62	8.72	8.35	8.72	8.50	8.60
6.25	8.40	8.50	8.10	8.46	8.25	8.34
6.50	8.19	8.25	7.85	8.21	8.01	8.10
6.75	7.95	7.90	7.58	7.98	7.79	7.87
7.00	7.70	7.73	7.28	7.75	7.56	7.63
7.25	7.42	7.45	6.96	7.56	7.38	7.45
7.50	7.15	7.14	6.64	7.37	7.20	7.27
7.75	6.90	6.82	6.34	7.18	7.02	7.08
8.00	6.68	6.56	6.13	7.01	6.85	6.91

Columns (1) - (3) list experimental stopping powers of propyl alcohol, i.e. $(CH_3)_2CHOH$ vapour and liquid (methods I and II) respectively.

Column (4) - (6) list calculated stopping powers.

the liquid obtained by method II at all energies. The differences between the vapour and liquid stopping powers at lower energies are 2 to 5% and at higher energies above 6 Mev are 3-8%.

To bring the experimental stopping power values for different phases into agreement with the calculated values in column (6), Z_{1eff} has been calculated and is shown in table 5.4a.

Energy Mev	(1)	(2)	(3)	Energy Mev	(1)	(2)	(3)
1.00	1.76		1.73	4.75	1.96	1.98	1.98
1.25	1.82		1.80	5.00	1.97	1.99	1.96
1.50	1.87		1.82	5.25	1.98	1.99	1.96
1.75	1.91		1.88	5.50	1.99	2.00	1.97
2.00	1.93	1.92	1.92	5.75	2.00	2.00	1.97
2.25	1.95	1.94	1.93	6.00	2.00	2.01	1.97
2.50	1.96	1.96	1.94	6.25	2.00	2.02	1.97
2.75	1.97	1.96	1.95	6.50	2.01	2.02	1.97
3.00	1.96	1.95	1.94	6.75	2.01	2.00	1.96
3.25	1.96	1.95	1.95	7.00	2.00	2.01	1.95
3.50	1.96	1.96	1.96	7.25	2.00	2.00	1.93
3.75	1.96	1.97	1.95	7.50	1.98	1.98	1.91
4.00	1.97	1.97	1.95	7.75	1.97	1.96	1.89
4.25	1.99	1.98	1.96	8.00	1.97	1.95	1.88
4.50	1.99	1.99	1.97				

Table 5.4a The value of Z_{1eff}.

Columns (1)-(3) give the value of Z_{1eff} of Propyl alcohol, i.e. $(CH_3)_2CHOH$ vapour and liquid (methods I and II) respectively.

5.5 Dichloromethane (CH_2Cl_2)

The molecular stopping powers of dichloromethane vapour and liquid (method II) as a function of energy are plotted in graph 5.5.

In table 5.5 the molecular stopping powers of CH_2Cl_2 vapour and liquid (method II) are shown in columns (1) and (2) respectively in comparison with calculated values in columns (3)-(5).

Column (3) gives the calculated molecular stopping power of dichloromethane obtained from the uncorrected Bethe formula. In column (4) the values in column (3) have been modified in accordance with the C_k corrections for carbon and chlorine as suggested by Walske (1952), and in accordance with the C_L corrections for chlorine as calculated by Khandelwal (1968). In column (5) a further correction has been made due to the Z_1^3 effect as suggested by Ashley et al (1973).

The C_k and C_L corrections increase the molecular stopping power values calculated from the uncorrected Bethe formula by 1.8% at 1 Mev. At energies above 1 Mev it decreases the value in column (3) by about 1-2.5%. The combined effect of this with the Z_1^3 correction increases the stopping power values, column (3), by about 19.5% at the lowest energy and by about 0.6% at the highest energy.

The experimental vapour values are 1.7 to 7.5% higher than those in liquid below 2 Mev. At higher energies the vapour values are only marginally higher and the differences are probably not significant.

The calculated stopping power values are significantly higher than the experimental values at low energies for both dichloromethane vapour

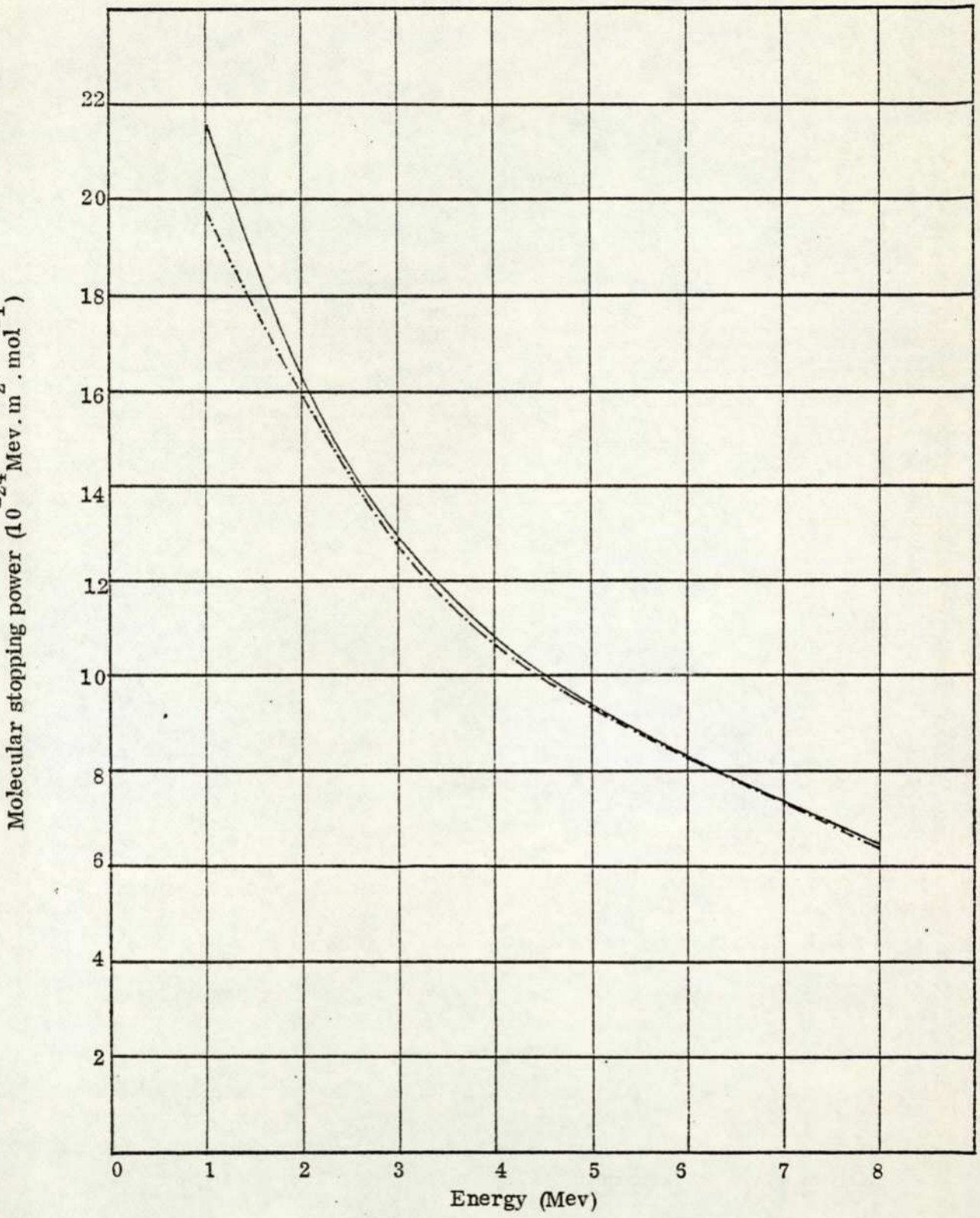

Graph 5.5. Variation of molecular stopping power of —— dichloromethane and —·—·— dichloromethane liquid (method II) with energy.

Table 5.5 Comparison of experimental and calculated stopping powers (10^{-24} Mev. m^2 . mol^{-1})

Energy (Mev)	(1)	(2)	(3)	(4)	(5)
1.00	21.31	19.82	21.58	21.97	25.78
1.25	20.05	18.54	20.14	20.12	23.17
1.50	18.80	17.67	18.74	18.49	20.95
1.75	17.39	16.81	17.48	17.22	19.27
2.00	16.11	15.84	16.37	16.07	17.80
2.25	15.17	14.97	15.39	15.08	16.56
2.50	14.26	14.11	14.53	14.21	15.49
2.75	13.46	13.30	13.77	13.44	14.56
3.00	12.80	12.66	13.09	12.82	13.81
3.25	12.30	12.08	12.48	12.21	13.09
3.50	11.71	11.51	11.92	11.64	12.42
3.75	11.22	11.01	11.43	11.15	11.86
4.00	10.76	10.66	10.97	10.68	11.32
4.25	10.39	10.26	10.56	10.27	10.85
4.50	10.05	9.94	10.17	9.89	10.42
4.75	9.72	9.61	9.82	9.59	10.07
5.00	9.36	9.25	9.50	9.26	9.70
5.25	9.10	8.96	9.19	8.97	9.38
5.50	8.82	8.72	8.91	8.71	9.09
5.75	8.53	8.50	8.65	8.48	8.83
6.00	8.27	8.30	8.40	8.23	8.56
6.25	8.04	8.11	8.17	8.00	8.31
6.50	7.81	7.85	7.95	7.78	8.07
6.75	7.58	7.60	7.75	7.59	7.86
7.00	7.35	7.34	7.56	7.41	7.66
7.25	7.15	7.11	7.37	7.22	7.46
7.50	6.92	6.84	7.20	7.04	7.26
7.75	6.68	6.54	7.04	6.88	7.09
8.00	6.50	6.40	6.88	6.72	6.92

Columns (1) and (2) list experimental stopping powers of dichloromethane (CH_2Cl_2) vapour and liquid (method II) respectively. Columns (3) - (5) list calculated stopping powers.

and liquid. To bring the experimental stopping power values for different phases into agreement with the calculated values in column (5), Z_{1eff} has been calculated and is shown in table 5.5a.

Energy Mev	(1)	(2)	Energy Mev	(1)	(2)
1.00	1.82	1.75	4.75	1.96	1.95
1.25	1.86	1.79	5.00	1.96	1.95
1.50	1.89	1.84	5.25	1.97	1.95
1.75	1.90	1.87	5.50	1.97	1.96
2.00	1.90	1.89	5.75	1.97	1.96
2.25	1.91	1.90	6.00	1.97	1.97
2.50	1.92	1.91	6.25	1.97	1.98
2.75	1.92	1.91	6.50	1.97	1.98
3.00	1.92	1.91	6.75	1.96	1.97
3.25	1.94	1.92	7.00	1.96	1.96
3.50	1.94	1.93	7.25	1.96	1.95
3.75	1.95	1.93	7.50	1.95	1.94
4.00	1.95	1.94	7.75	1.94	1.92
4.25	1.96	1.94	8.00	1.94	1.92
4.50	1.96	1.95			

Table 5.5a The value of Z_{1eff}.

Columns (1) and (2) give the value of Z_{1eff} of dichloromethane vapour and liquid respectively.

5.6 Trichloromethane ($CHCl_3$).

The molecular stopping powers of trichloromethane vapour and liquid (method II) as a function of energy are plotted in graph 5.6.

In table 5.6 the molecular stopping powers of $CHCl_3$ vapour and liquid (method II) are shown in columns (1) and (2) respectively in comparison with calculated values in columns (3)-(5).

Column (3) gives the calculated molecular stopping powers of trichloromethane obtained from the uncorrected Bethe formula. In column (4) the values in column (3) have been modified for the K shell electrons in carbon and chlorine in accordance with the C_k corrections calculated by Walske (1952), and for the L shell electrons in chlorine in accordance with the C_L corrections calculated by Khandewal (1968). In column (5) a further correction has been made due to the Z_1^3 effect as suggested by Ashley et al (1973).

The C_K and C_L corrections increase the molecular stopping power values calculated from the uncorrected Bethe formula by about 2% at 1 Mev, and fall to zero at 1.25 Mev. At energies above 1.25 Mev they decrease the values in column (3) by about 1.3 to 3%. The combined effect of this with the Z_1^3 correction increases the stopping power values, column (3), by about 21% at lowest energy and 0.6% at the highest energy.

The experimental stopping power values in trichloromethane vapour are higher than those in liquid by about 0.9 to 2% below 4 Mev. At energies above 2 Mev these differences are reasonably small except at energies $4.5 < E < 6$ Mev in which the experimental vapour values are about 0.6-3.3% higher than those in liquid.

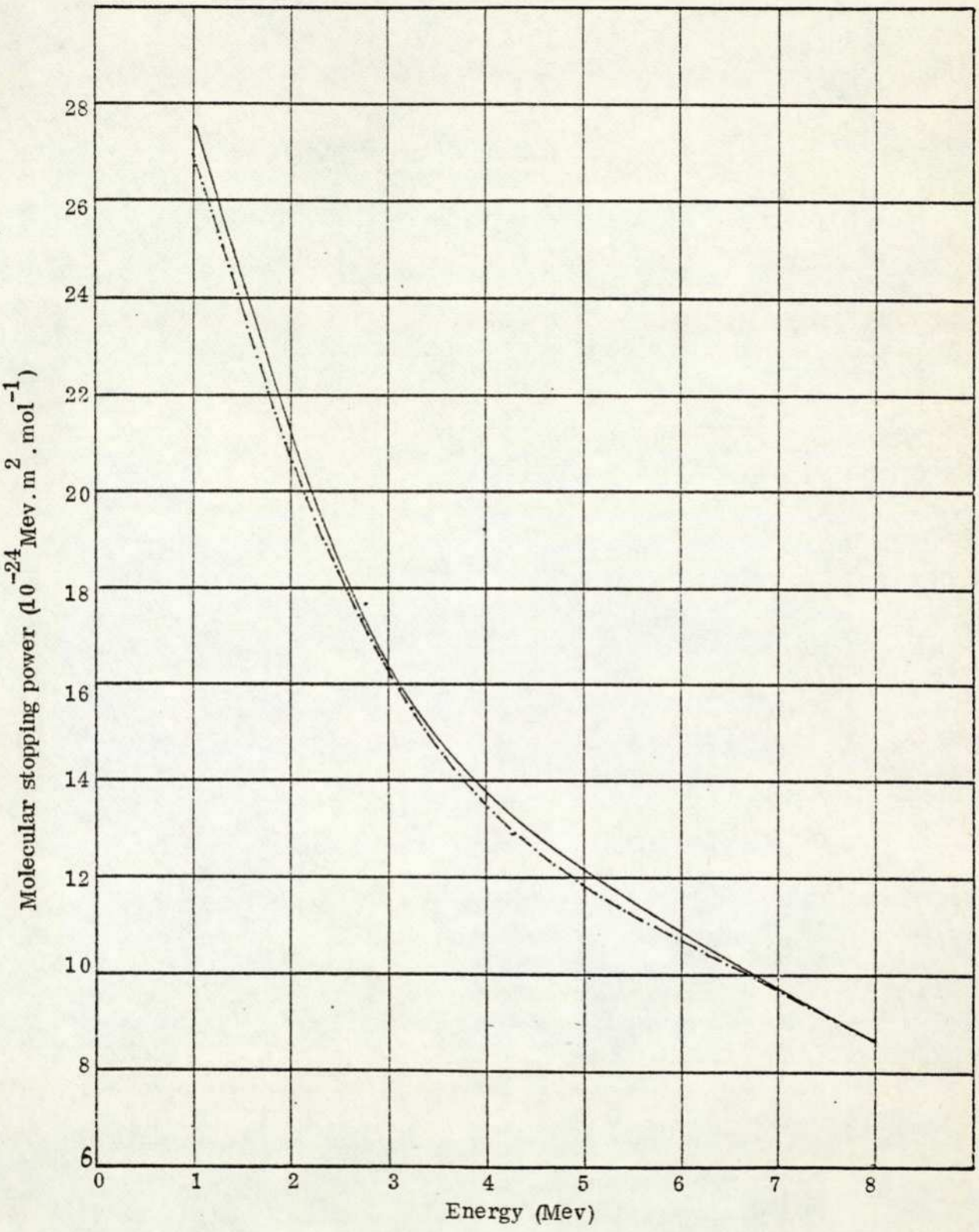

Graph 5.6. Variation of molecular stopping power of—— trichloromethane vapour and—·—·—trichloromethane liquid (method II) with energy.

Table 5.6 Comparison of experimental and calculated stopping powers (10^{-24} Mev.m^2.mol^{-1})

Energy (Mev)	(1)	(2)	(3)	(4)	(5)
1.00	27.39	26.85	27.57	28.13	33.32
1.25	26.17	25.72	26.02	26.02	30.17
1.50	24.25	23.81	24.38	24.07	27.43
1.75	22.57	22.13	22.86	22.54	25.40
2.00	20.93	20.58	21.48	21.18	23.57
2.25	19.70	19.19	20.26	19.87	21.91
2.50	18.31	17.97	19.17	18.76	20.53
2.75	17.42	17.22	18.20	17.76	19.32
3.00	16.56	16.35	17.33	16.98	18.37
3.25	15.75	15.50	16.54	16.19	17.42
3.50	14.81	14.59	15.83	15.47	16.57
3.75	14.20	14.00	15.18	14.71	15.69
4.00	13.58	13.46	14.59	14.20	15.09
4.25	13.24	13.13	14.05	13.66	14.47
4.50	12.81	12.64	13.55	13.18	13.92
4.75	12.49	12.21	13.09	12.74	13.42
5.00	12.19	11.78	12.67	12.34	12.97
5.25	11.89	11.44	12.27	11.97	12.55
5.50	11.57	11.27	11.90	11.64	12.18
5.75	11.23	11.04	11.55	11.32	11.82
6.00	10.90	10.83	11.23	11.00	11.47
6.25	10.57	10.57	10.93	10.70	11.14
6.50	10.25	10.24	10.64	10.42	10.83
6.75	9.98	9.89	10.37	10.15	10.53
7.00	9.67	9.68	10.11	9.91	10.27
7.25	9.39	9.45	9.87	9.66	10.00
7.50	9.13	9.20	9.64	9.43	9.75
7.75	8.87	8.96	9.43	9.21	9.51
8.00	8.67	8.69	9.22	9.00	9.28

Columns (1) and (2) list experimental stopping powers of trichloromethane ($CHCl_3$) vapour and liquid (method II) respectively. Columns (3) - (5) list calculated stopping powers.

The calculated stopping power values are consistently higher than the experimental values at all energies 1 to 8 Mev for both trichloromethane vapour and liquid. To bring the experimental stopping power values for different phases into agreement with the calculated values in column (5), Z_{1eff} has been calculated and is shown in table 5.6a.

Energy Mev	(1)	(2)	Energy Mev	(1)	(2)
1.00	1.81	1.80	4.75	1.93	1.91
1.25	1.86	1.85	5.00	1.94	1.91
1.50	1.88	1.86	5.25	1.95	1.91
1.75	1.89	1.87	5.50	1.95	1.92
2.00	1.88	1.87	5.75	1.95	1.93
2.25	1.90	1.87	6.00	1.95	1.94
2.50	1.89	1.87	6.25	1.95	1.95
2.75	1.90	1.89	6.50	1.95	1.95
3.00	1.90	1.89	6.75	1.95	1.94
3.25	1.90	1.89	7.00	1.94	1.94
3.50	1.89	1.88	7.25	1.94	1.94
3.75	1.90	1.89	7.50	1.94	1.94
4.00	1.90	1.89	7.75	1.94	1.94
4.25	1.91	1.91	8.00	1.93	1.94
4.50	1.92	1.91		1.93	1.94

Table 5.6a. The value of Z_{1eff}.

Columns (1) and (2) give the value of Z_{1eff} trichloromethane vapour and liquid respectively.

5.7 Carbontetrachloride (CCl_4).

The molecular stopping power of carbontetrachloride vapour and liquid (method II) as a function of energy are plotted in graph 5.7. These results are compared with recent stopping power measurement (Palmer 1973), (and are seen to be consistently higher by between 2 and 8%).

In table 5.7 the molecular stopping power of CCl_4 vapour and liquid (method II) are shown in columns (1) and (2) respectively in comparison with calculated values in columns (3)-(5).

Column (3) gives the calculated molecular stopping powers of carbontetrachloride obtained from the uncorrected Bethe formula. In column (4) the values in column (3) have been corrected for the K shell electrons in carbon and chlorine in accordance with the C_k corrections calculated by Walske (1952), and L shell electrons in chlorine in accordance with the C_L corrections calculated by Klandelwal (1968). In Column (5) a further correction has been made due to the Z_1^3 effect as suggested by Ashley et al (1973).

The C_K and C_L corrections increase the molecular stopping power values calculated from the uncorrected Bethe formula by about 2.2% at 1 Mev, falling to zero at 1.25 Mev. At energies above 1.25 Mev they decrease the values in column (3) by about 1.2 to 2.8%. The combined effect of this together with the Z_1^3 correction increases the stopping power values, column (3), by about 22% at the lowest energy and by 0.7% at the highest energy.

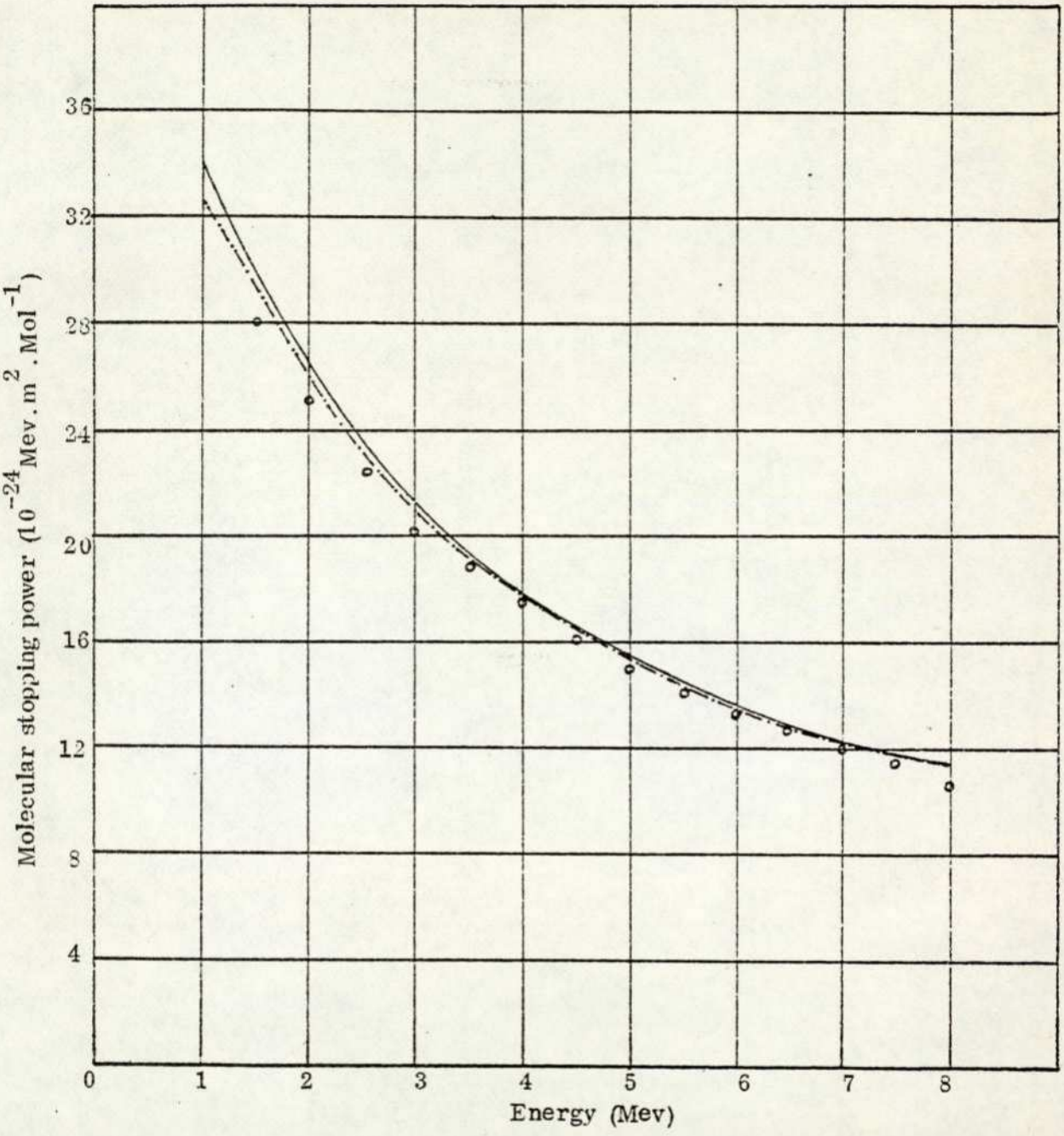

Graph 5.7. Variation of molecular stopping power of —— carbontetrachloride vapour and —·—·— carbontetrachloride liquid (method II) with energy: O Palmer (1973).

Table 5.7 Comparison of experimental and calculated stopping powers.

(10^{-24} Mev.m^2.mol^{-1})

Energy (Mev)	(1)	(2)	(3)	(4)	(5)
1.00	33.48	32.49	33.62	34.36	40.89
1.25	31.73	31.03	31.95	31.95	37.19
1.50	29.85	29.41	30.07	29.70	34.01
1.75	27.99	27.88	28.27	27.88	31.50
2.00	26.29	26.07	26.63	26.17	29.25
2.25	24.67	24.46	25.16	24.68	27.35
2.50	23.39	23.14	23.84	23.34	25.64
2.75	22.22	22.07	22.65	22.11	24.12
3.00	21.18	21.00	21.59	21.16	22.95
3.25	20.20	20.05	20.62	20.19	21.78
3.50	19.34	19.25	19.75	19.30	20.72
3.75	18.59	18.47	18.96	18.50	19.78
4.00	17.91	17.73	18.23	17.75	18.91
4.25	17.34	17.30	17.56	17.07	18.12
4.50	16.76	16.66	16.95	16.48	17.44
4.75	16.19	16.12	16.38	15.93	16.82
5.00	15.64	15.52	15.85	15.44	16.26
5.25	15.10	14.98	25.36	14.98	15.73
5.50	14.62	14.43	14.90	14.57	15.27
5.75	14.15	13.96	14.47	14.18	14.83
6.00	13.71	13.57	14.07	13.78	14.39
6.25	13.29	13.20	13.69	13.40	13.97
6.50	12.95	12.85	13.34	13.06	13.59
6.75	12.70	12.56	13.00	12.73	13.23
7.00	12.44	12.31	12.68	12.42	12.89
7.25	12.18	12.08	12.38	12.11	12.55
7.50	11.90	11.83	12.10	11.83	12.24
7.75	11.65	11.60	11.83	11.55	11.94
8.00	11.48	11.42	11.57	11.28	11.65

Columns (1) and (2) list experimental stopping power of carbontetrachloride (CCl_4) vapour and liquid (method II) respectively. Column (3) - (5) list calculated stopping powers.

The experimental stopping power values in carbontetrachloride vapour and liquid are the same within the limits of experimental error except at low energies. The vapour values are 2-3% higher than the liquid values below 1.5 Mev.

The calculated stopping power values are significantly higher than the experimental values at all energies 1 to 8 Mev for both Carbontetrachloride vapour and liquid. To bring the experimental stopping power values for different phases into agreement with the calculated values in column (5), Z_{1eff} has been calculated and is shown in table 5.7a.

Energy Mev	(1)	(2)	Energy Mev	(1)	(2)
1.00	1.81	1.78	4.75	1.96	1.96
1.25	1.85	1.83	5.00	1.96	1.95
1.50	1.87	1.86	5.25	1.96	1.95
1.75	1.89	1.88	5.50	1.96	1.95
2.00	1.90	1.89	5.75	1.95	1.94
2.25	1.90	1.89	6.00	1.95	1.94
2.50	1.91	1.90	6.25	1.95	1.94
2.75	1.92	1.91	6.50	1.95	1.94
3.00	1.92	1.91	6.75	1.96	1.95
3.25	1.93	1.92	7.00	1.96	1.95
3.50	1.93	1.93	7.25	1.97	1.96
3.75	1.94	1.93	7.50	1.97	1.97
4.00	1.95	1.94	7.75	1.98	1.97
4.25	1.96	1.95	8.00	1.99	1.98
4.50	1.96	1.95			

Table 5.7a. The value of Z_{1eff}.

Columns (1) and (2) give the value of Z_{1eff} of carbontetrachloride vapour and liquid respectively.

6. Discussion.

6.1 Stopping cross-sections determined by using Bragg's Rule.

From the experimental values presented here it is possible to calculate stopping cross-sections for various elements and molecular groups i.e. for O, - Cl -, - C - and - CH_2 -. No experimental values have been obtained for H_2, but a number of published experimental results are available which show good agreement (Bourland et al 1971, Lodhi and powers 1974, Venkataraman et al 1975 and Hanke and Laursen 1978). These have been used in the stopping cross-section calculations and a distinction has been made between calculations using the liquid and vapour forms of the different types of organic materials and water. In certain cases a distinction is also made between values obtained using methods I and II for the liquids so that an estimate of reliability can be made.

6.1a Oxygen.

Stopping cross-sections for oxygen are shown in table 6.1. These are calculated by subtracting hydrogen molecular cross-sections from the values for water vapour and water (methods I and II). The hydrogen values are those of Hanke and Laursen because they cover the whole energy range and they are in good agreement with other published results, mentioned above.

Molecular hydrogen cross-sections here are being subtracted from measured molecular cross-sections. If the Bragg Rule is valid at all, it should be permissible to apply it under these conditions for molecules which are in the same phase. The indications in the literature are that this is

probably sound at energies above 2 Mev, but that there may be inaccuracy in applying the Bragg Rule at lower energies. If this is so, one would expect the oxygen stopping cross-sections calculated in this way from water vapour to differ from the experimental oxygen cross-section by an amount greater than the experimental uncertainty. The calculations from the liquid water experiments should show whether the use of the Bragg Rule can be extended to oxygen when incorporated into molecules in the liquid phase.

From table 6.1 it may be seen that the calculated stopping cross sections of oxygen in vapour phase are about 11-13% higher than those in water liquid (method II) at energies below 1.25 Mev. The difference becomes insignificant between 1.5 and 3 Mev but above 4 Mev it increases again.

The stopping cross-sections of oxygen calculated from the vapour state measurements are higher than values of the experimental stopping power (table 4.3) by between 1 and 6% at energies below 6 Mev. At higher energies this difference increases.

Table 6.1. Stopping cross sections for oxygen i.e. $(H_2O-H_2)2$ calculated using the Bragg's Rule from experimental values for H_2 published by Hanke and Laursen (1978) and (a) water vapour (table 4.4), (b) water liquid method I (table 4.11) and (c) water liquid method II (table 1, Palmer and Akhavan-Rezayat (1978) (10^{-24} Mev. m^2. $atom^{-1}$). (d) Shows the experimental oxygen values as from table 4.3 for comparison.

Energy (Mev)	(a)	(b)	(c)	(d)
1.00	9.22		8.02	8.85
1.25	9.02		7.96	8.45
1.50	8.00		7.94	7.91
1.75	7.62		7.48	7.51
2.00	7.10	6.80	7.08	7.09
2.50	6.37	5.93	6.35	6.26
3.00	5.68	5.10	5.50	5.56
3.50	5.26	4.54	4.96	5.07
4.00	4.82	4.50	4.50	4.65
4.50	4.46	4.40	4.16	4.28
5.00	4.15	4.23	3.85	4.00
5.50	3.96	3.92	3.64	3.75
6.00	3.80	3.60	3.44	3.54
6.50	3.68	3.44	3.22	3.30
7.00	3.53	3.27	3.01	3.08
7.50	3.35	3.05	2.75	2.90
8.00	3.11	2.73		2.71

6.1b. $-CH_2-$

Stopping cross-sections for - CH_2 - are shown in table 6.2. These are calculated by, (a) subtracting the experimental molecular stopping powers of methyl alcohol vapour (table 4.5) from the values for ethyl alcohol vapour (table 4.6) ($C_2H_5OH - CH_3OH$), (b) subtracting ethyl alcohol vapour values from the values for propyl alcohol vapour (table 4.7), $(CH_3)_2CHOH - C_2H_5OH$ and (c) subtracting methyl alcohol vapour values from the values for propyl alcohol vapour and dividing by two. $\frac{(CH_3)_2 CHOH - CH_3OH}{2}$ The mean values of (a), (b) and (c) have been taken as the - CH_2 - vapour stopping power. Similar calculations have been made in the liquid phase from tables 4.5, 4.6 and 4.7 for each liquid stopping power measurement method (I and II) separately and the mean values in all cases for different energies have been taken as stopping power values for - CH_2 - liquid. The stopping power values calculated from vapour measurements for - CH_2 - are higher than those calculated from liquid measurements by within 0-3% between 2 and 6.5 Mev. At higher energies the vapour values are appreciably higher than those calculated from liquid measurements, outside the estimated limits of experimental error.

Table 6.2. Stopping cross-sections for - CH_2 - calculated from experimental measurements using Bragg's Rule (10^{-24}. Mev. m^2. mol^{-1}).

Energy (Mev)	- CH_2 - liquid	- CH_2 - vapour
1.00	5.43	5.53
1.25	5.04	5.10
1.50	4.33	4.70
1.75	4.30	4.42
2.00	4.05	4.14
2.25	3.79	3.88
2.50	3.81	3.78
2.75	3.45	3.46
3.00	3.21	3.27
3.25	3.05	3.02
3.50	2.95	2.87
3.75	2.80	2.71
4.00	2.70	2.67
4.25	2.62	2.62
4.50	2.50	2.52
4.75	2.33	2.30
5.00	2.28	2.25
5.25	2.19	2.21
5.50	2.16	2.19
5.75	2.14	2.15
6.00	2.07	2.09
6.25	2.01	2.04
6.50	1.96	2.00
6.75	1.86	1.95
7.00	1.81	1.89
7.25	1.71	1.82
7.50	1.63	1.75
7.75	1.55	1.68
8.00	1.50	1.62

6.1c Carbon - C -.

Stopping cross-sections for carbon are shown in table 6.3. These are calculated by subtracting hydrogen molecular cross-sections from the values for - CH_2 - vapour and liquid (table 6.2.). The hydrogen values are those of Hanke and Laursen 1978. The results obtained are compared in table 6.3 with recent measured stopping power values (Chu and Powers 1969 and Venkataraman et al 1975). The stopping power values calculated from vapour measurements for carbon are higher than those calculated from liquid measurements by between 1 and 4.5% below 3 Mev. At higher energies up to 6.5 Mev they are in good agreement, but at energies above 7 Mev the vapour values increase again relative to those calculated from the liquid measurements.

The stopping cross-section values for carbon published by Chu and Powers (obtained by carbon foil measurements) are higher than those calculated in this work from experimental measurements with vapours by between 1.5 and 14% at energies below 2 Mev, and the values presented by Venkataraman et al (calculated stopping power of gaseous carbon from a knowledge of ethane and hydrogen stopping powers by use of Bragg's Rule) are appreciably higher than those calculated in this work for all energy regions.

Table 6.3. Stopping cross-sections for - C - i.e. (CH_2 - H_2) calculated using the Bragg Rule from experimental values for H_2 presented by Hanke and Laursen (1978) and (a) - CH_2 - vapour, (b) - CH_2 - liquid (Table 6.2) (10^{-24} Mev. m^2. $atom^{-1}$). (c) Shows the experimental carbon values by Chu and Powers 1969 and (d) shows the calculated carbon values by Venkataraman et al 1975.

Energy (Mev)	(a)	(b)	(c)	(d)
1.00	3.09	3.01	3.61	4.09
1.25	2.96	2.90	3.30	
1.50	2.82	2.45	3.04	3.39
1.75	2.74	2.62	2.86	
2.00	2.61	2.52	2.65	2.88
2.50	2.48	2.51		2.66
3.00	2.14	2.08		2.44
3.50	1.87	1.95		2.26
4.00	1.77	1.80		2.11
4.50	1.70	1.86		1.97
5.00	1.50	1.53		1.86
5.50	1.49	1.46		1.75
6.00	1.43	1.42		1.66
6.50	1.39	1.35		
7.00	1.31	1.23		
7.50	1.21	1.09		
8.00	1.11	0.98		

6.1d Chlorine - Cl -.

Stopping cross-sections for chlorine are shown in table 6.4. These are calculated by (a) subtracting the calculated stopping cross-sections of - CH_2 - vapour (table 6.2) from the molecular stopping powers of dichloromethane vapour (table 4.8) and dividing by two $\left(\frac{CH_2Cl_2 - CH_2}{2}\right)$, (b) subtracting the hydrogen molecular cross-sections (Hanke and Laursen 1978) and calculated stopping cross-sections for carbon table (6.2) from the experimental molecular stopping powers of trichloromethane vapour (table 4.9) and dividing by three $\left(\frac{CHCl_3 - H - C}{3}\right)$, and (c) subtracting the calculated stopping cross-sections for carbon (table 6.2) from the experimental molecular stopping powers of carbontetrachloride vapour (table 4.10) and dividing by four $\left(\frac{CCl_4 - C}{4}\right)$. The mean values of (a), (b), and (c) have been taken for chlorine vapour stopping powers. Similar calculations have been made for chlorine in the liquid phase by using method II liquid experimental measurements. The stopping power values calculated from vapour measurements for chlorine are higher than those calculated from liquid measurements by between 1 and 4.5% below 5.5. Mev. At energies above 6 Mev the liquid values are about 1% higher than those calculated from vapour measurements.

Table 6.4. Stopping cross-sections for - Cl - calculated from experimental measurements using Bragg's Rule (10^{-24} Mev. m^2. $atom^{-1}$).

Energy (Mev)	Cl Vapour	Cl liquid
1.00	7.73	7.38
1.25	7.35	7.01
1.50	6.88	6.74
1.75	6.38	6.27
2.00	5.92	5.85
2.50	5.18	5.08
3.00	4.72	4.68
3.50	4.31	4.22
4.00	3.96	3.90
4.50	3.70	3.66
5.00	3.51	3.43
5.50	3.28	3.22
6.00	3.07	3.06
6.50	2.88	2.90
7.00	2.73	2.75
7.50	2.61	2.64
8.00	2.49	2.52

The reliability of stopping cross-sections determined by using Bragg's Rule has been investigated by number of workers (Tschalar and Bichsel 1968, Bourland and Power 1971, Ladhi and Powers 1974 and Zeiss et al 1977). These studies were based either on a comparison of different experimental energy loss measurements or on a comparison of I (the mean excitation energy) values obtained by fitting the Bethe formula to experimental stopping cross sections with or without shell corrections.

Experimental measurements are subject to error, sometimes systematic errors which are not always appreciated. Theoretical calculations, especially at low energies, are not reliable since shell corrections, the Z_1^3 corrections and the value assumed for Z_{1eff} may all be inaccurate. This has been discussed in section 1.3d.

It is important when comparing experimental results to choose those which are, as far as possible, relating to the same conditions e.g. comparison of stopping cross-sections of - CH_2 - should be in the same phase material and, if possible derived from similar molecules. Provided that this is adhered to. it would seem that it is valid in general to use the Bragg Rule in molecular calculations over the energy range investigated to the order of accuracy of the present experimental work.

In the stopping cross-section tables presented here, comparisons with other workers results are made where these are felt to be valid.

6.2. The ratio of the molecular stopping powers in the vapour and liquid phases for water, methyl, ethyl and propyl alcohol, dichloromethane, trichloromethane and carbontetrachloride for various alpha-particle energies

are shown in tables 6.5 and 6.6 . All molecules concerned contain hydrogen except carbontetrachloride and it is noticeable that the higher stopping powers in the vapour phase are more pronounced in the molecules which contain a higher proportion of hydrogen. This would suggest that the phase effect can be partly explained by the modification of the outer electronic wave-functions in the liquid phase since this would be most easily observed in hydrogenous materials (Bichsel 1975, Matteson et al 1977 and Ziess et al 1977).

It can be seen from the experimental stopping powers that phase effects occur clearly in the stopping of low energy alpha-particles in water and alcohols, the stopping powers in the liquid states being lower than those in the corresponding vapour states. Present results for dichloromethane (above 2 Mev), trichloromethane and carbontetrachloride (tables 5.5, 5.6 and 5.7) indicate that the molecular stopping powers are not significantly different in the liquid and vapour phases over most of the energy range investigated, and the slightly higher value in the vapour phase at the lower energies could be within the limits of experimental uncertainty.

As discussed in section 1.3d, there is evidence from other workers that the molecular stopping power of a material is different in different phases. The reasons for these differences could be an increase in the mean excitation potential I in liquid states, caused by the change in molecular structure, because only the outer electrons are involved in the molecular bond, or it could be that at lower energies, the value of the alpha-particle mean charge in the vapour phase is likely to be a little higher than that in the liquid medium, because the probability of electron capture is greater when the elctron density is increased.

Table 6.5. Ratio of experimental stopping powers in the vapour phase to those in the liquid phase.

(1) Methyl alcohol vapour and liquid (method I)
(2) Methyl alcohol vapour and liquid (method II)
(3) Ethyl alcohol vapour and liquid (method I)
(4) Ethyl alcohol vapour and liquid (method II)
(5) Propyl alcohol vapour and liquid (method I)
(6) Propyl alcohol vapour and liquid (method II)

Energy (Mev)	(1)	(2)	(3)	(4)	(5)	(6)
1.00		1.04		1.08		1.03
1.25		1.03		1.08		1.02
1.50		1.03		1.04		1.05
1.75		1.03		1.02		1.03
2.00	1.02	1.01	1.05	1.05	1.02	1.02
2.25	1.01	1.01	1.04	1.03	1.01	1.02
2.50	1.03	1.00	1.02	1.02	1.01	1.03
2.75	1.02	1.00	1.03	1.04	1.01	1.01
3.00	1.04	1.00	1.03	1.04	1.01	1.02
3.25	1.05	1.00	1.03	1.03	1.01	1.01
3.50	1.05	1.00	1.03	1.03	1.00	1.00
3.75	1.05	1.00	1.03	1.04	0.99	1.01
4.00	1.05	1.00	1.03	1.04	1.00	1.02
4.25	1.04	1.01	1.03	1.05	1.00	1.02
4.50	1.02	1.01	1.04	1.05	1.00	1.02
4.75	1.01	1.01	1.05	1.07	0.98	0.99
5.00	1.01	1.01	1.06	1.08	0.99	1.01
5.25	0.99	1.01	1.09	1.11	0.99	1.02
5.50	0.99	1.02	1.11	1.13	0.99	1.03
5.75	0.99	1.02	1.12	1.15	0.99	1.03
6.00	1.00	1.03	1.13	1.15	0.99	1.03
6.25	0.99	1.03	1.14	1.16	0.99	1.04
6.50	1.00	1.03	1.13	1.15	0.99	1.04
6.75	1.00	1.03	1.12	1.14	1.01	1.05
7.00	0.99	1.02	1.12	1.14	1.00	1.05
7.25	0.99	1.02	1.11	1.13	1.00	1.07
7.50	0.99	1.03	1.12	1.14	1.00	1.08
7.75	1.00	1.03	1.11	1.15	1.01	1.09
8.00	1.01	1.04	1.10	1.18	1.02	1.09

Table 6.6. Ratio of experimental stopping powers in the vapour phase to those in the liquid phase.

(1) Water vapour and liquid water (method I).
(2) Dichloromethane vapour and liquid (method II).
(3) Trichloromethane vapour and liquid (method II).
(4) Carbontetrachloride vapour and liquid (method II).

Energy (Mev)	(1)	(2)	(3)	(4)
1.00		1.08	1.02	1.03
1.25		1.08	1.02	1.02
1.50		1.06	1.02	1.01
1.75		1.03	1.02	1.00
2.00	1.03	1.02	1.02	1.01
2.25	1.03	1.01	1.03	1.01
2.50	1.05	1.01	1.02	1.01
2.75	1.09	1.01	1.01	1.01
3.00	1.08	1.01	1.02	1.01
3.25	1.10	1.02	1.02	1.01
3.50	1.10	1.02	1.02	1.00
3.75	1.08	1.02	1.01	1.01
4.00	1.08	1.01	1.01	1.01
4.25	1.03	1.01	1.01	1.00
4.50	1.01	1.01	1.01	1.01
4.75	1.00	1.01	1.02	1.00
5.00	0.99	1.01	1.03	1.01
5.25	0.99	1.02	1.04	1.01
5.50	1.00	1.01	1.03	1.01
5.75	1.02	1.00	1.02	1.01
6.00	1.04	1.00	1.01	1.01
6.25	1.05	0.99	1.00	1.01
6.50	1.05	0.99	1.00	1.01
6.75	1.05	1.00	1.01	1.01
7.00	1.05	1.00	1.00	1.01
7.25	1.06	1.01	0.99	1.01
7.50	1.07	1.01	0.99	1.01
7.75	1.08	1.02	0.99	1.00
8.00	1.10	1.02	1.00	1.01

6.3. Suggestions for further work.

It would be desirable for more accurate experimental work to be carried out at lower energies especially with liquids, because calculated molecular stopping powers obtained from the Bethe formula are unreliable since there is no definite theory from which an accurate value of the effective charge can be calculated at low energies.

Further measurements with vapours, especially water and the alcohols under lower pressure conditions should be carried out. This would eliminate uncertainties due to the possible association of the molecules in the vapour phase. In order to investigate the full range-energy relation in some of the vapours, it was necessary to use methal foils of uniform thickness, e.g. for water vapour measurement 3-42 μm (Section 4.2b), for ethyl alcohol vapour 6-18 μm (Section 4.2d) of rolled Aluminium foils have been used. There is some evidence (Sofield et al 1977) that the alpha-particle straggling in rolled Aluminium foils is considerably higher than that in evaporated Aluminium foils of the same thickness, presumably due to slight variations in thickness or density. Greater accuracy in the vapour measurements could probably be obtained if evaporated Aluminium foils were to be used instead of rolled foils.

In order to eliminate considerations of charge exchange effects influencing the stopping power in liquids and vapours comparable measurements with protons would also be of interest.

6.4. Conclusion.

The experimental measurements presented indicate that there is, in general, some difference in molecular stopping powers in liquids and their corresponding vapours. This effect is most pronounced in molecules with a high hydrogen content and is small, and sometimes insignificant in halogenated compounds, although there are indications that the effect is present at low energies. Use of the Bragg Rule for calculating stopping powers of substances from the constituent atoms would seem to be valid provided that data is used from measurements derived from bound atoms in molecules of the same phase. Use of atomic data derived from measurements on a material in another phase may not be valid e.g. results from carbon foil measurements may not be reliable when used in molecular calculations, and this is particularly true at low energies.

7. Appendix (I).

The listings of the programs used to calculate $\frac{dE}{dx}$ with both methods.

7.1. Master Poly.

In the programme standard techniques are used to fit a polynominal of any required order to experimental points by the criterion of least squares fit. The polynomials used were of 2nd, 3rd and 4th order for the current experiments, and since only limited regions of the range-energy curve were fitted each time e.g. between 2 and 5 Mev the quadratic fit was usually considered to be the most appropriate. The number of points fitted was usually between 30 and 50. The programme gave the coefficients for the quadratic, cubic and 4th power curves. A subsidiary programme differentiated these polynomials and hence gave the gradient $\frac{dE}{dx}$ at stated energy intervals. Comparison of the values of $\frac{dE}{dx}$ at the same energy for the three polynomials gave some indication of reliability. It was observed that values of $\frac{dE}{dx}$ were most consistent with all curves when taken near the middle of the energy range of the experimental points i.e. at $3\frac{1}{2}$ Mev for the 2 to 5 Mev section.

Results from the cubic and 4th power curves were sometimes found to be inconsistent due to a point of inflexion in the calculated curve. Such results were discarded. A mean value was taken of $\frac{dE}{dx}$ values obtained in this way and a measure of uncertainty could be estimated from the variations.

The listing of this program is as follows:

7.1. Program polynomial fit.

```
      MASTER POLY
      DIMENSION TITLE(3),XR(250),YE(250),W(250),R(250),A(5),P(228),
     1DEG(5),RMS(5),COEF(5,5),E(3,110),X1(110),Y1(5,110),DIFF(5,110),
     2X(110),Y(110)
      READ(1,100) (TITLE(K), K=1,3)
100   FORMAT(3A8)
      READ(1,101) NO
101   FORMAT(I3)
      M=NO
      READ(1,102)(YE(K),XR(K),K=1,M)
102   FORMAT(500F0.0)
IS THIS LARGE A REPEAT COUNT INTENDED AT ABOUT COLUMN 15, LINE 0018

      CALL SORT(XR,YE,M)
      WRITE(2,99)(TITLE(K),K=1,3),YE(1),YE(M)
99    FORMAT(1H1,40X,37HA LEAST-SQUARES POLYNOMIAL CURVE FIT.,//,
     131X,3A8,15H  ENERGIES FROM,F6.2,4H TO ,F6.2,4HMEV.,//)
      WRITE(2,999) M
999   FORMAT(1H ,12HDATA POINTS=,I3,/,8X,1HE,9X,1HR)
      WRITE(2,1000)(YE(K),XR(K),K=1,M)
1000  FORMAT(1H ,2F10.2)
      EPS1=0.0
      EPS2=3.0
20    M=0
      DO 1  I=1,NO
      IF(YE(I) .GE. EPS1 .AND. YE(I) .LE. EPS2) GO TO 30
      GO TO 1
30    M=M+1
      Y(M)=YE(I)
      X(M)=XR(I)
1     CONTINUE
      P(1)=-1.0
      P(3)=1.0
      P(4)=1.0
      P(5)=0.0
      NMAX=5
      MM=5*NMAX+2*M+3
      DO 33  II=1,NMAX
33    A(II)=0.0
      WRITE(2,99)(TITLE(K),K=1,3),EPS1,EPS2
      WRITE(2,999) M
      WRITE(2,1000)(Y(J),X(J),J=1,M)
      DO 3  NN=1,NMAX
      CALL F4CFORP1(M,NMAX,MM,X,Y,R,W,A,P)
      DEG(NN)=P(1)
      RMS(NN)=P(2)
```

```
      DO 4  I=1,NMAX
4     COEF(NN,I)=A(I)
3     CONTINUE
      WRITE(2,99)(TITLE(K),K=1,3),EPS1,EPS2
      WRITE(2,105)(DEG (NN),NN=1,NMAX)
105   FORMAT(1H ,11X,5(6X,4HORD=,F4.1,6X)//)
      WRITE(2,106)((I,(COEF(NN,I),NN=1,NMAX),I=1,NMAX))
106   FORMAT(//(1H ,I2,8X,5(4X,F12.8,4X)))
      WRITE(2,107)(RMS(NN),NN=1,NMAX)
107   FORMAT(1H0,10HRMS ERROR=,5(4X,F12.8,4X))
      L=1
      DO 5  K=3,5
      DO 6  J=1,M
6     E(L,J)=COEF(K,1)+COEF(K,2)*X(J)+COEF(K,3)*X(J)**2+
     1COEF(K,4)*X(J)**3+COEF(K,5)*X(J)**4
      L=L+1
5     CONTINUE
      WRITE(2,108)
108   FORMAT(1H ,/////,21X,12HEXPERIMENTAL,32X,
     124HCALCULATED   POLYNOMIALS,//)
      WRITE(2,109)
109   FORMAT(1H ,13X,1HR,20X,1HE,14X,12HSECOND ORDER,8X,
     111HTHIRD ORDER,8X,12HFOURTH ORDER,//)
      WRITE(2,110)((X(J),Y(J),(E(L,J),L=1,3),J=1,M))
110   FORMAT(1H ,5E20.8)
      BIGX=X(M)
      SMALLX=X(1)
      STEP=(BIGX-SMALLX)/100.
      DO 7  K=2,5
      XX=SMALLX
      DO 7  J=1,100
      X1(J)=XX
      Y1(K,J)=COEF(K,1)+COEF(K,2)*X1(J)+COEF(K,3)*X1(J)**2+
     1COEF(K,4)*X1(J)**3+COEF(K,5)*X1(J)**4
      DIFF(K,J)=COEF(K,2)+2*COEF(K,3)*X1(J)+
     13*COEF(K,4)*X1(J)**2+4*COEF(K,5)*X1(J)**3
7     XX=XX+STEP
      WRITE(2,111)
111   FORMAT(1H1,//,43X,35HTHEORETICAL VALUES OF R,E AND DE/DR,//)
      WRITE(2,112) COEF(2,2)
112   FORMAT(1H ,28X,10HD(E1)/DR= ,F20.8,///)
      WRITE(2,114)
114   FORMAT(1H ,10X,1HR,14X,2HE1,12X,2HE2,12X,2HE3,
     112X,2HE4,11X,14H  D(E2)/DR    ,14H  D(E3)/DR    ,
     214H  D(E4)/DR    )
      WRITE(2,115)(X1(J),Y1(2,J),Y1(3,J),Y1(4,J),Y1(5,J),
     1DIFF(3,J),DIFF(4,J),DIFF(5,J),J=1,100)
115   FORMAT(1H ,8E15.8)
      EPS1=EPS1+0.5
      EPS2=EPS2+0.5
      IF(EPS2 .GT. YES NO)+0.5) GO TO 60
      GO TO 20
60    STOP
      END
```

7.2. Fit 1.

This programme fitted a curve of the form of mentioned in section 3.3. to the complete set of experimental results, and a subsidiary programme differentiated the curve and gave values of the gradient of the curve over the full range of x so that $\frac{dE}{dx}$ could be noted for any required energy value.

The sum of the squares of the deviations of the experimental values from the curve was given, and points on the calculated curve were printed out so that a comparison could be made with the experimental values and the reliability of fit over various parts of the curve could be ascertained.

If the fit was deemed to be unsatisfactory, modifications Fit 2 and Fit 3 were fitted to the experimental results. These were similar to Fit 1 but used further variables to give more flexibility in the curve fitting.

7.3. Comparison of methods.

The polynomial fit and the experiential fit methods were found to give results which in most cases were in agreement with the limits of uncertainty set by the experimental variations.

```
STARTED
0010                  MASTER CURVE
0011                  DOUBLE PRECISION X(150),Y(150),C(7),CT(7),
0012                 1A(7,15),V(7)
0013                  C(1)=0.5D0
0014                  C(2)=0.064D0
0015                  C(3)=0.04D0
0016                  READ(1,150)NPTS
0017          150     FORMAT(I0)
0018                  READ(1,151)(Y(I),X(I),I=1,NPTS)
0019          151     FORMAT(2D0.0)
0020                  CALL FIT(NPTS,X,Y,3,C,CT,7,A,20,V,1)
0021                  CALL DIFF(NPTS,C,X)
0022                  STOP
0023                  END

END OF SEGMENT,LENGTH    89, NAME  CURVE

0024                  DOUBLE PRECISION FUNCTION F(NC,C,X)
0025                  DOUBLE PRECISION C(NC),X,P
0026                  P=DEXP(-C(2)*X)
0027                  F=(C(1)+C(3)*X)*(1-P)
0028                  RETURN
0029                  END

END OF SEGMENT,LENGTH    85, NAME  F


0030                  SUBROUTINE DERIV(NC,C,X,V)
0031                  DOUBLE PRECISION C(NC),X,P,V(NC)
0032                  P=DEXP(-C(2)*X)
0033                  V(1)=1-P
0034                  V(2)=X*(C(1)+C(3)*X)*P
0035                  V(3)=X*V(1)
0036                  RETURN
0037                  END

END OF SEGMENT, LENGTH  130, NAME  DERIV

0038                  SUBROUTINE DIFF(NPTS,C,X)
0039                  DOUBLE PRECISION X(150),C(7),P,G
0040                  DO 1 I=1,NPTS
0041                  P=DEXP(-C(2)*X(I))
0042                  G=C(3)+C(1)*C(2)*P+(C(3)*(C(2)*X(I)-1.0D0)*P)
0043                  WRITE(2,150)X(I),G
0044          150     FORMAT(1H ,2D20.6)
0045          1       CONTINUE
0046                  RETURN
0047                  END
```

```
STARTED
0010                MASTER CURVE
0011                DOUBLE PRECISION X(150),Y(150),C(9),CT(9),
0012               1A(9,19),V(9)
0013                C(1)=0.5D0
0014                C(2)=0.064D0
0015                C(3)=0.04D0
0016                C(4)=1.0D0
0017                READ(1,150)NPTS
0018          150   FORMAT(I0)
0019                READ(1,151)(Y(I),X(I),I=1,NPTS)
0020          151   FORMAT(2D0.0)
0021                CALL FIT(NPTS,X,Y,4,C,CT,9,A,20,V,1)
0022                CALL DIFF(NPTS,C,X)
0023                STOP
0024                END

END OF SEGMENT, LENGTH   100, NAME  CURVE

0025                DOUBLE PRECISION FUNCTION F(NC,C,X)
0026                DOUBLE PRECISION C(NC),X,P
0027                P=DEXP(-C(2)*X)
0028                F=(C(1)+C(3)*X)*(1-C(4)*P)
0029                RETURN
0030                END

END OF SEGMENT, LENGTH   89,  NAME  F

0031                SUBROUTINE DERIV(NC,C,X,V)
0032                DOUBLE PRECISION C(NC),X,P,V(NC)
0033                P=DEXP(-C(2)*X)
0034                V(1)=1-C(4)*P
0035                V(2)=X*C(4)*P*(C(1)+C(3)*X)
0036                V(3)=X*V(1)
0037                V(4)=-(C(1)+C(3)*X)*P
0038                RETURN
0039                END

END OF SEGMENT, LENGTH  178,  NAME  DERIV

0040                SUBROUTINE DIFF(NPTS,C,X)
0041                DOUBLE PRECISION X(150),C(9),P,G
0042                DO 1  I=1,NPTS
0043                P=DEXP(-C(2)*X(I))
0044                G=C(3)+C(4)*(C(1)*C(2)-C(3)+C(2)*C(3)*X(I))*P
0045                WRITE(2,150)X(I),G
0046          150   FORMAT(1H  ,2D20.6)
0047          1     CONTINUE
0048                RETURN
0049                END
```

```
STARTED
0010                  MASTER CURVE
0011                  DOUBLE PRECISION X(150),Y(150),C(11),CT(11),
0012                 1A(11,23),V(11)
0013                  C(1)=0.5D0
0014                  C(2)=0.16D0
0015                  C(3)=0.1D0
0016                  C(4)=1.0D0
0017                  C(5)=0.1D0
0018                  READ(1,150)NPTS
0019           150    FORMAT(I0)
0020                  READ(1,151)(Y(I),X(I),I=1,NPTS)
0021           151    FORMAT(2D0.0)
0022                  CALL FIT(NPTS,X,Y,5,C,CT,11,A,20,V,1)
0023                  CALL DIFF(NPTS,C,X)
0024                  STOP
0025                  END


END OF SEGMENT,  LENGTH   111,  NAME  CURVE

0026                  DOUBLE PRECISION FUNCTION F(NC,C,X)
0027                  DOUBLE PRECISION C(NC),X,P
0028                  P=DEXP(-C(2)*X)
0029                  F=(C(1)+C(3)*X+C(5)*X*X)*(1-C(4)*P)
0030                  RETURN
0031                  END


END OF SEGMENT,  LENGTH   109,  NAME  F

0032                  SUBROUTINE DERIV(NC,C,X,V)
0033                  DOUBLE PRECISION C(NC),X,P,V(NC)
0034                  P=DEXP(-(2)*X)
0035                  V(1)=1-C(4)*P
0036                  V(2)=(C(1)+C(3)*X+C(5)*X*X)*X*C(4)*P
0037                  V(3)=X*V(1)
0038                  V(4)=-(C(1)+C(3)*X+C(5)*X*X)*P
0039                  V(5)=X*X*V(1)
0040                  RETURN
0041                  END


END OF SEGMENT,  LENGTH   241,  NAME  DERIV

0042                  SUBROUTINE DIFF(NPTS,C,X)
0043                  DOUBLE PRECISION X(150),C(11),P,G
0044                  DO 1  I=1,NPTS
0045                  P=DEXP(-C(2)*X(I))
0046                  G=(C(3)+2.0*C(5)*X(I))*(1.-C(4)*P)+(C(1)+C(3)*X(I)
0047                 1+C(5)*X(I)*X(I))*C(2)*C(4)*P
0048                  WRITE(2,150)X(I),G
0049           150    FORMAT(1H  ,2D20.6)
0050             1    CONTINUE
0051                  RETURN
0052                  END
```

REFERENCES

Allison, S. K. Experimental results on charge-changing collisions of Hydrogen and Helium atoms and ions at kenetic energies above 0.2 Mev. Rev. Mod. Phys. 30, 1137-1168 (1958).

Andersen, H. H., Sorensen, H. and Vadja, P. Excitation potentials and Shell corrections for the elements $Z_2 = 20$ to $Z_2 = 30$. Phys. Rev. 180, 373-380 (1969).

Andersen, H. H., Bak, J. F., Knudsen, H, Moller Pëtersen, P. and Nielsen, B. R. Experimental investigation of higher-order Z_1 corrections to the Bethe stopping-power formula. Nucl.Instrum.Meth. 140, 537-540 (1977).

Ashley, J. C. Influence of the Z_1^3 contribution to stopping power on the evaluation of mean excitation potentials and shell corrections. Phys. Rev. B9 334-6 (1973).

Ashley, J. C. and Ritchie, R. H. Z_1^3 - Dependent stopping power and range contributions. Phy.Rev. A8, 1402-8 (1973).

Ashley, J. C. and Ritchie, R. H. Z_1^3 Effect in the stopping power of matter for charged particles. Phys. Rev. B5 2393-7 (1972).

Baglin, J. E. E. and Ziegler, J. F. Tests of Bragg rule for energy loss of ^4H_e ions in solid compounds. J. Appl. Phys. 45. No.3, 1413-15 (1973).

Baker, C. J. and Segrè, E. Stopping power and energy loss for ion pair production for 340-Mev protons. Phys. Rev. 81. 489-92 (1951).

Barkas, H. D. Nuclear Research Emulsions (New York: Academic Press) (1963).

Bell, G. I. The capture and loss of electrons by fission fragments. Phys. Rev. 90. 548-57 (1953).

Bethe, H. A. Passage of heavy particles through matter. Ann. Physik, 5, 325 (1930).

Bethe, H. A. Moliere's theory of multiple scattering. Phys. Rev. 89. 1256-66 (1953)

Betz, H. D. Charge states and charge-changing cross sections of fast heavy ions penetrating through gaseous and solid media. Rev. Mod. Phys. 44 (1972).

Betz, H. D. Ionization and excitation of fast heavy ions inside and outside solid targets. Proc. Isr. Phys. Soc.1(1976).

Bichsel, H. Passage of charged particles through matter. University of Washington, U.S.C. 136-150 (1970).

Bichsel, H. Sympo en neutron dosimetry. 1974 (Luxembuorg: Commission of the European Communities) Vol 1, 191-225 (1975).

Bichsel, H. Considerations concerning the straggling of 100-Mev proton in X_e. Phys.Rev.A9. 571-5 (1974).

Bloch, F. Braking capacity of atoms with several electrons. Ann.Phys. 16. 285 (1933).

Bohr N. Scattering and stopping of fission fragments. Phys.Rev. 58. 654-5 (1940).

Bohr, N. Velocity - range relation for fission fragments. Phys. Rev. 59. 270-5 (1941).

Bohr, N. The penetration of atomic particles through matter. Dan.Mat. Fys. Medd. 18.8 (1948).

Bonderup, E. Kgl. Danshe. Viderskab Selskab Matt. Phys. Medd. 35 No 17 (1967).

Bourland, P. D. and Powers, D. Bragg Rule applicability to stopping cross sections of gases for alpha particles of Energy 0.3-2.0 Mev. Phys. Rev. 3. 3635-3641 (1971).

Burgess, V.W.E. The stopping power of organic compounds for alpha particles in the range 1.5-8 Mev. J.Phys.D.Appl.Phys. 8, 782-9 (1975).

Chau, E.K.L., and Powers, D. Measurement of molecular stopping cross-sections of aldehydes and ketones and calculation of the atomic stopping cross-section of oxygen in double-bonded and three-membered ring-structure C-H-O compounds. J.Appl.Phys. 49(5). 2611-15 (1978).

Chu, W. K. and Powers, D. Alpha-particle stopping cross section in solids from 400 Kev to 2 Mev. Phys. Rev. 187. 478-490 (1969).

Chu, W. K., Braun, M., Davies, J. A. Matsunami, N. and Thompson, D.A. Energy loss of the ions in solidified gases. Nucl.Instrum.Meth. 149. 115-120 (1978).

Dalton, P. and Turner, J. E. New evaluation of mean excitation energies for use in radiation dosimetry. Health Phys. 15. 257-262 (1968).

Evans, R. D. The atomic nuclear (New York: McGraw-Hill) p.636 (1955).

Fano, U. Ed. Studies in penetration of charged particles in matter. Publication 1133 (National Academy of Sciences - National Research Council, Washington, D.C. (1964).

Feng, J. S. Y., Chu, W.K. and Nicolet, M.A. Stopping-cross-section additivity for 1-2 Mev $^4He^+$ in solid oxides. Phy.Rev.B10. 3781-8 (1974).

Gluckstern, R. L. Electron capture and loss by ions in gases. Phys. Rev. 93. 1817-21 (1955).

Hanke, C. and Laursen, J. Stopping cross sections for alpha-particles from 1.0 to 8.5 Mev in H_2, He, N_2, O_2, Ne, Kr and Xe. Nucl. Instrum. Meth. 151. 253-260 (1978).

Heckman, H. H., Hubbard, E. L. and Simon, W. G. Electronic charge distributions for heavy ions at high velocities. Phys. Rev. 129. 1240-9 (1963).

Heckman, H. H. and Lindstrom, P. J. Stopping power differences between positive and negative pions at low velocities. Phys. Rev. Let. 22, 1969-74 (1969).

Inokuti, M. Mean excitation energies for stopping power as derived from oscillator-strength distribhtions. Six symposium on microdosimetry, Brussels 22-26, May (1978).

Jackson, J. D. and McCarthy, R. L. Z_1^3 Corrections to energy loss and range. Phys. Rev. B6. 4131-41 (1972).

Khandelwal, G. S. Shell corrections for K- and L- electrons. Nucl. Phys. A116. 97-111 (1968).

Khandelwal, G. S. and Merzbacher, E. Stopping power of M electrons. Phys. Rev. 144. 349-352 (1966).

Brunings, J. H. M., Knipp, J. K. and Teller, E. On the momentum loss of heavy ions. Phys. Rev. 60. 657-60 (1941).

Lindhard, J. The Barkas effect - or Z_1^3, Z_1^4 - corrections to stopping of swift charged particles. Nucl. Instrum. Meth. 132. 1-5 (1976).

Lodhi, A. S. and Powers, D. Energy loss of alpha-particles in gaseous C-H and C-H-F compounds. Phys. Rev. A10. 2131-40 (1974).

Matteson, S. Powers, D. and Chau, E. K. L. Physical-state effect in the stopping cross section of H_2O ice and vapour for 0.3-2.0 Mev alpha-particles. Phys. Rev. A15. 856-64 (1977).

Mapleton, R. A. Theory of charge exchange (New York: Wiley) (1972).

Massey, H. S. W. and Gilbody, H. B. Electronic and Ionic impact phenomena Vol. 4 (London: Oxford UP) pp 2841-47 (1974).

Meckbach, W. and Allison, S.K. Ratio of the effective charge of the beam traversing gaseous and metallic calmium. Phys. Rev. 132. 294-304 (1963).

Palmer, R. B. J. and Simons, H.A.B. The experimental determination of the range-energy relations for alpha-particles in water and water vapour for alpha-particles at energies below 8.78 Mev. Proc. Phys. Soc. 74. 585-98 (1959).

Palmer, R. B. J. The stopping power for alpha-particles of ethyl alcohol and carbontetrachloride in the liquid and vapour states. Proc. Phys. Soc. 78. 766-773 (1961).

Palmer, R. B. J. The stopping power of hydrogen and hydro carbon vapours for alpha particles over the energy range 1 to 8 Mev. Proc. Phys. Soc. 87. 681-8 (1963).

Palmer, R. B. J. The stopping power of organic liquids for alpha-particles over the energy range 1-8 Mev. J.Phys.B: Atom. Molec. Phys. 6. 384-92 (1973).

Palmer, R. B. J. and Akhavan-Rezayat, A. The stopping power of water, water vapour and aqueous tissue equivalent solution for alpha particles, over energy range 0.5-8 Mev. J.Phys. D: Appl. Phys. 11. 605-15 (1978).

Ritchie, R. H. and Brandt, W. Projectile-charge dependence of stopping powers. Phy.Rev.A17. 2102-5 (1978).

Segre, E. Experimental nuclear physics. Pt.II. Sec.1A (1953).

Sofield, C. J.. Cowern, N. E. B., Freeman, J. M. and Parthasaradhi, K. Energy straggling of 5.486 Mev alpha particles in Al. Phys. Rev. A15. 2221-6 (1977).

Thwaites, D.I. and Watt, D.E. Similarity treatment of phase effects in stopping power for low energy heavy charged particles. Phys. Med. Biol. 23, 426-37 (1978).

Tschalar, C. and Bichsel, H. Mean excitation potential of light compounds. Phys. Rev. 187. 478-490 (1969).

Turner, J. E., Roecklein, P. D. and Vora, R. B. Mean excitation energies for chemical elements. Health. Phys. 18. 159-160 (1970).

Venkataraman, G., Murthy, M.S.S. and Viswakarma, R.R. Stopping powers of some low atomic number materials for alpha particles of energies up to 6 Mev. Health. Phys. 28. 461-4 (1975).

Walsh, J. Numerical analysis: An introduction (Acad. Press) (1966).

Walsh, P. J. Stopping power and range of alpha-particles. Health Phys. 19 312-6 (1970).

Walske, M.C. The stopping power of K-electrons. Phys.Rev. 88. 1283-9 (1952).

Walske, M.C. Stopping power of L-electrons. Phys.Rev.101. 940-4 (1955).

Whillock, M.J. and Edwards, A.A. Comparison of the stopping cross-sections of ethylene and polyethylene using alpha-particles in the energy range 1.5-4.2 Mev. Phys.Med. Biol. 23. 416-25 (1978).

Williamson, J. and Watt, D. E. The influence of molecular binding on the stopping power of alpha-particles in hydrocarbons. Phy.Med.Biol. 17. 486-92 (1972).

Ziegler, J. F. The calculation of low energy He ion stopping powers. Nucl. instrum. Meth. 149. 129-135 (1978).

Ziess, G. D., Meath, W. J.. MacDonald, J. C. F. and Dawson, D. J. Accurate evaluation of stopping and straggling mean excitation energies for N, O, H_2, N_2, NO, NH_3, H_2O and N_2O using dipole oscillator strength distributions. A test of the validity of Bragg's Rule. Radiat. Res. 70. 284-303 (1977).